

Filamentary Structures and Compact Objects in the Aquila and Polaris Clouds Observed by *Herschel*

Gould Belt GT KP

SPIRE SAG3



energie atomique • énergies alternatives

Alexander Men'shchikov

Ph. André, P. Didelon, V. Könyves, N. Schneider,
F. Motte, S. Bontemps, D. Arzoumanian, M. Attard

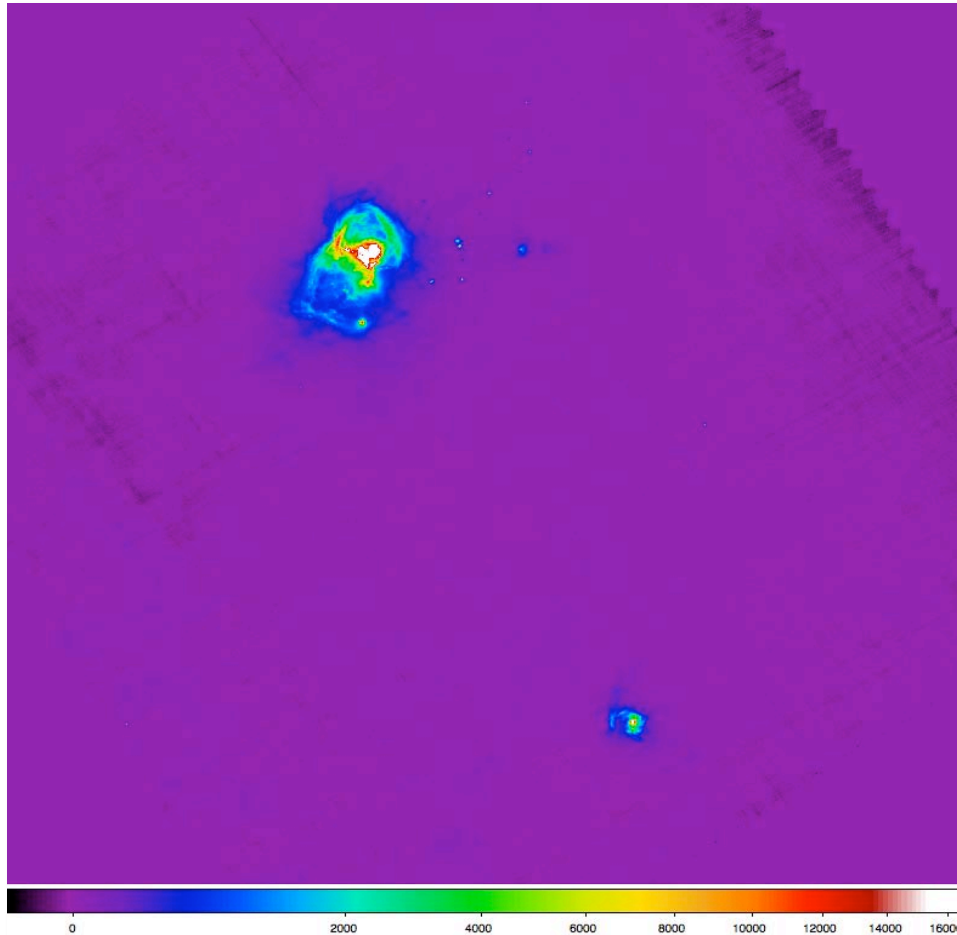
A. Abergel, J.-P. Baluteau, J.-Ph. Bernard, L. Cambrésy, P. Cox,
J. Di Francesco, M. Griffin, P. Hargrave, M. Huang, J. Kirk, J. Z. Li, P. Martin,
V. Minier, M.-A. Miville-Deschênes, S. Molinari, G. Olofsson, S. Pezzuto,
H. Roussel, D. Russeil, P. Saraceno, M. Sauvage, B. Sibthorpe, L. Spinoglio,
L. Testi, G. White, C. D. Wilson, A. Woodcraft, A. Zavagno

Herschel Science Demonstration

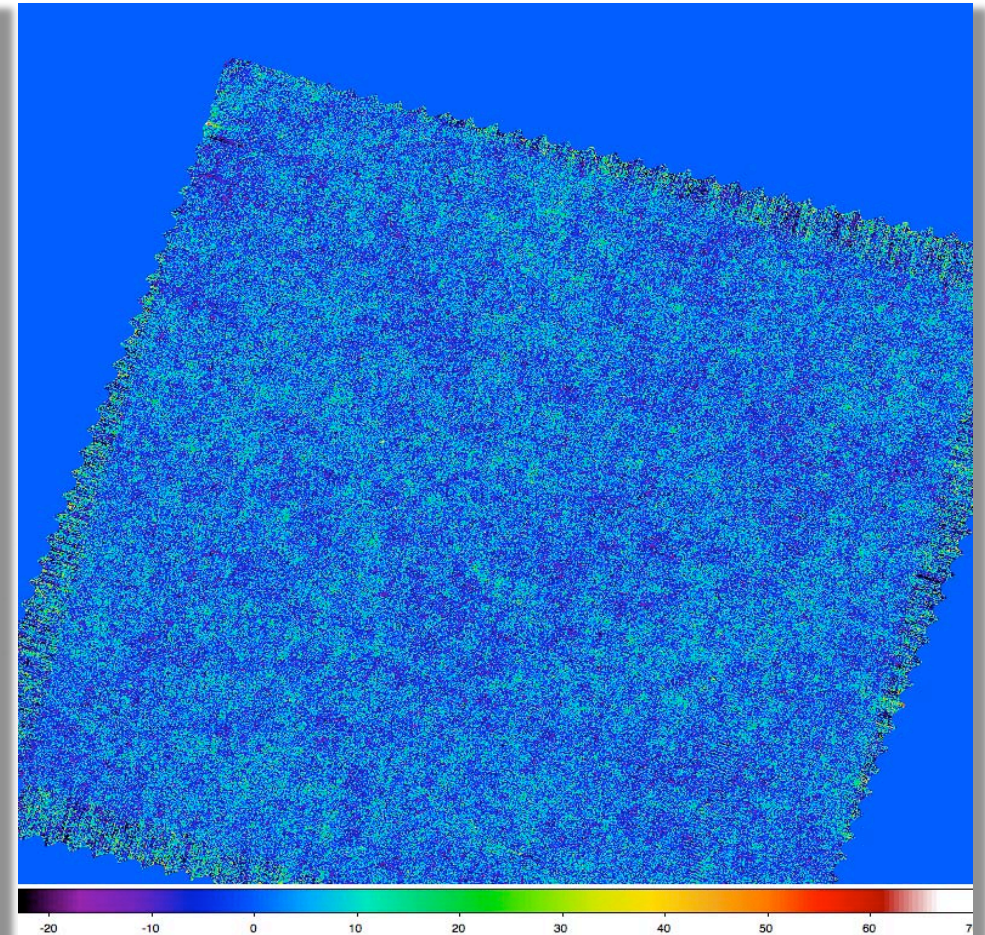
- Part of the large Gould Belt KP survey of the nearby star-forming regions
 - More results in talks by Philippe André, Vera Könyves, Sylvain Bontemps
- Aquila Rift and Polaris Flare fields ($D \sim 260$ pc and ~ 150 pc)
 - Cores in active star-forming region vs. high-latitude cirrus clouds
 - SPIRE/PACS parallel mode at 70, 160, 250, 350, 500 μm
 - Angular resolutions of $\sim 8, 13, 18, 25, 37$ arcsec
 - Fields $\sim 3 \times 3^\circ$, cross-scans at $60''/\text{s}$

Herschel Images of the Aquila and Polaris Fields

Aquila and Polaris: PACS 70 μm resolution $\sim 8''$

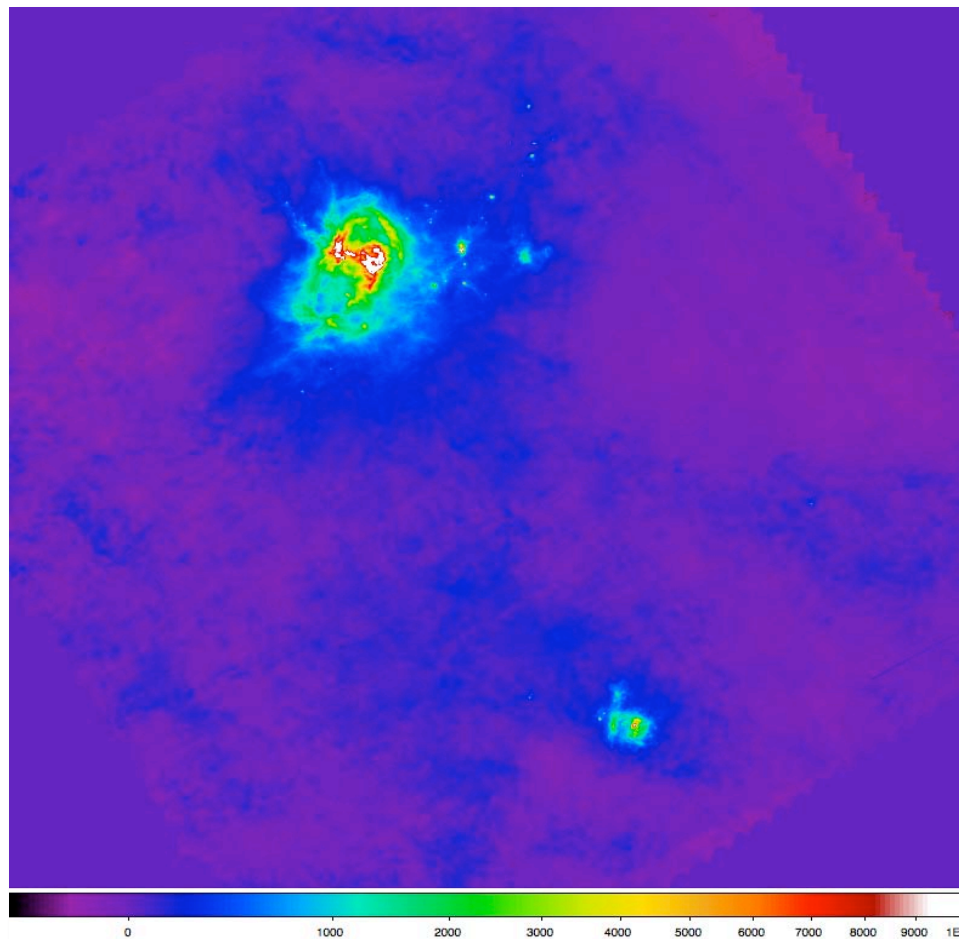


3.3°

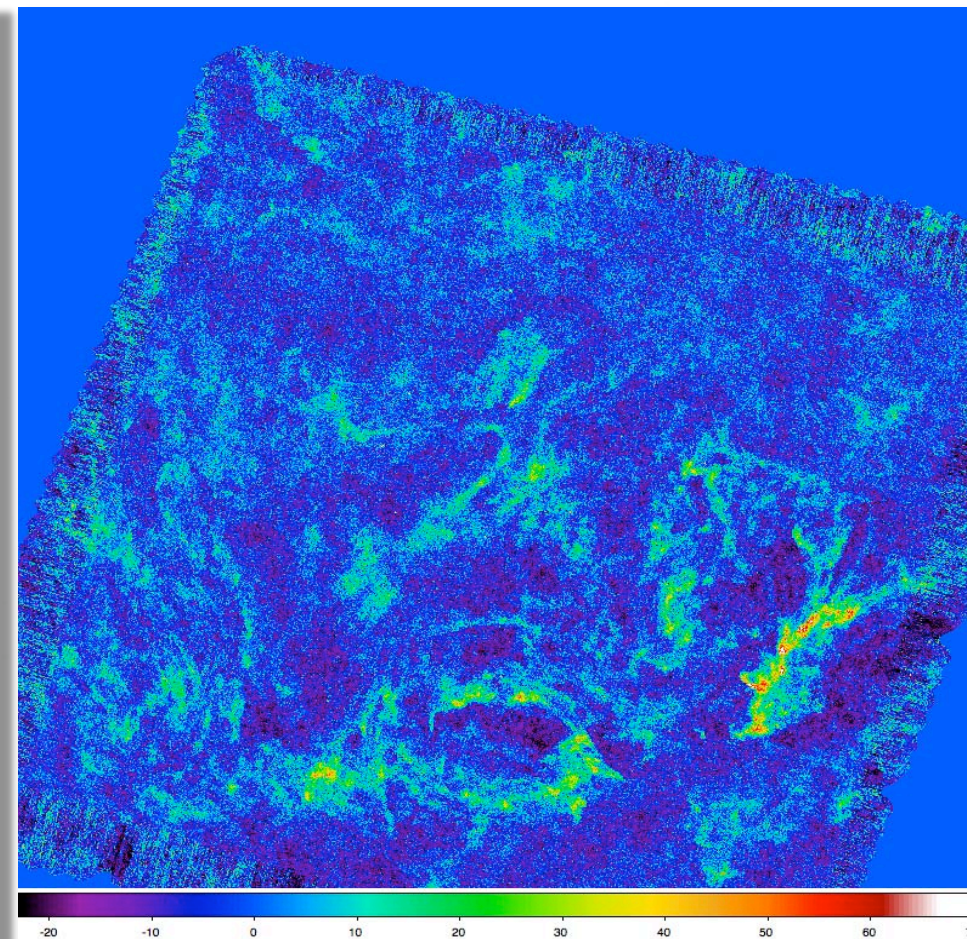


3.3°

Aquila and Polaris: PACS 160 μm resolution $\sim 13''$

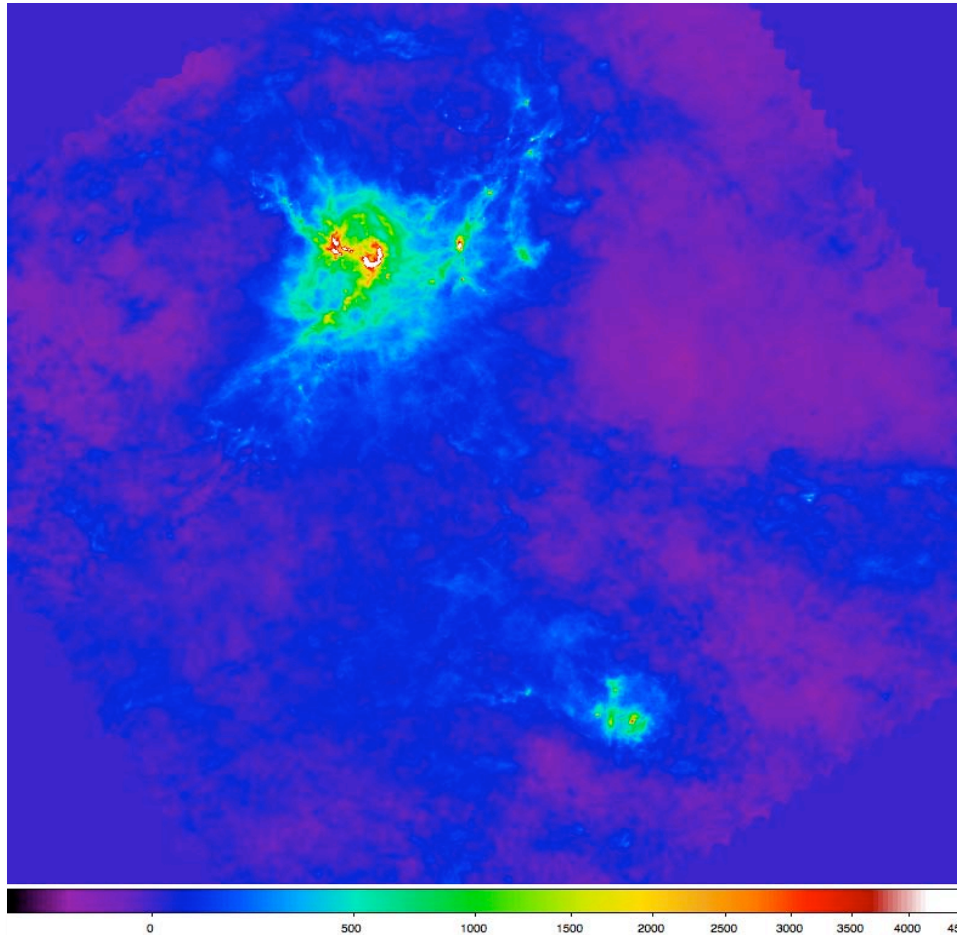


3.3°

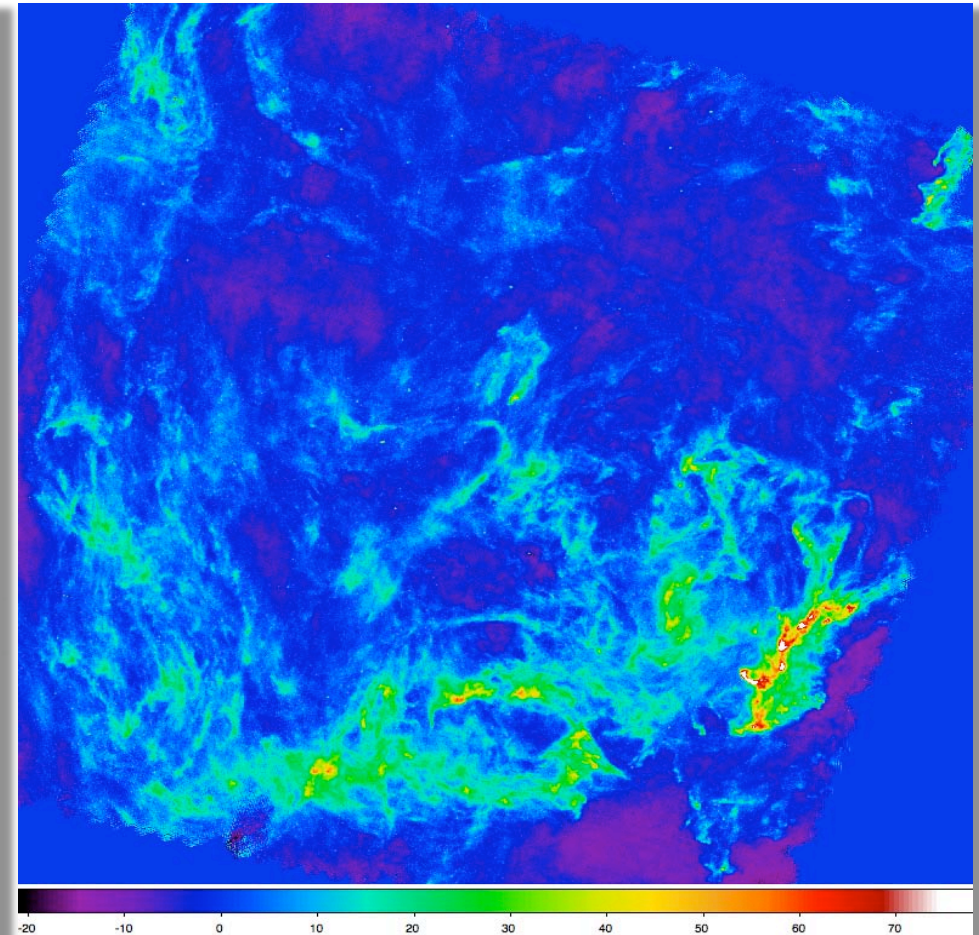


3.3°

Aquila and Polaris: SPIRE 250 μm resolution $\sim 18''$

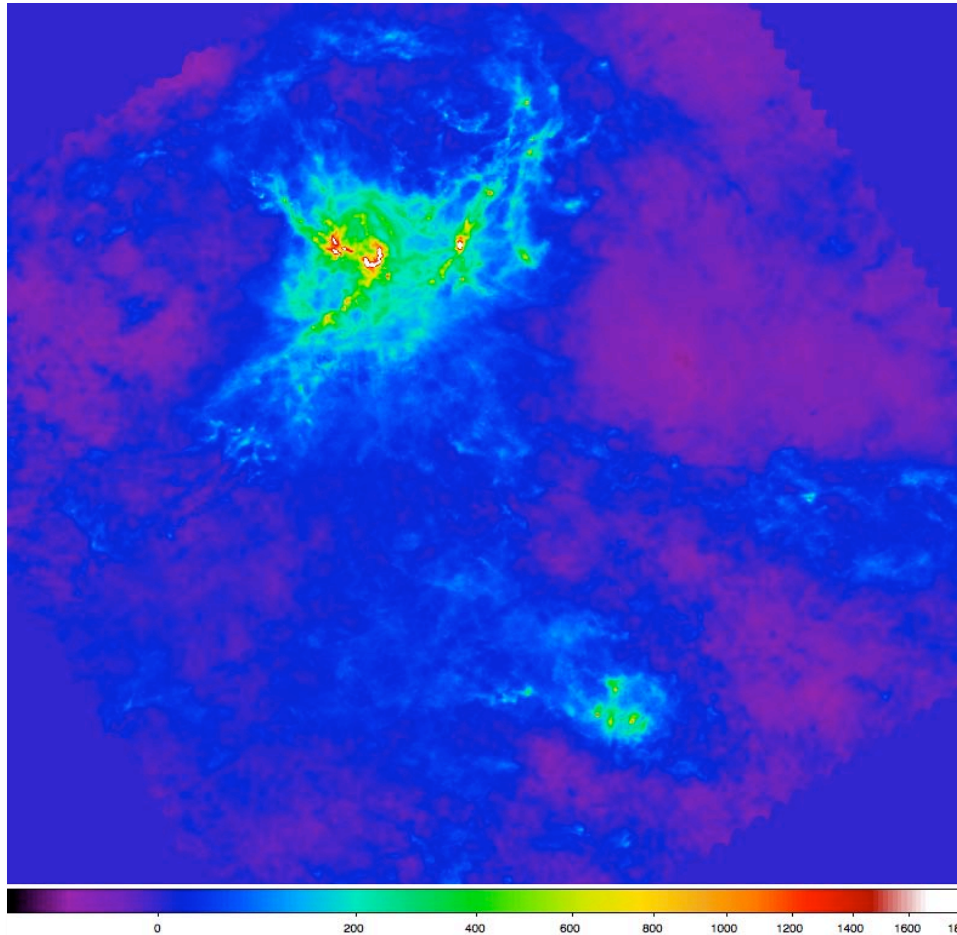


3.3°

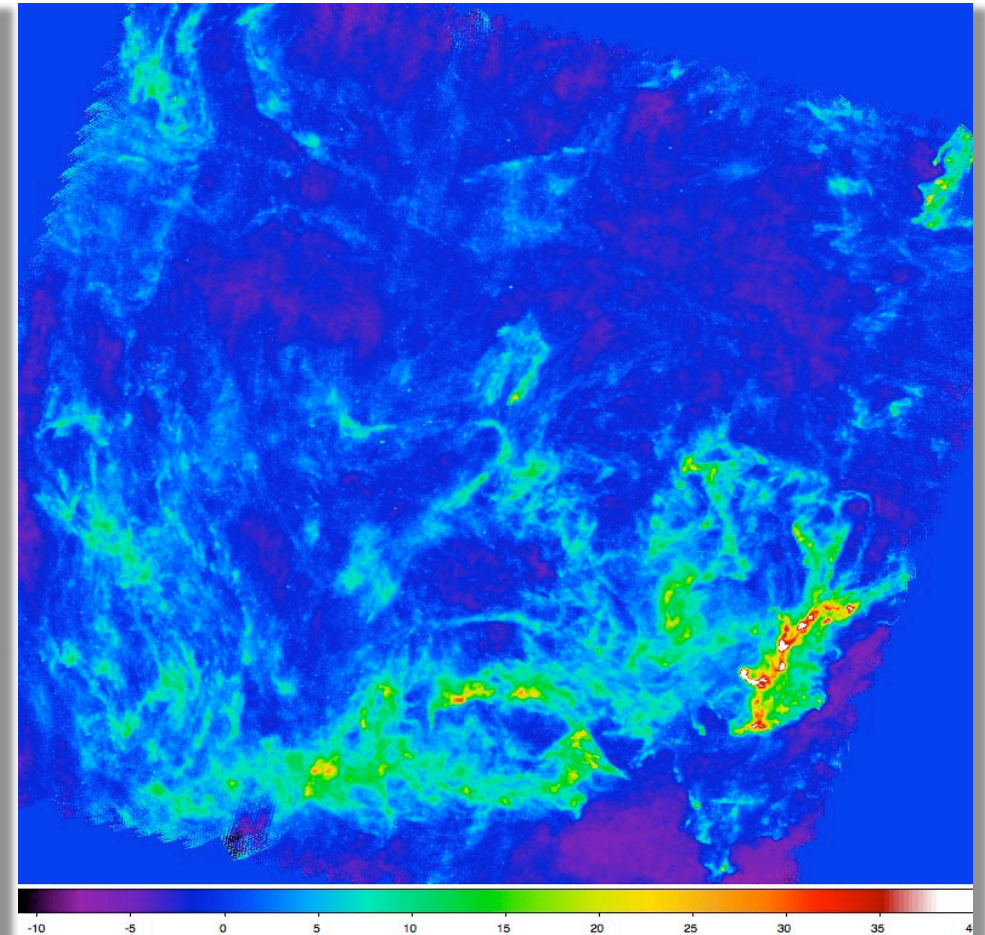


3.3°

Aquila and Polaris: SPIRE 350 μm resolution $\sim 25''$

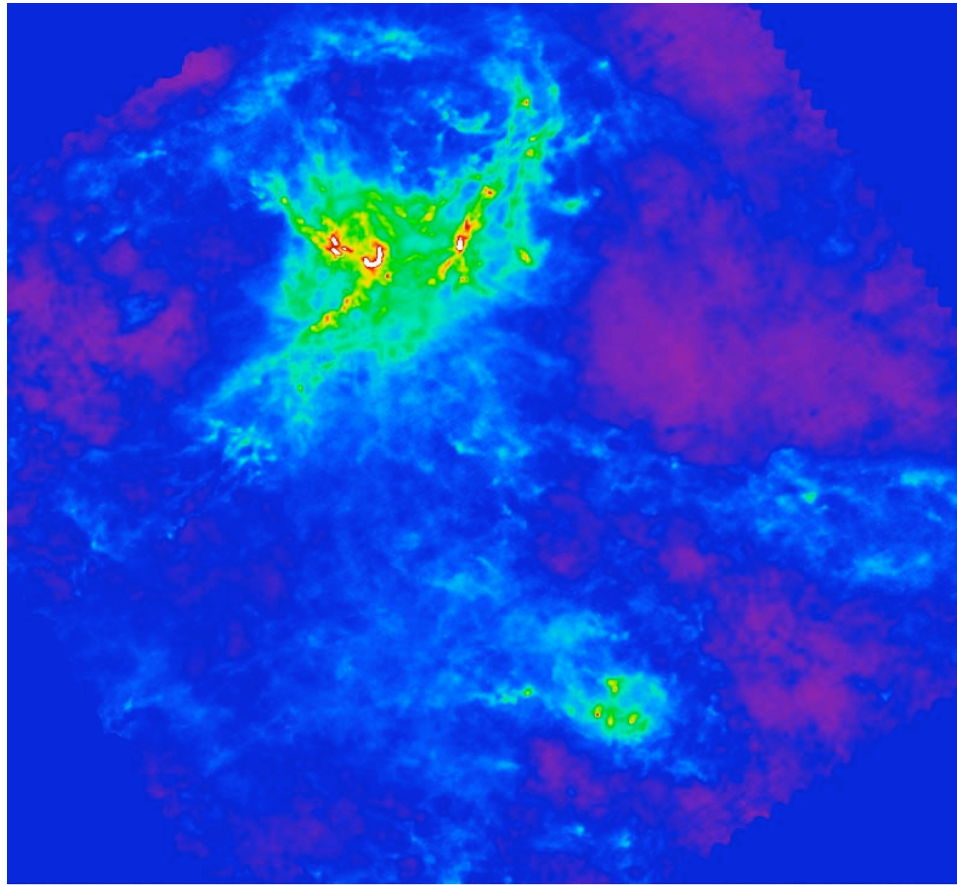


3.3°

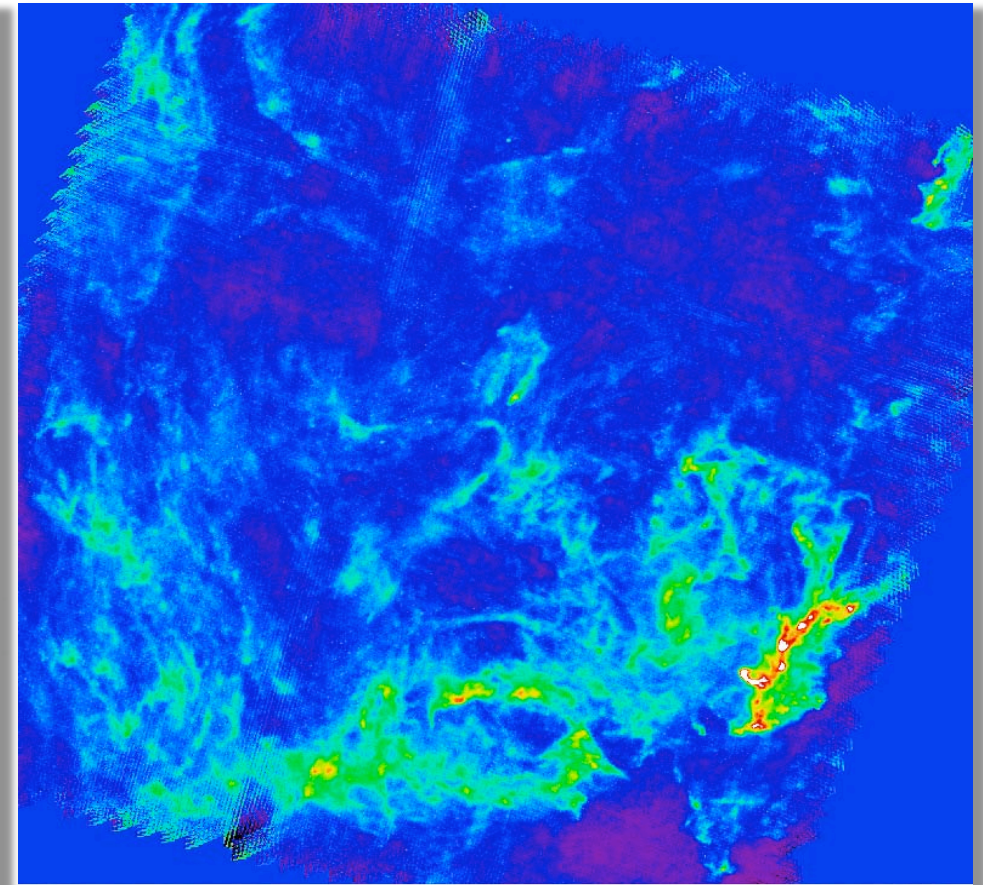


3.3°

Aquila and Polaris: SPIRE 500 μm resolution $\sim 37''$



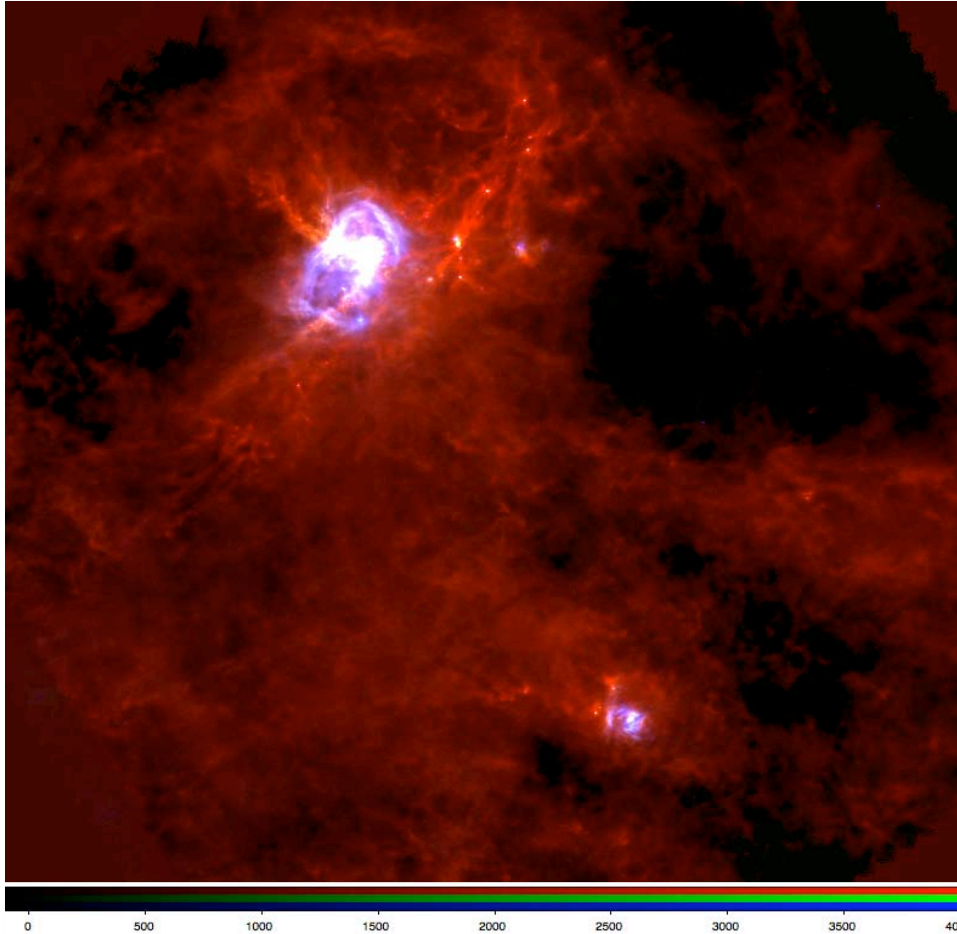
3.3°



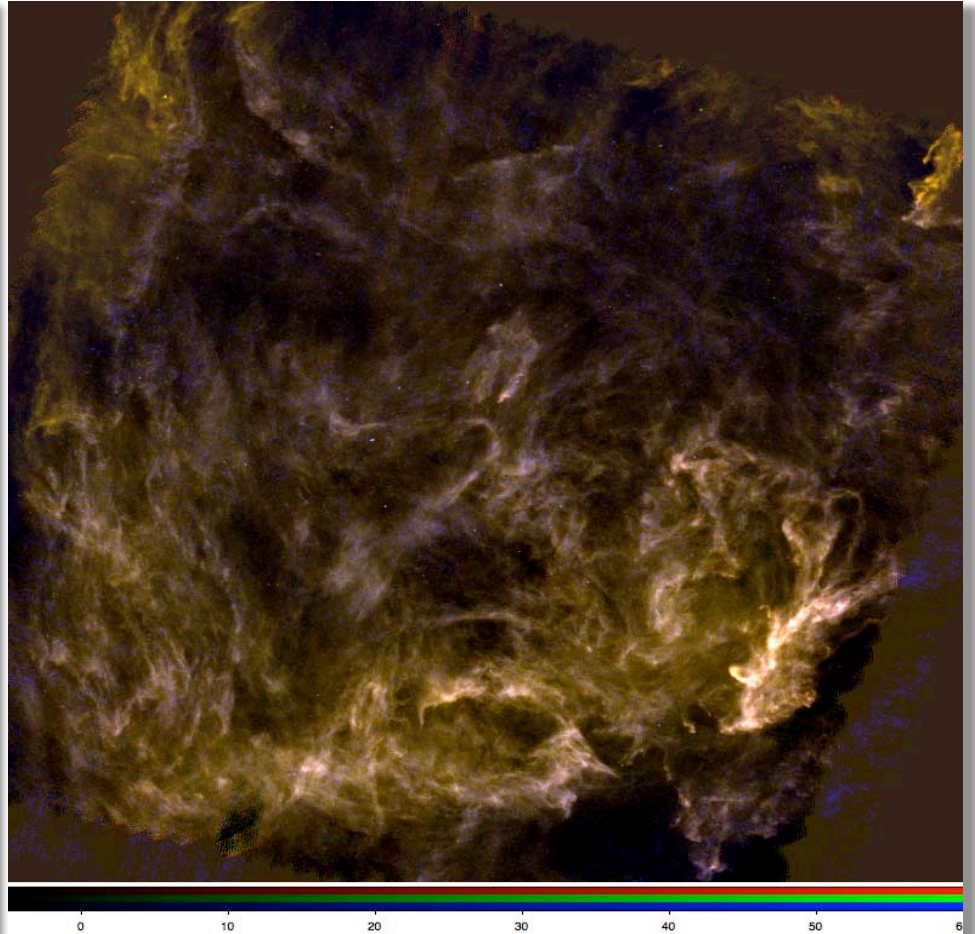
3.3°

Aquila and Polaris: SPIRE/PACS

RGB 350+160+70 μm and 350+250+160 μm



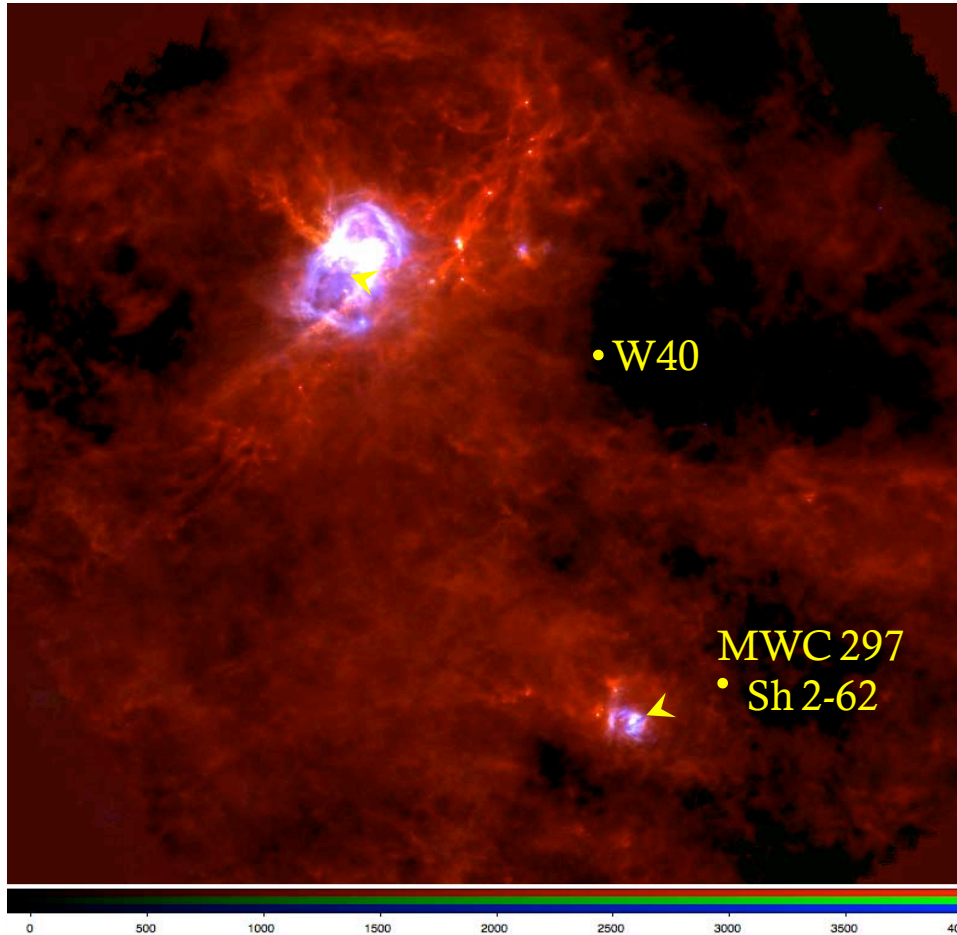
3.3°



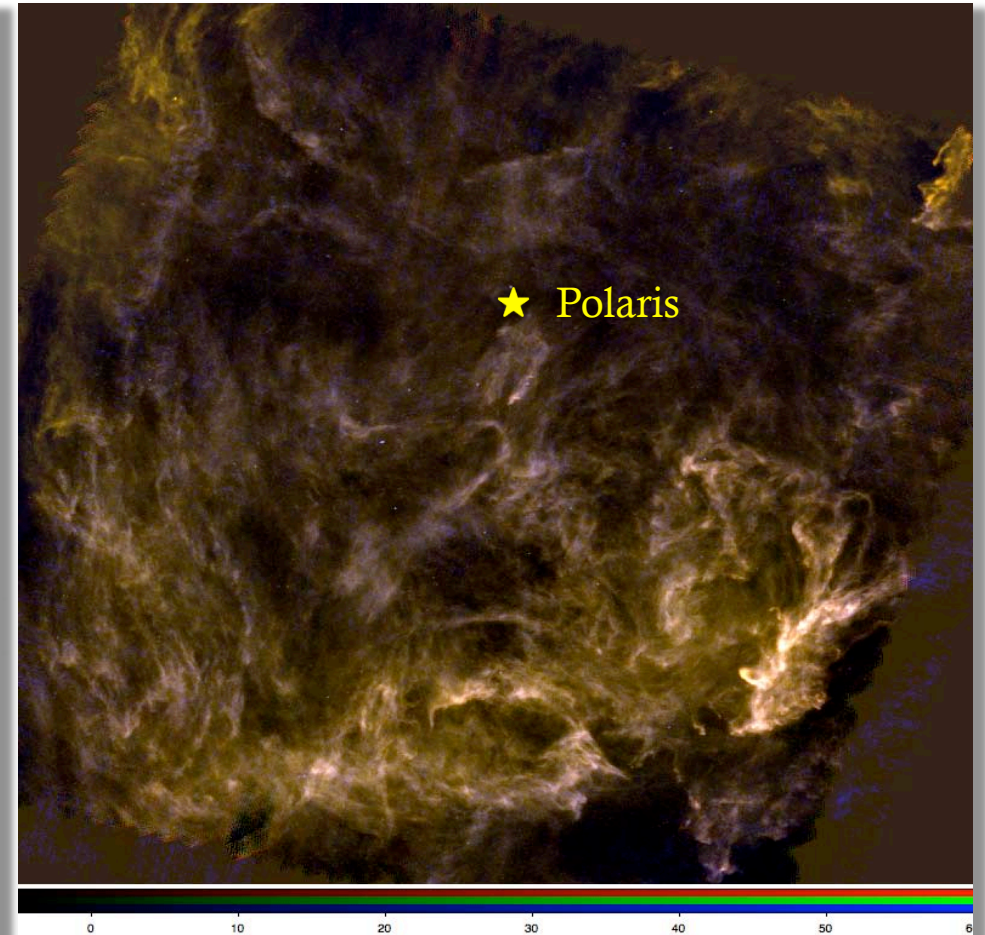
3.3°

Aquila and Polaris: SPIRE/PACS

RGB 350+160+70 μm and 350+250+160 μm



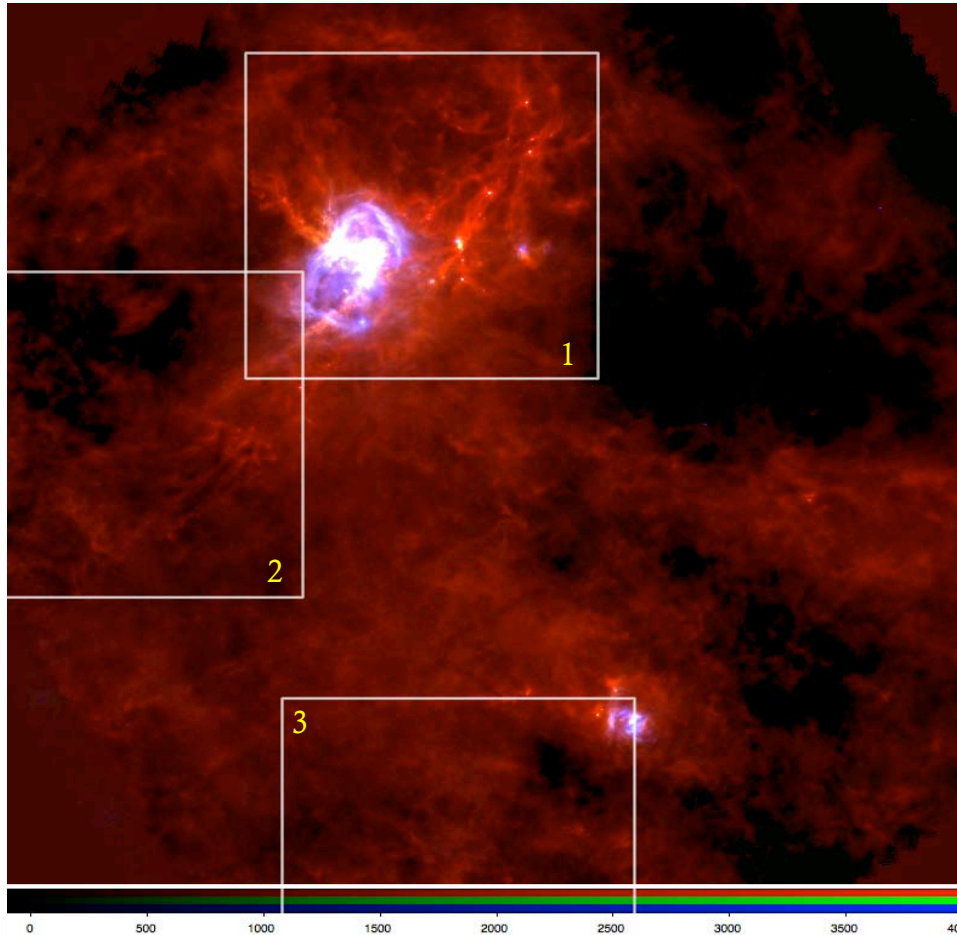
3.3°



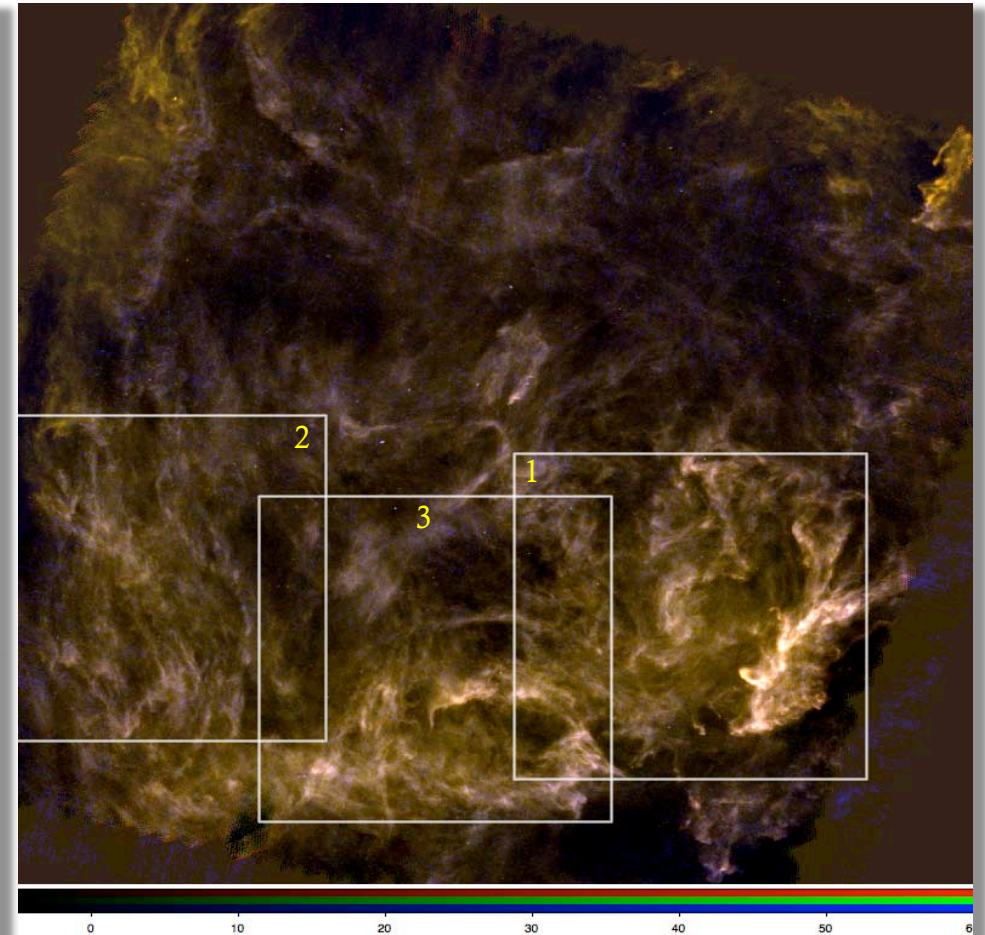
3.3°

Aquila and Polaris: SPIRE/PACS

RGB 350+160+70 μm and 350+250+160 μm



3.3°



3.3°

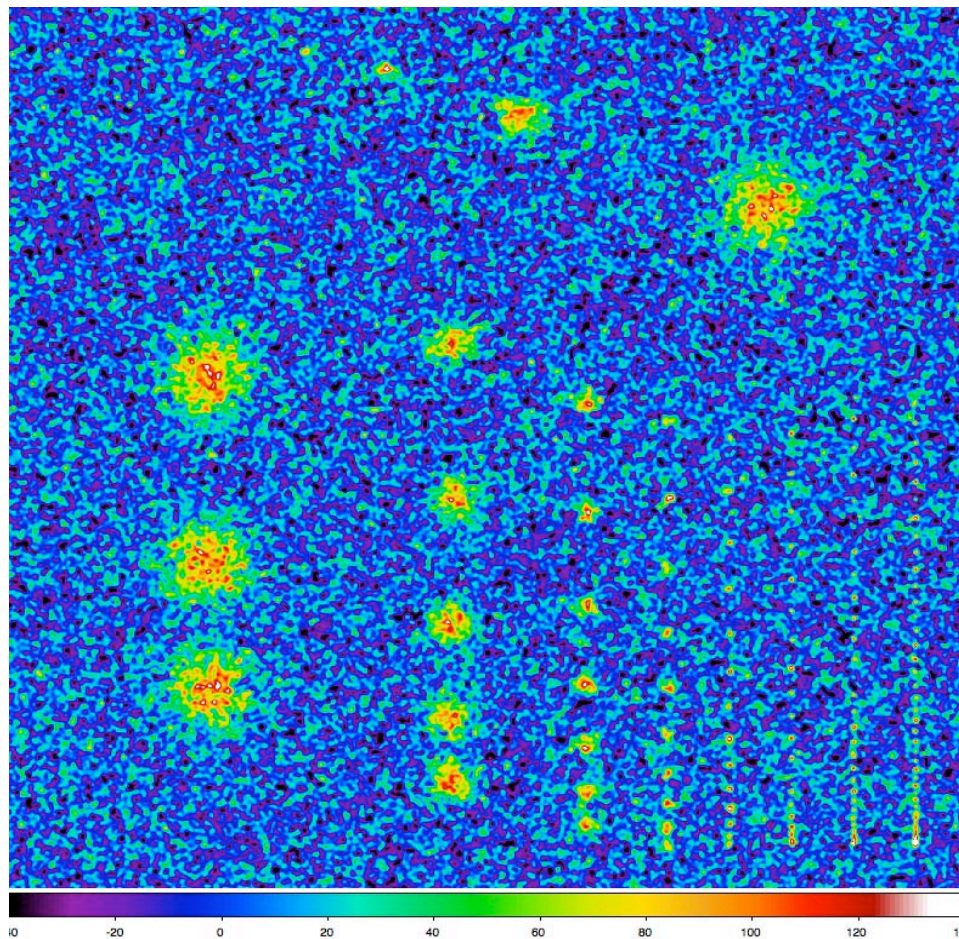
Extracting Sources

Multi-Scale, Multi-Wavelength Extraction

- New method and code *getsources* developed and used at CEA Saclay
 - No *multi-wavelength* extraction techniques existed for our *Herschel* projects
 - Must use higher resolution or sensitivity information across wavelengths
- Extensively verified at each step of its development
 - Multiple test images, simulated star-forming regions for *Herschel*
 - Star-forming regions NGC 2264, NGC 2068, W 43, Cyg X
- Benchmarked for the Gould Belt consortium, along with several other algorithms using simulated skies of various degree of complexity
 - *gaussclumps* (Stutzki & Guesten 1990)
 - *clumpfind* (Williams et al. 1994)
 - *sExtractor* (Bertin & Arnouts 1996)
 - *mre-gcl* (Motte et al. 2007)
 - *derivatives* (Molinari et al. 2010)
 - *csar* (J. Kirk, private comm.)
 - *reinhold* (CUPID software)
 - *fellwalker* (CUPID software)

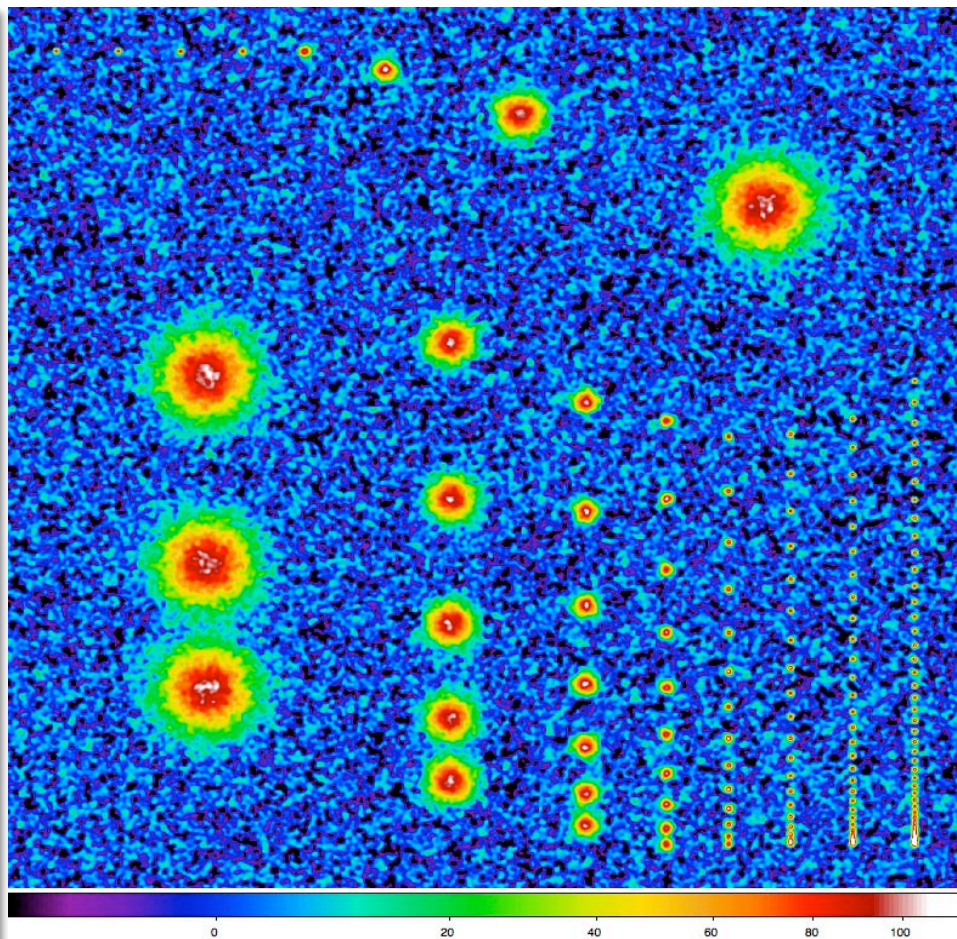
Benchmark 1: Simple Images

139 objects at 250 μm : effects of S/N, sizes, and separation



S/N = 5

1.0°

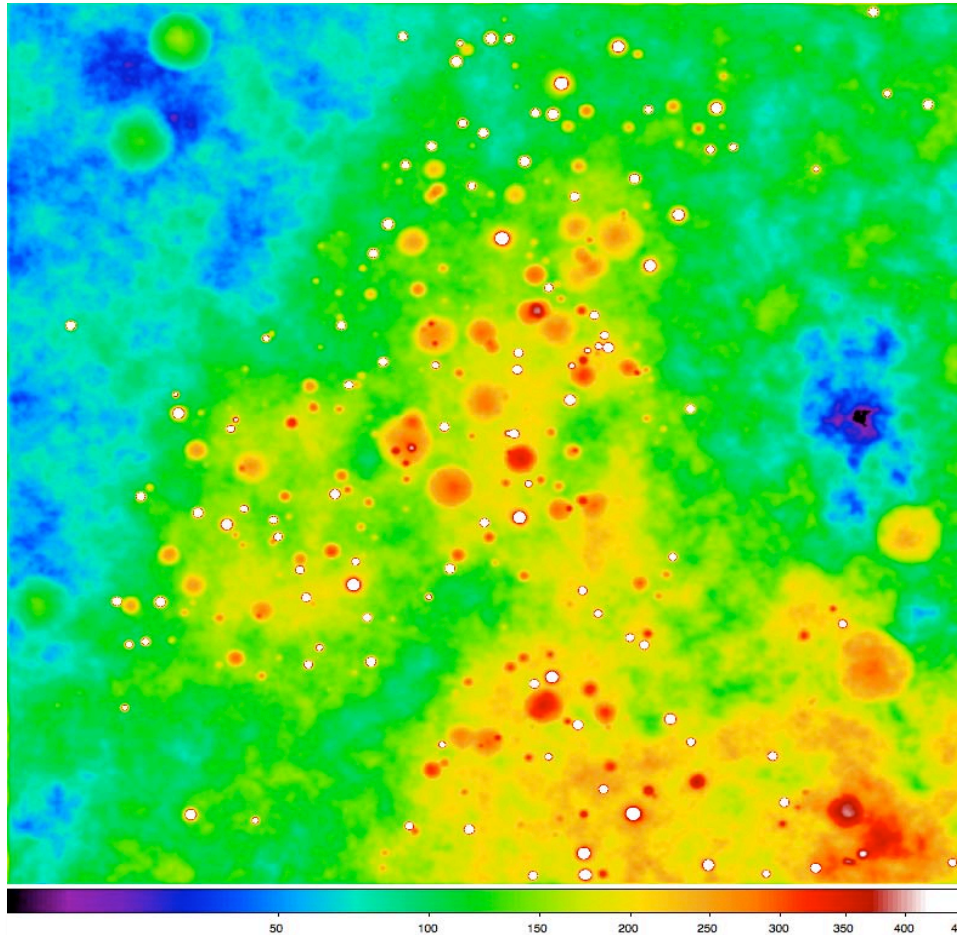


1.0°

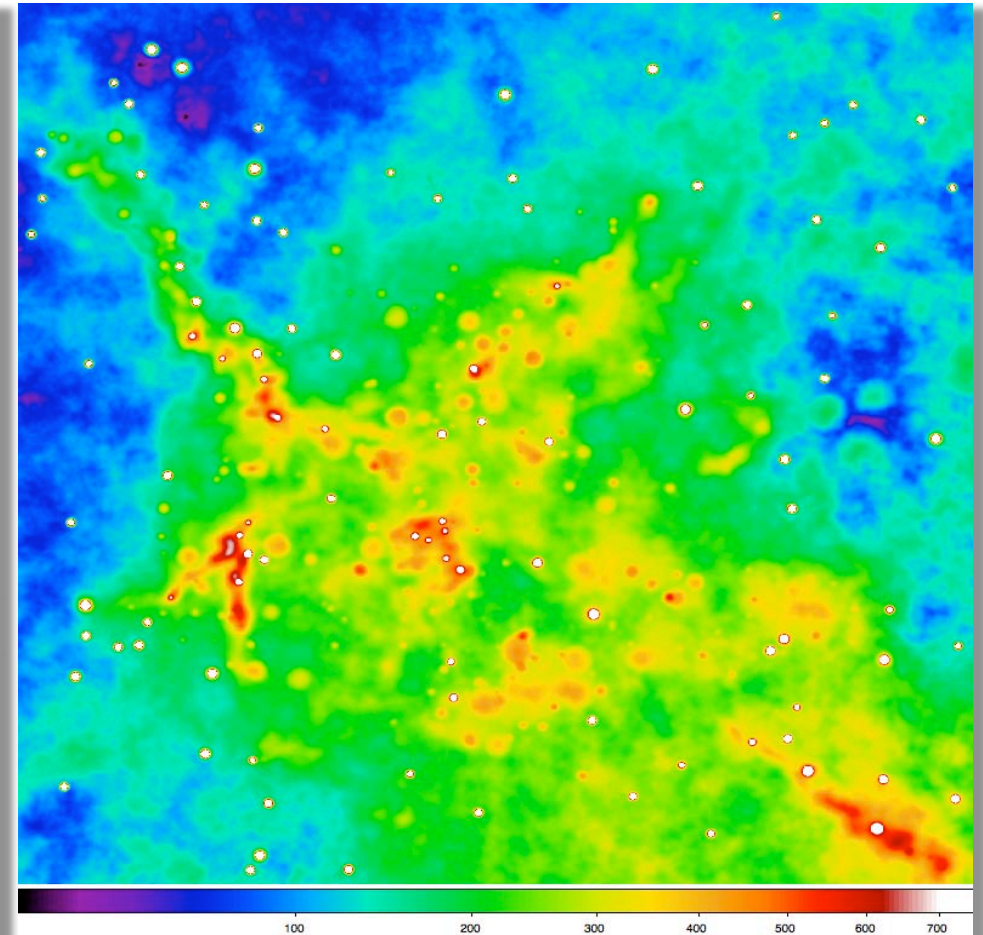
S/N = 20

Benchmarks 2 and 3: All *Herschel* Bands

350 cores and 100 protostars, shown at 350 μm



1.0°

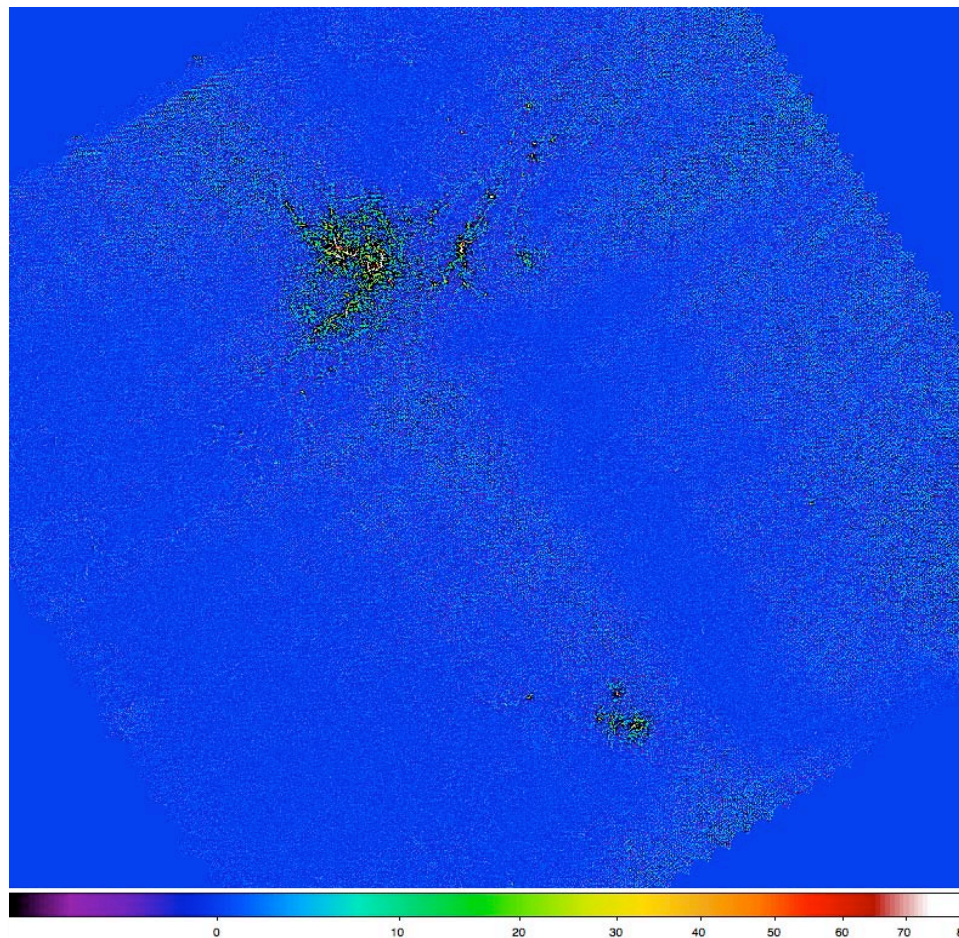


background: Bate, Bonnell, & Bromm (2003)

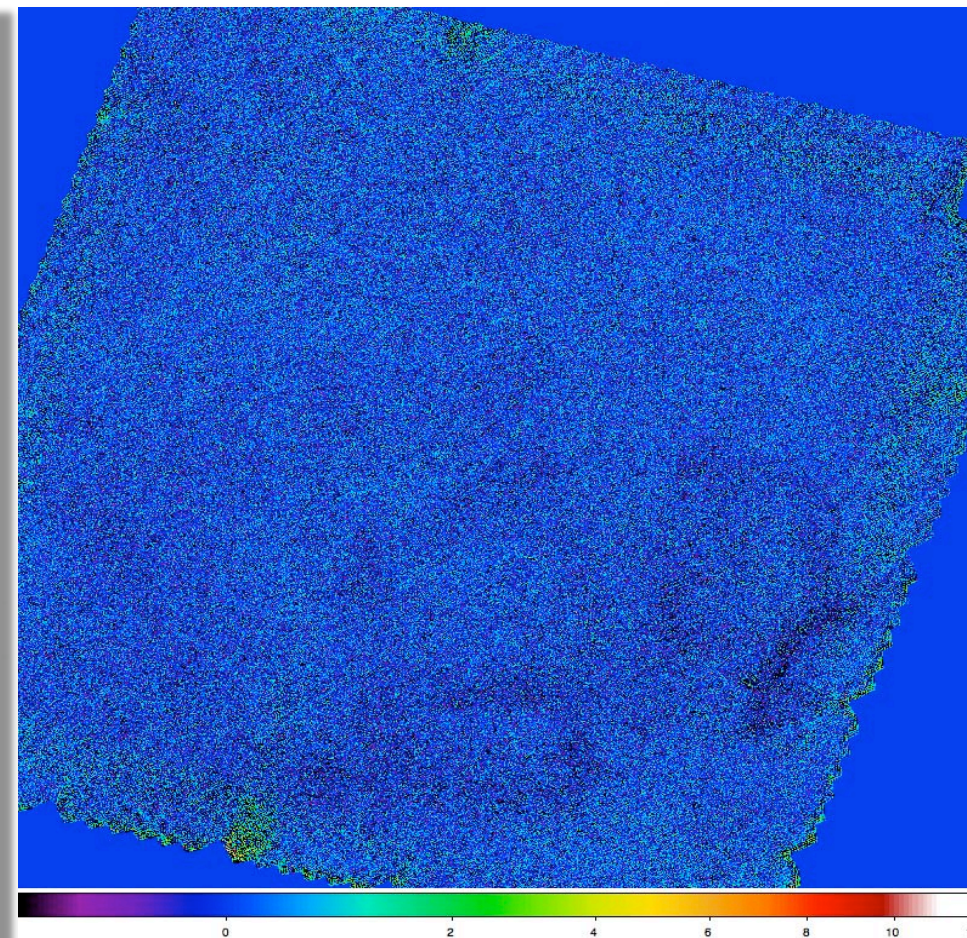
Outline of the *getsources* Algorithm

- Cleaning: original observed images at each wavelength λ
 - Create a set of filtered “*single scales*” separated by a factor of ~ 1.05
 - successive unsharp masking*: $I_j(\lambda) = G_{j-1} * I(\lambda) - G_j * I(\lambda)$, $j=1, 2, \dots, N$
 - Clean each of those scales of noise/background by iterating to $5\sigma_\lambda$ cut-offs
 - Re-normalize clean scales, sum up over all λ into *combined* detection images
- Detection: combined single-scale detection images, independent of λ
 - Track objects’ appearance, “evolution”, and disappearance: small to large scales
 - Find objects’ positions, S/N, characteristic scales, and footprints
- Measurements: original observed images at each λ
 - Subtract background under the footprints and deblend overlapping objects
 - Measure their fluxes, sizes, and intensity profiles at each wavelength

Aquila and Polaris: SPIRE at 250 μm single scale $\sim 10''$

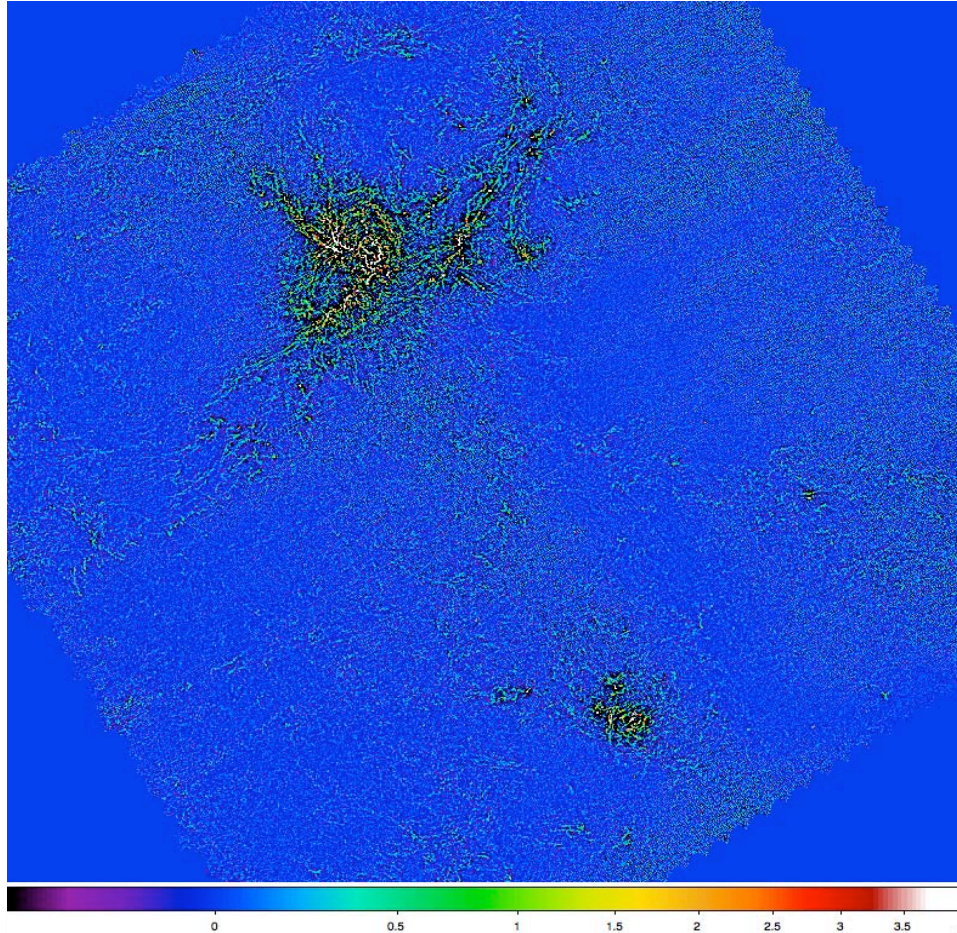


3.3°

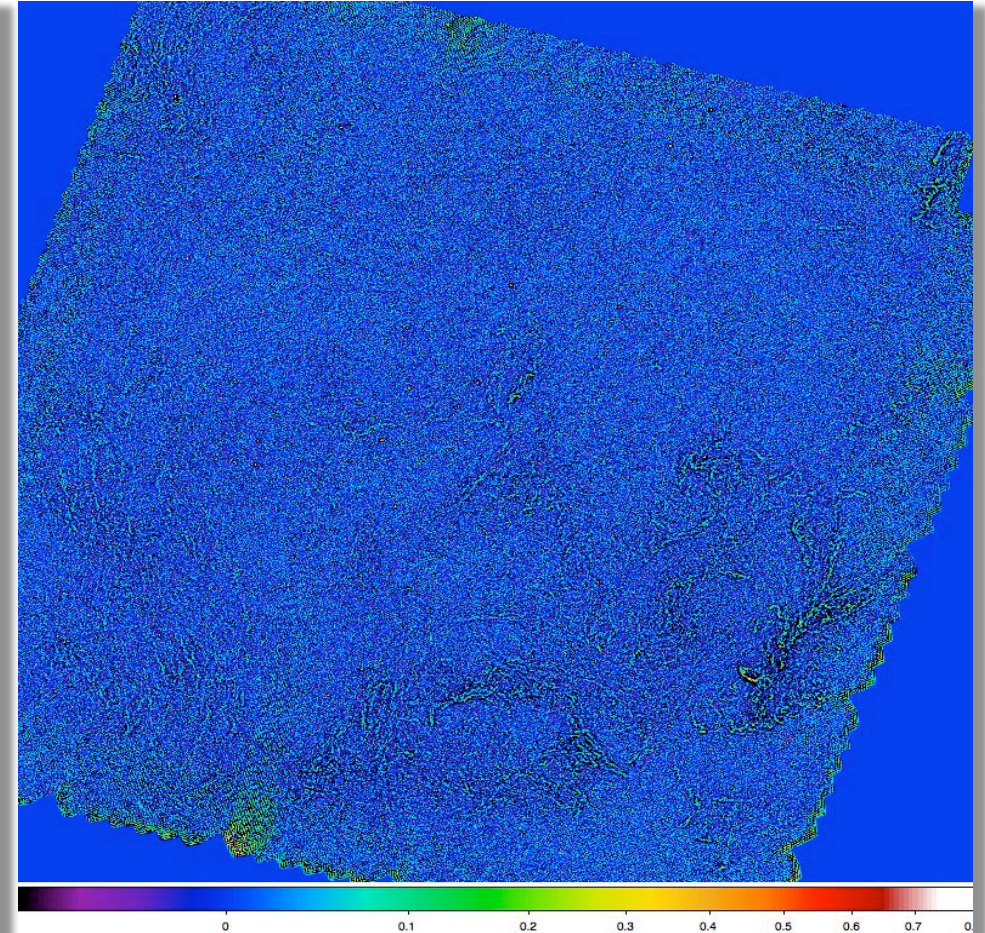


3.3°

Aquila and Polaris: SPIRE at 250 μm single scale $\sim 20''$

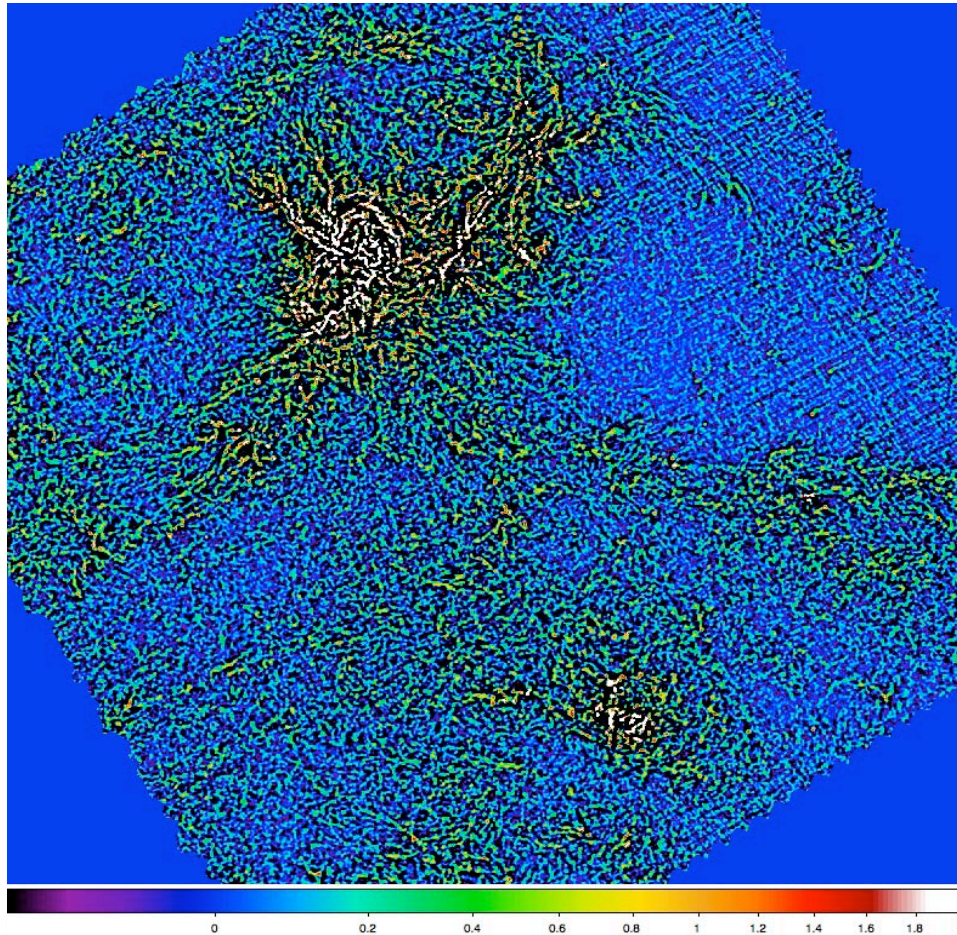


3.3°

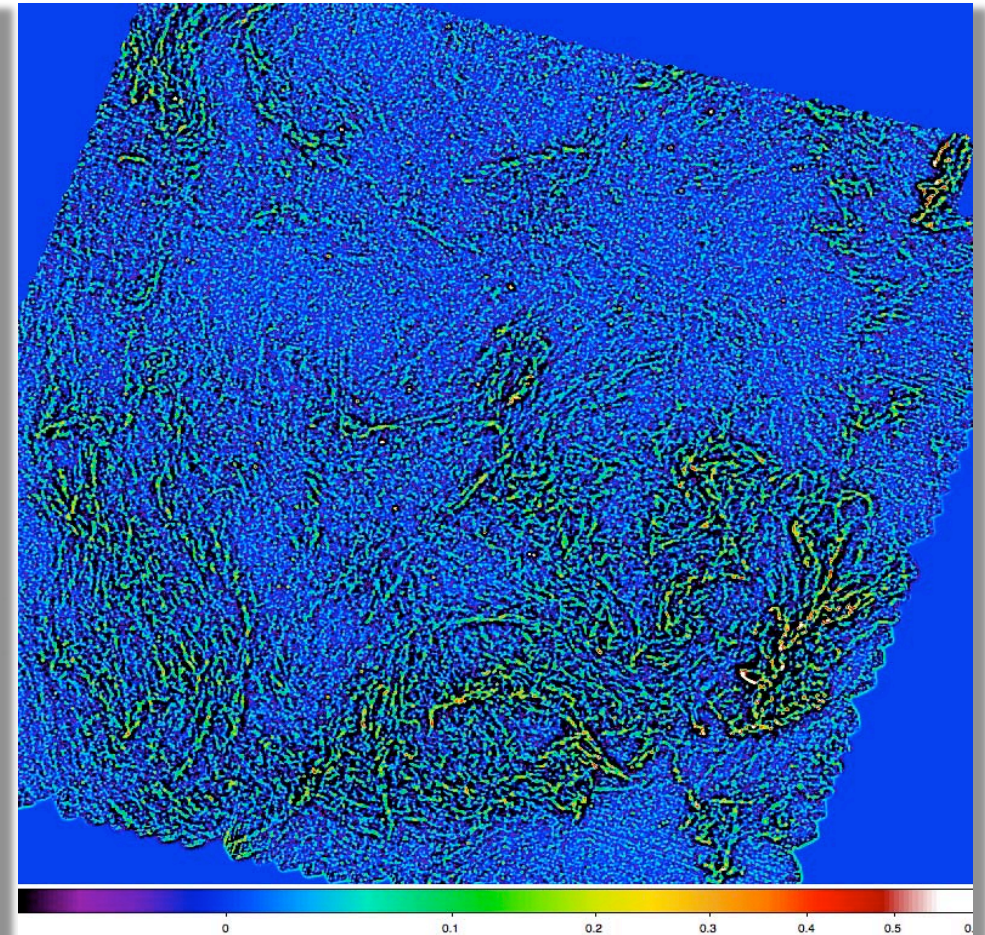


3.3°

Aquila and Polaris: SPIRE at 250 μm single scale $\sim 40''$

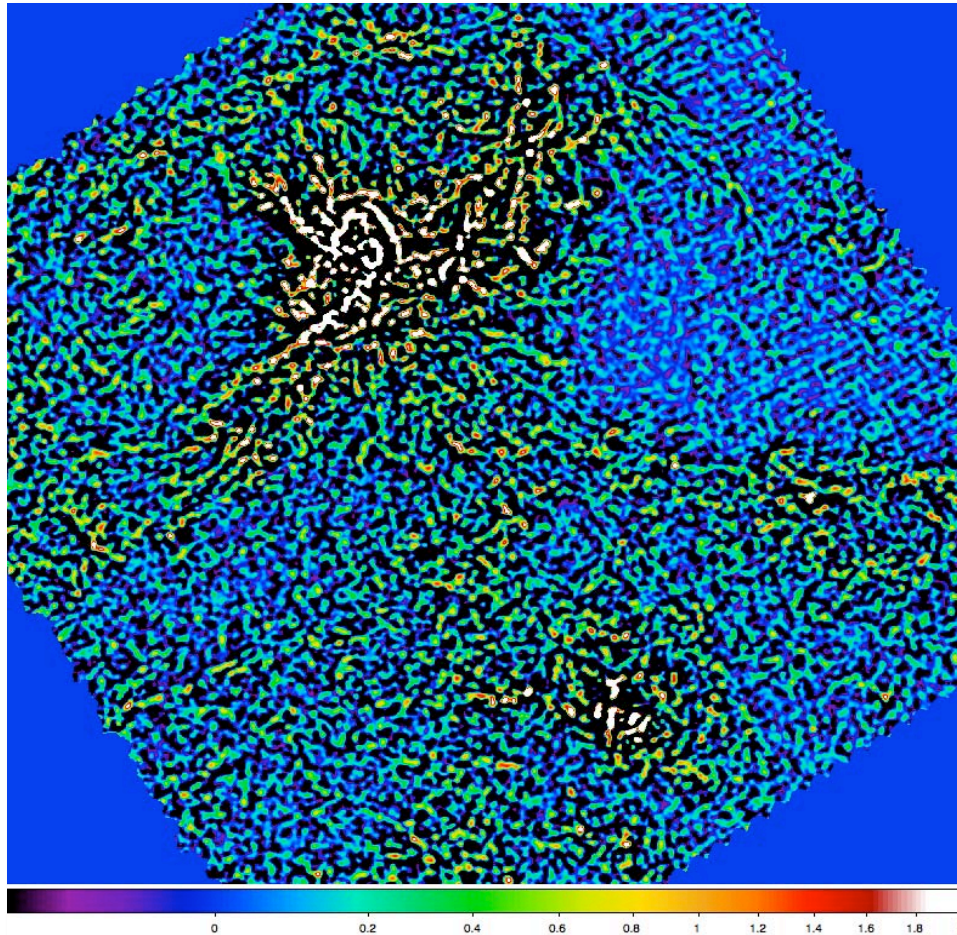


3.3°

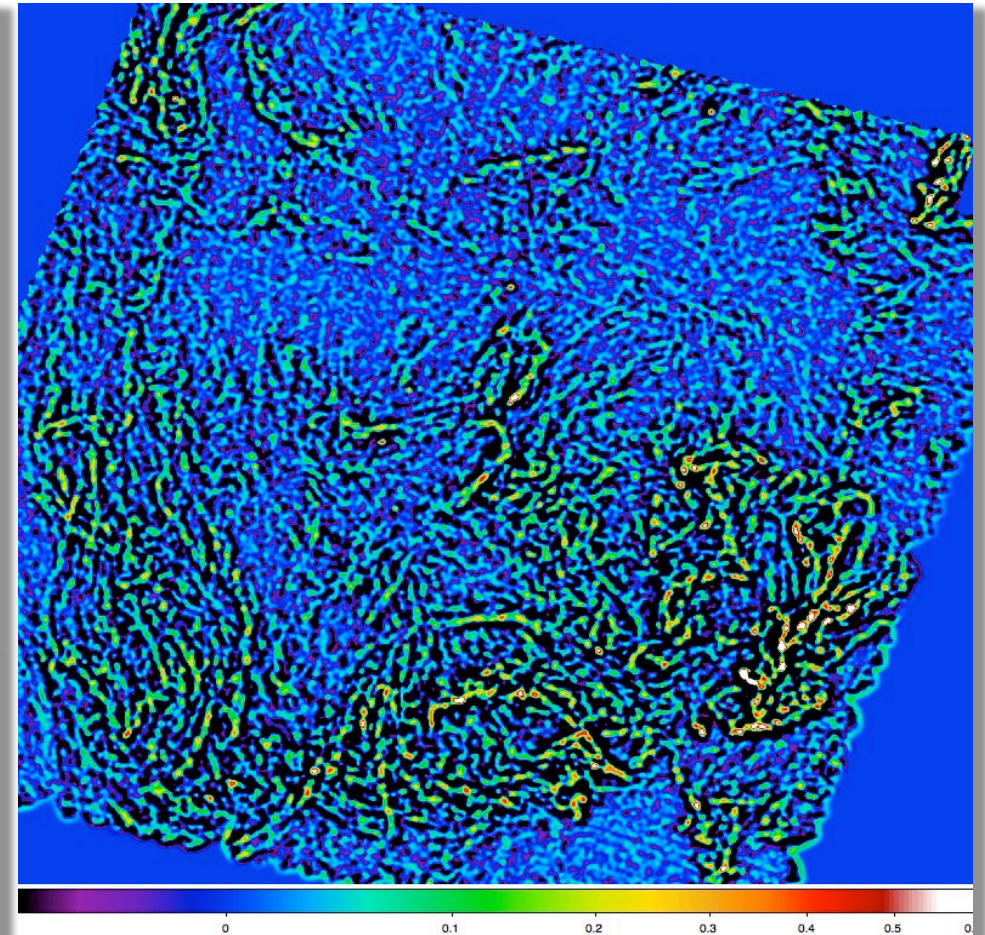


3.3°

Aquila and Polaris: SPIRE at 250 μm single scale $\sim 80''$

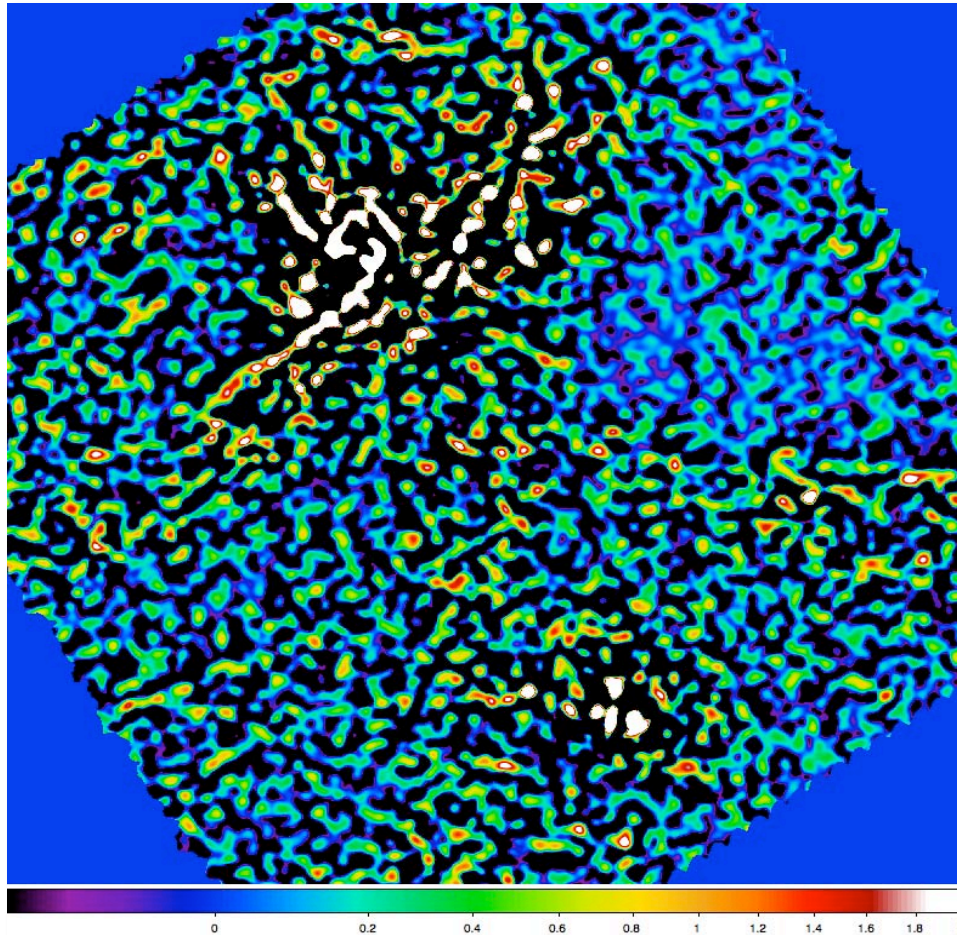


3.3°

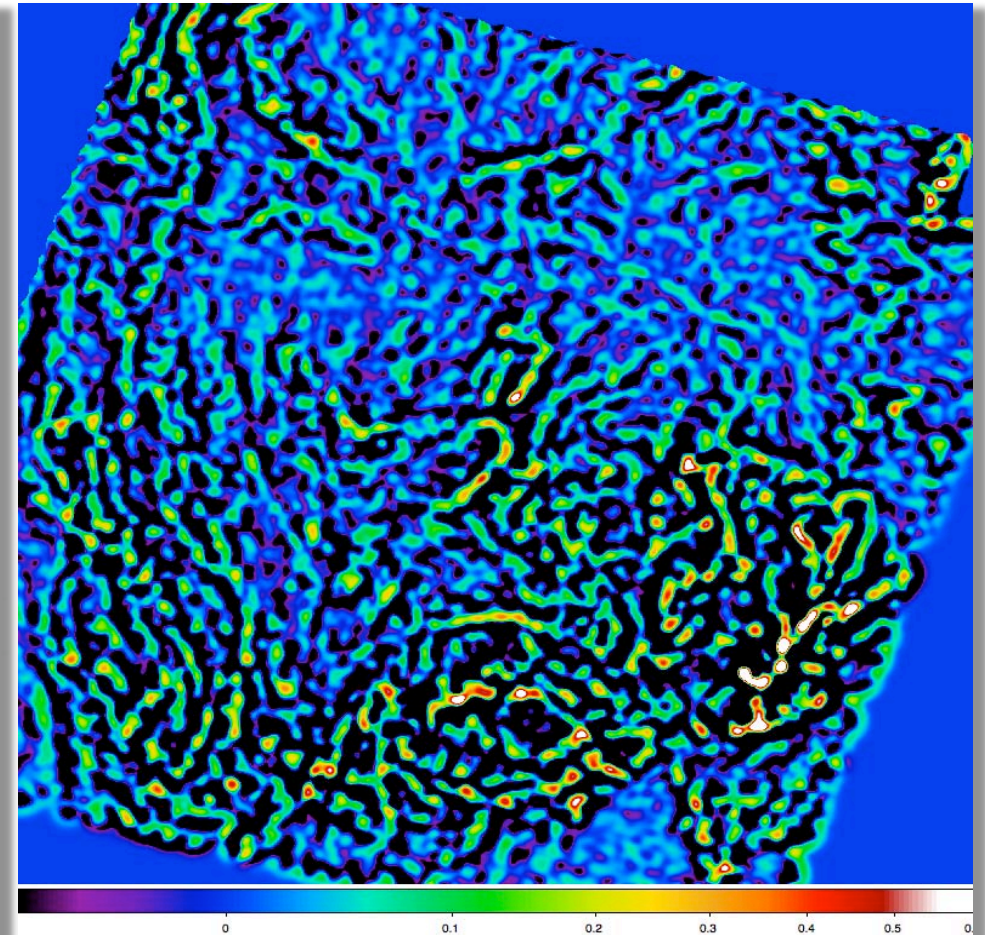


3.3°

Aquila and Polaris: SPIRE at 250 μm single scale $\sim 160''$

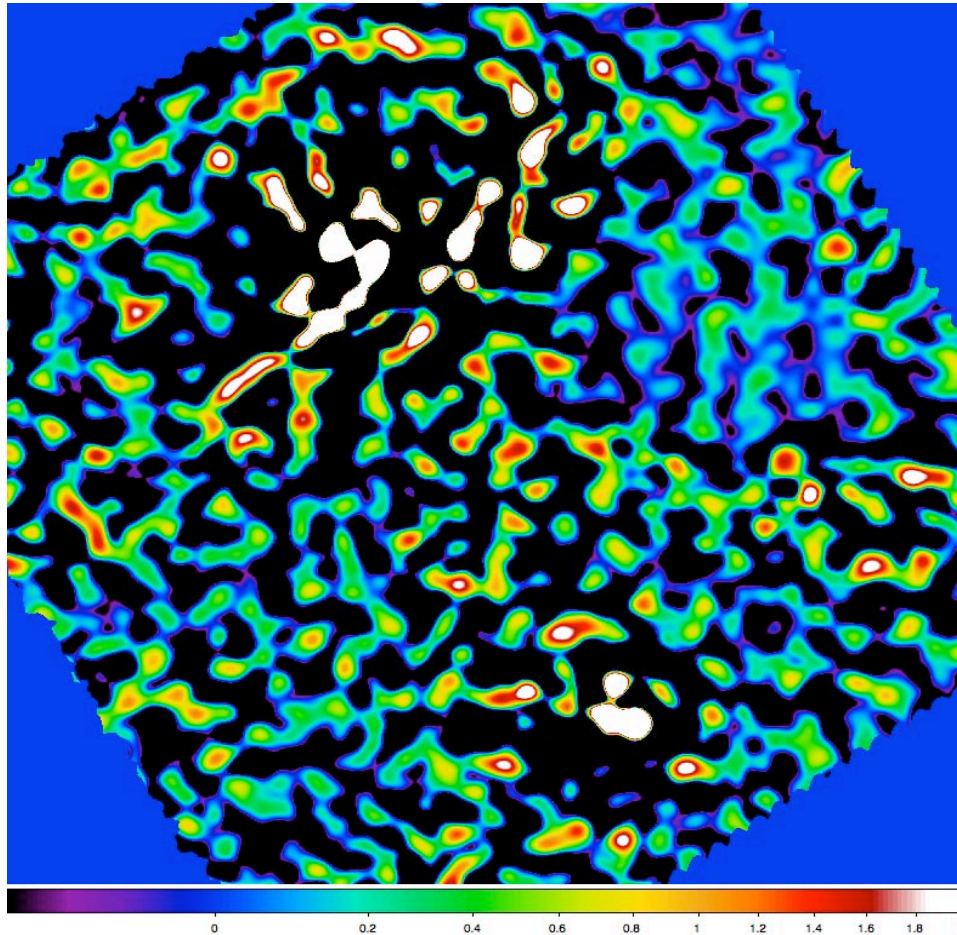


3.3°

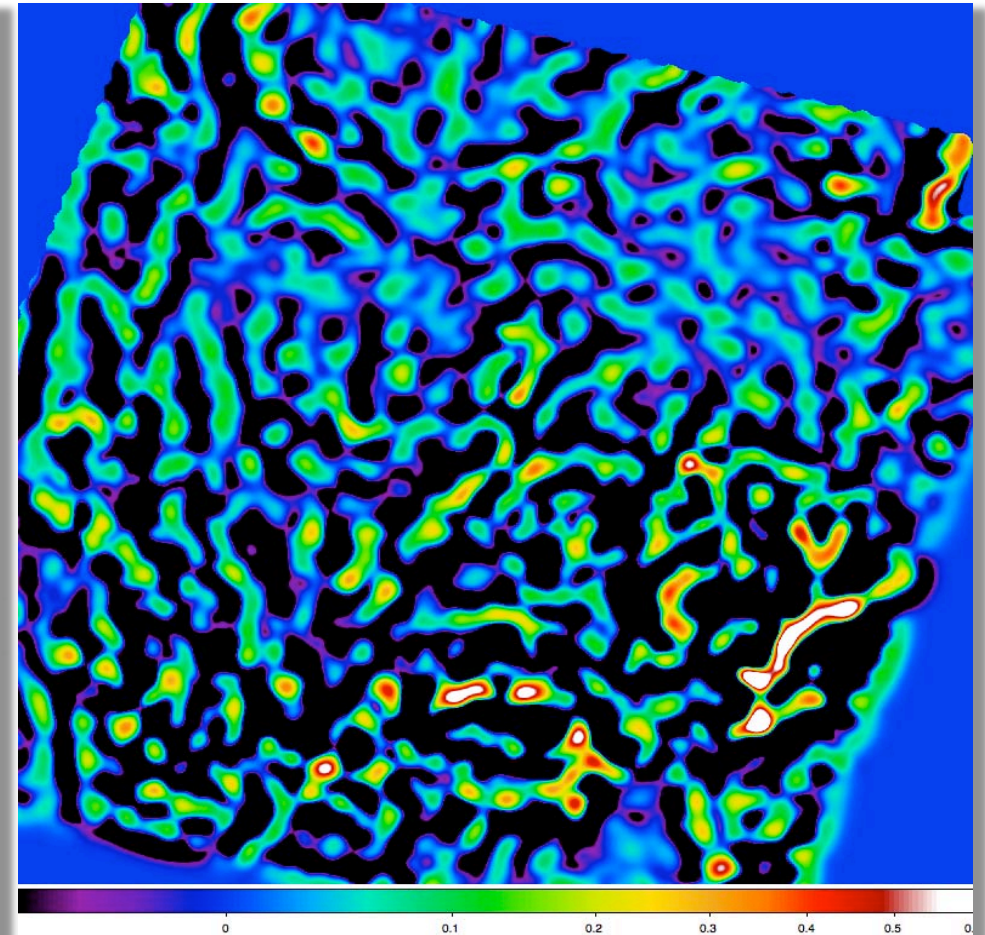


3.3°

Aquila and Polaris: SPIRE at 250 μm single scale $\sim 320''$

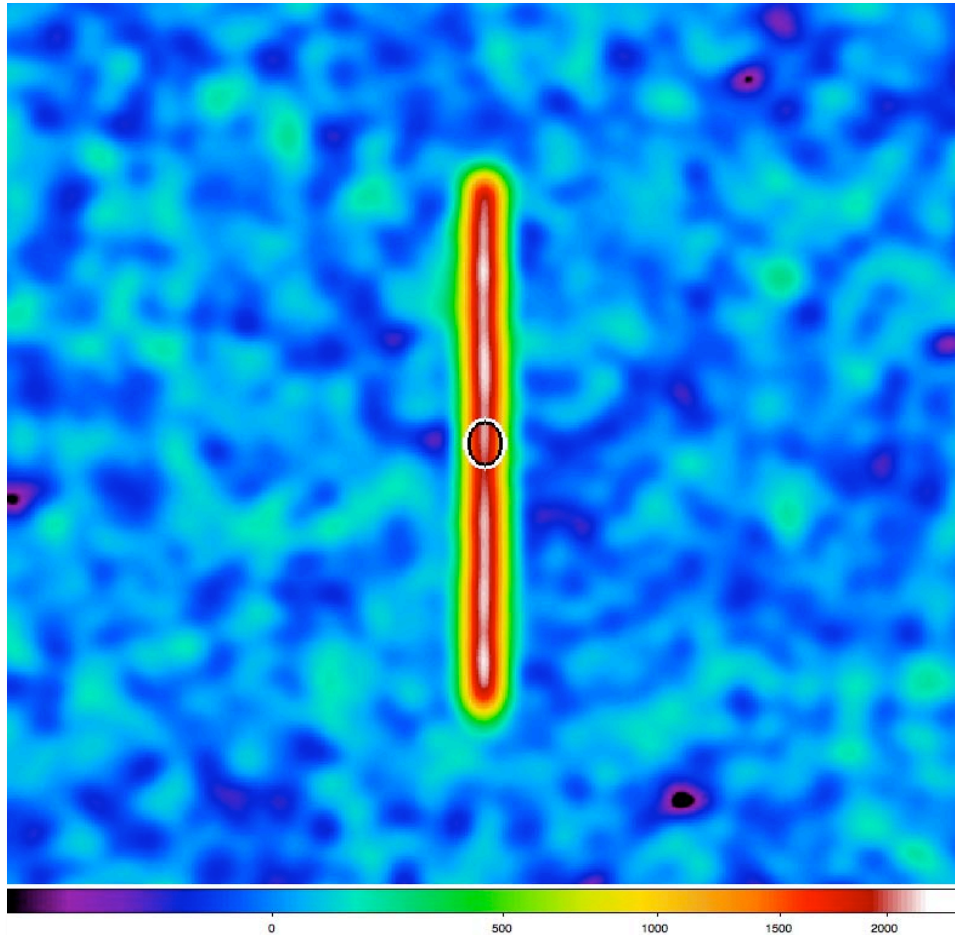


3.3°

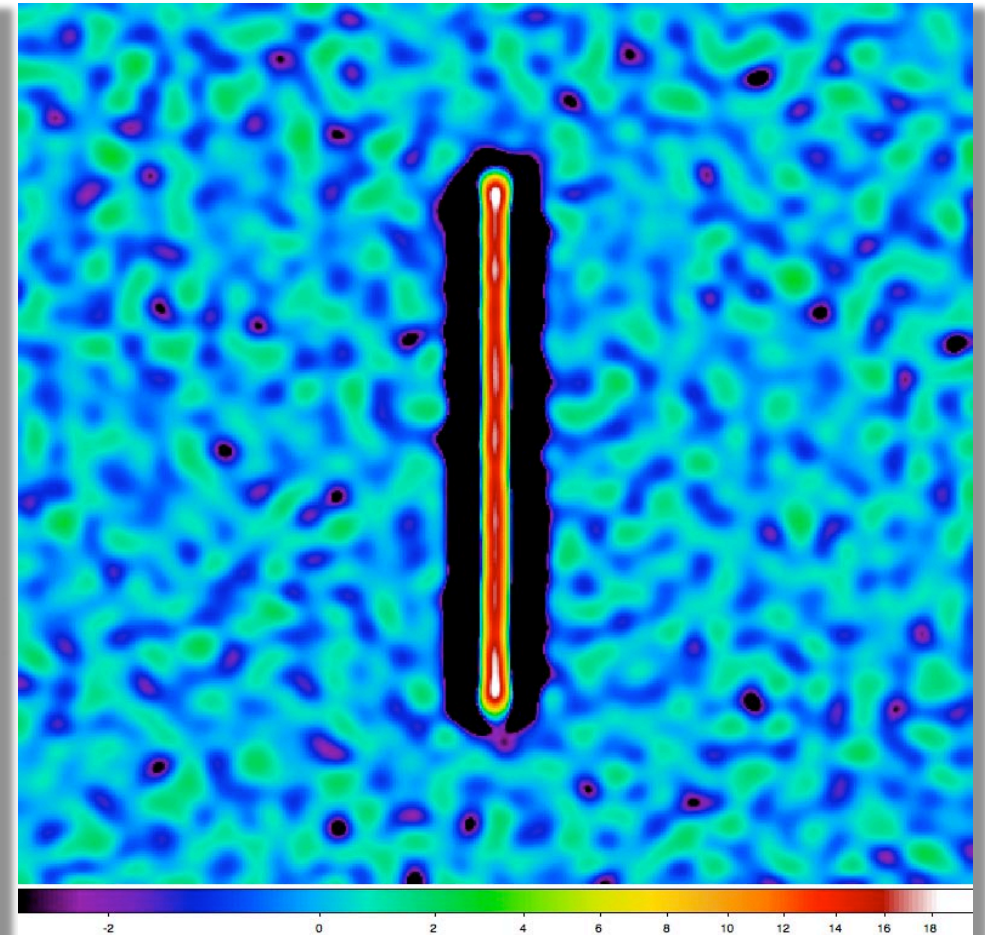


3.3°

Example of Test “Filaments”: Cylinder *getsources* does *not* break uniform filaments



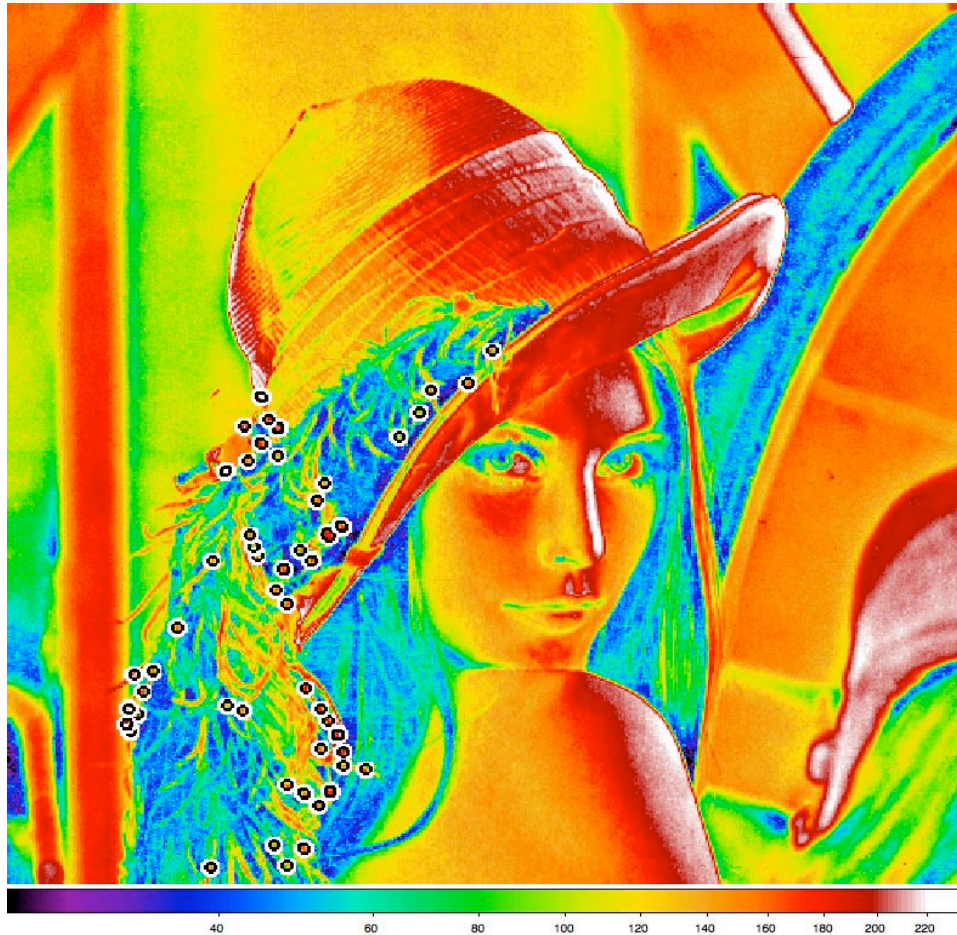
full image



single scale

Example of Test “Filaments”: Lena

getsources finds significant peaks that *are present*



full image



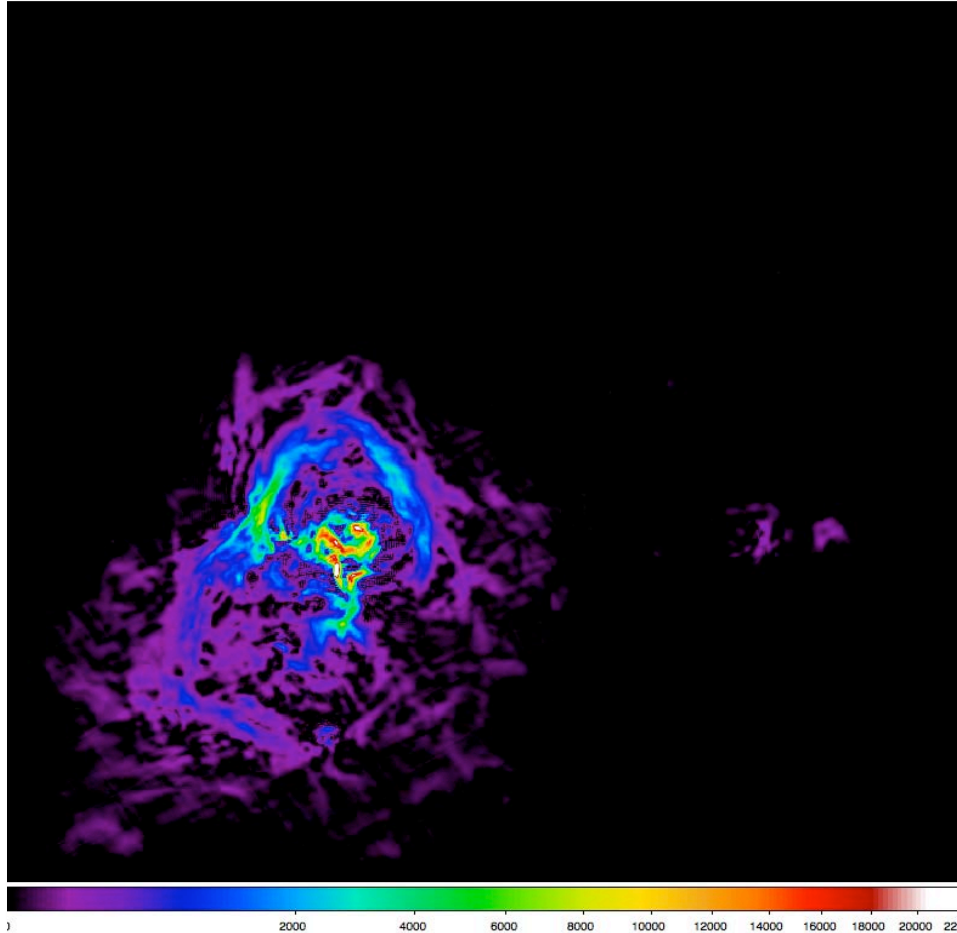
single scale

Extracting Filaments

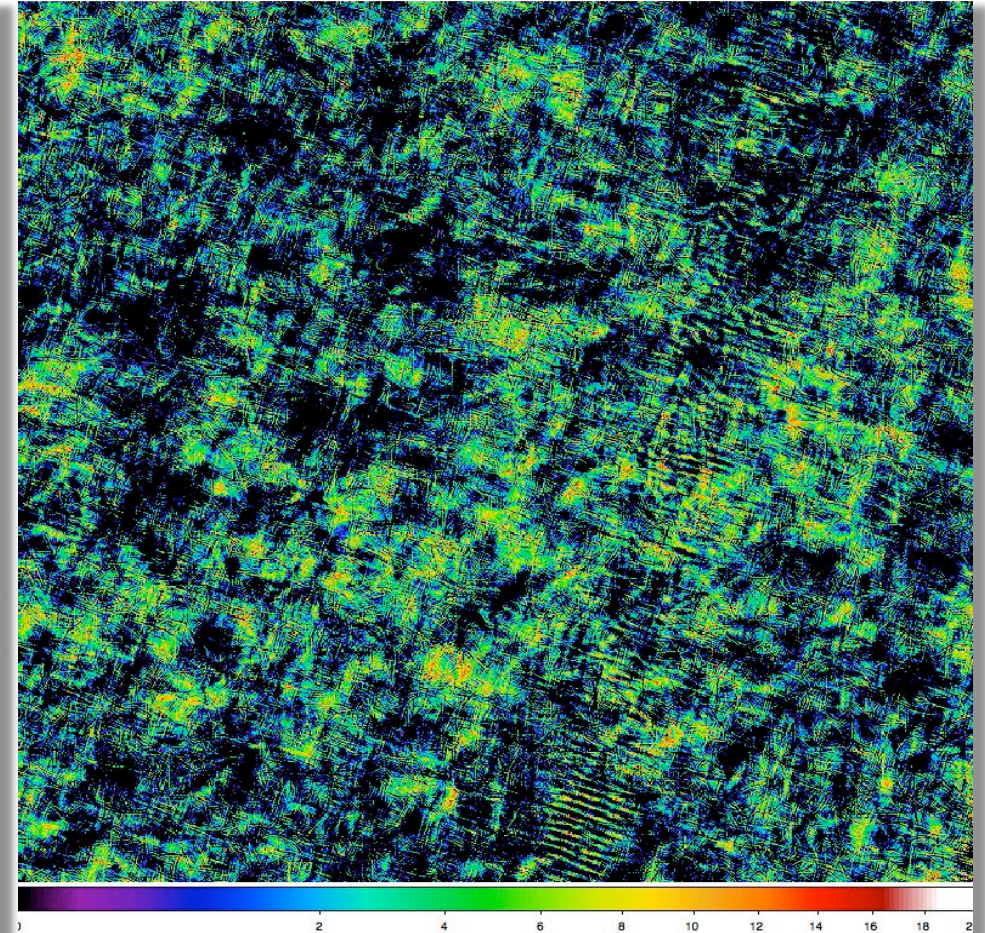
Morphological Component Analysis

- The MCA method and code *cb_mca* developed by J.-L. Starck et al. (2004)
 - Decompose a signal into its morphological building blocks represented by the isotropic wavelets, ridgelets, or curvelets
- Applied the method to analyze large, complex *Herschel* images
 - Separate filamentary structures from the more isotropic structures
 - Decompose images alternating between the curvelet and wavelet transforms
 - Iterate until convergence in both wavelet and curvelet representations

Aquila and Polaris Sub-Fields 1: PACS 70 μm curvelet components by *cb_mca*

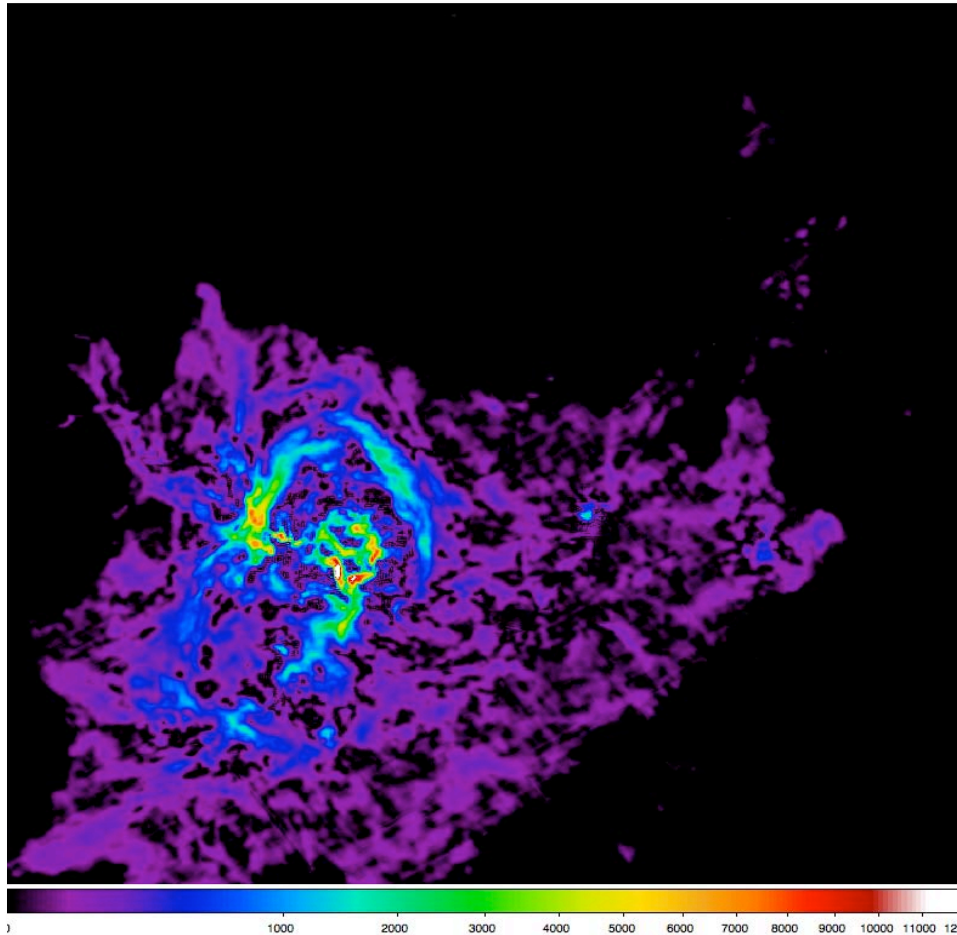


1.2°

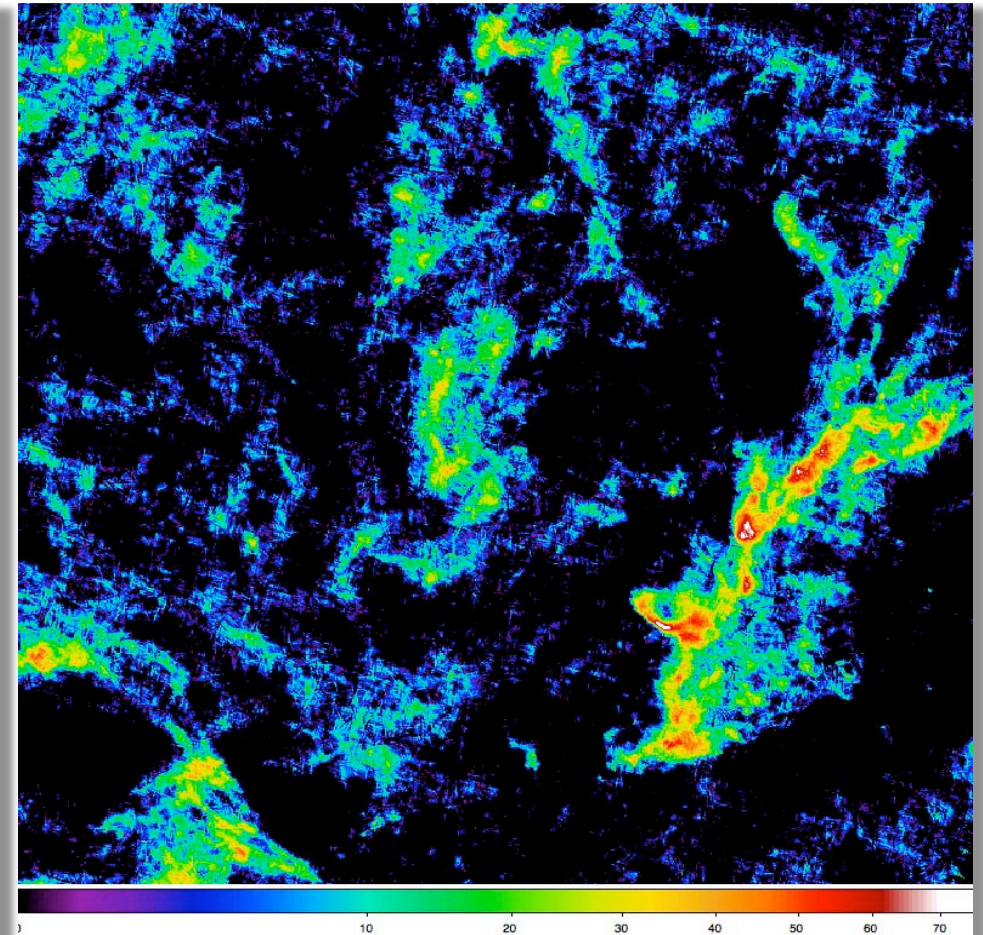


1.2°

Aquila and Polaris Sub-Fields 1: PACS 160 μm curvelet components by *cb_mca*

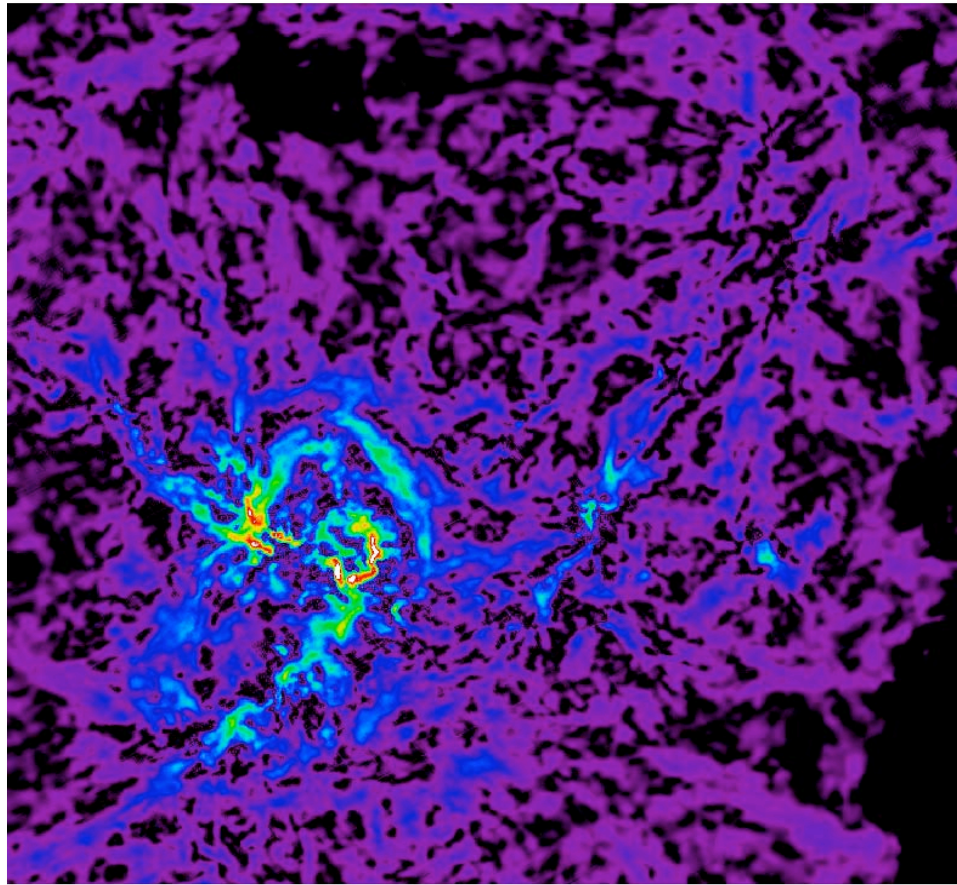


1.2°

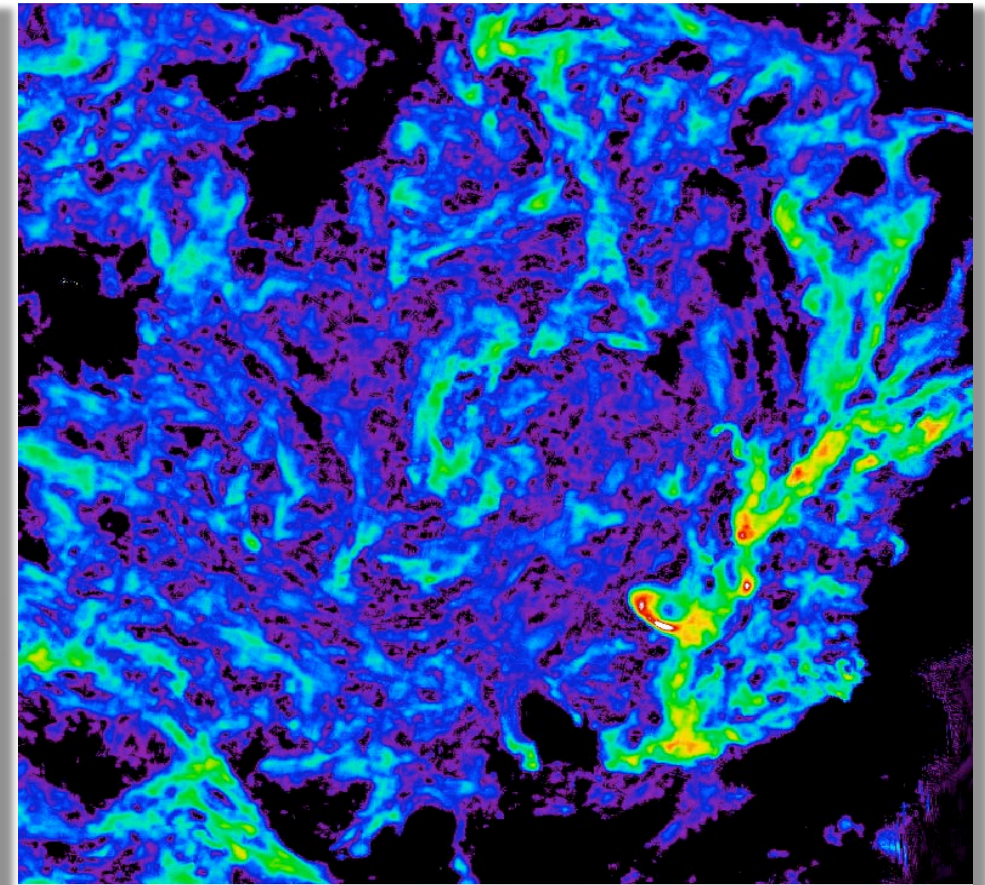


1.2°

Aquila and Polaris Sub-Fields 1: SPIRE 250 μm curvelet components by *cb_mca*

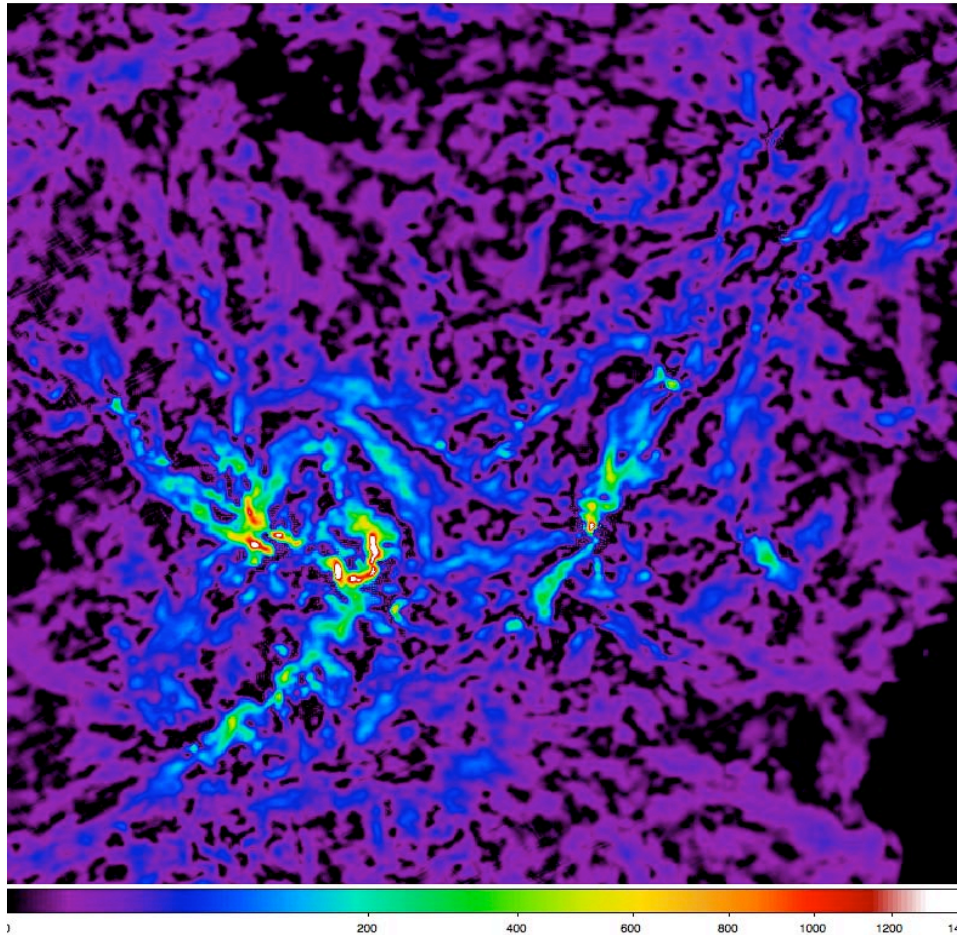


1.2°

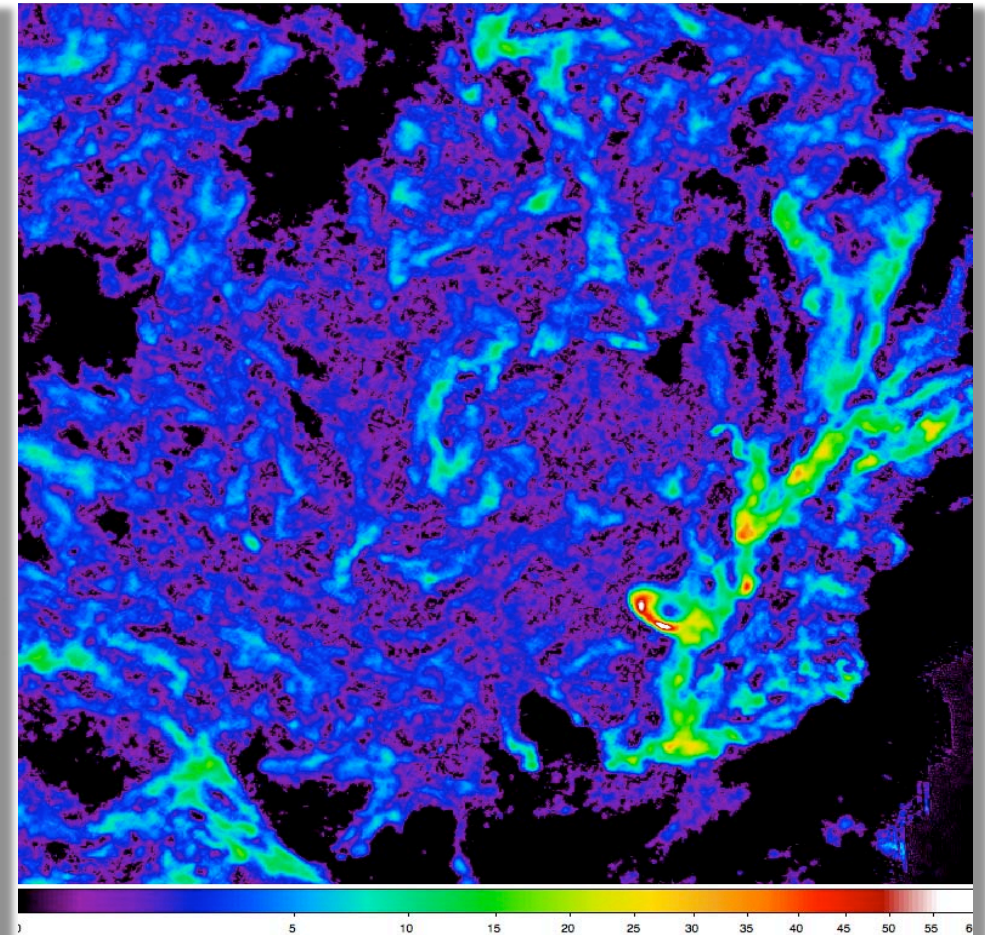


1.2°

Aquila and Polaris Sub-Fields 1: SPIRE 350 μm curvelet components by *cb_mca*

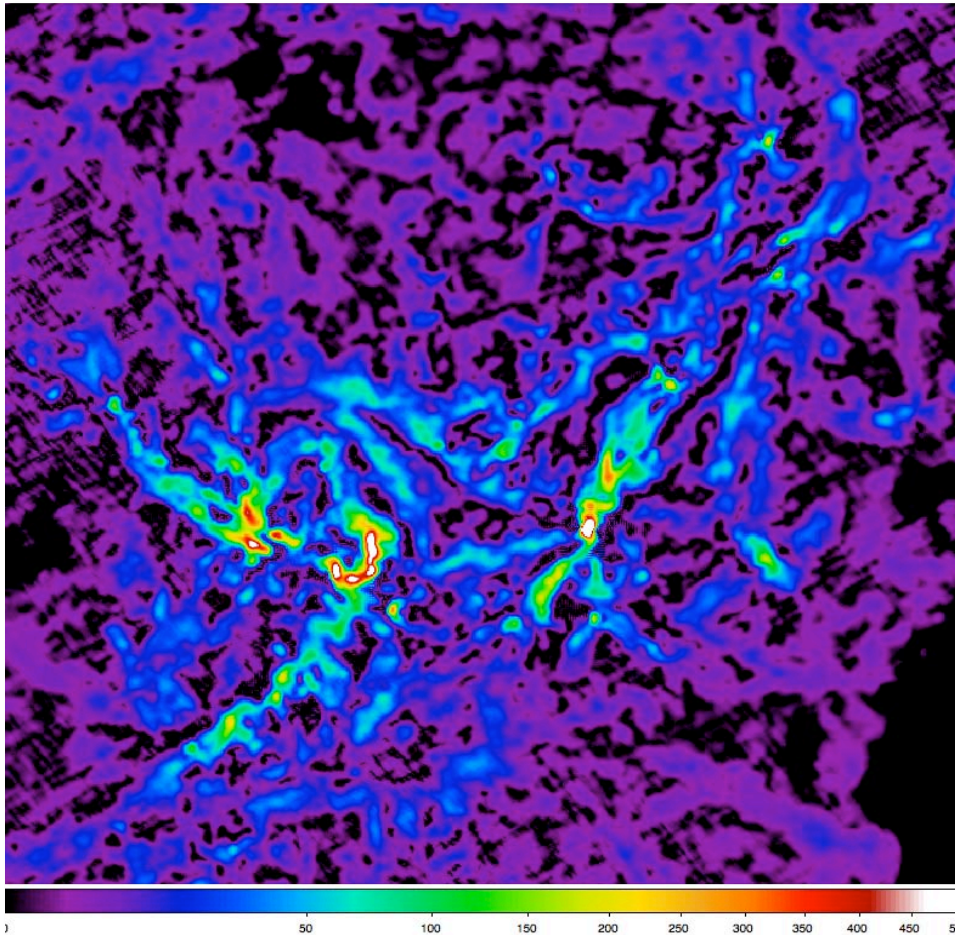


1.2°

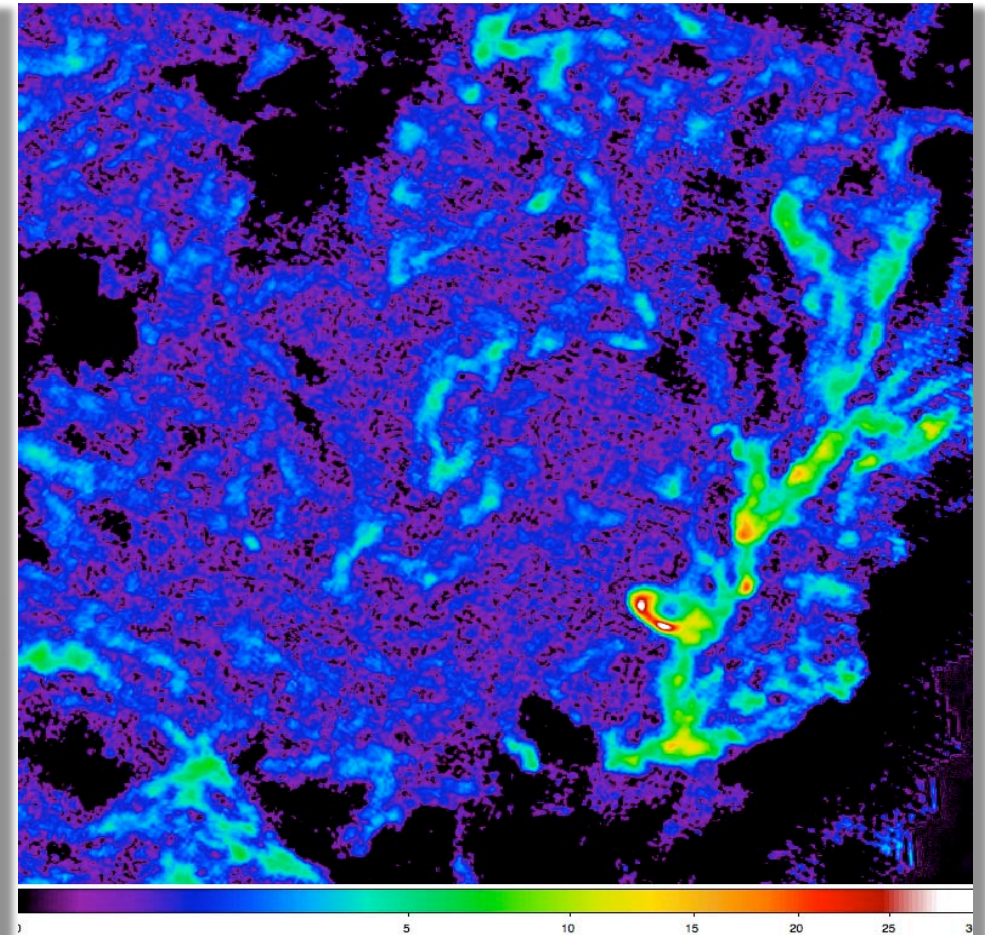


1.2°

Aquila and Polaris Sub-Fields 1: SPIRE 500 μm curvelet components by *cb_mca*



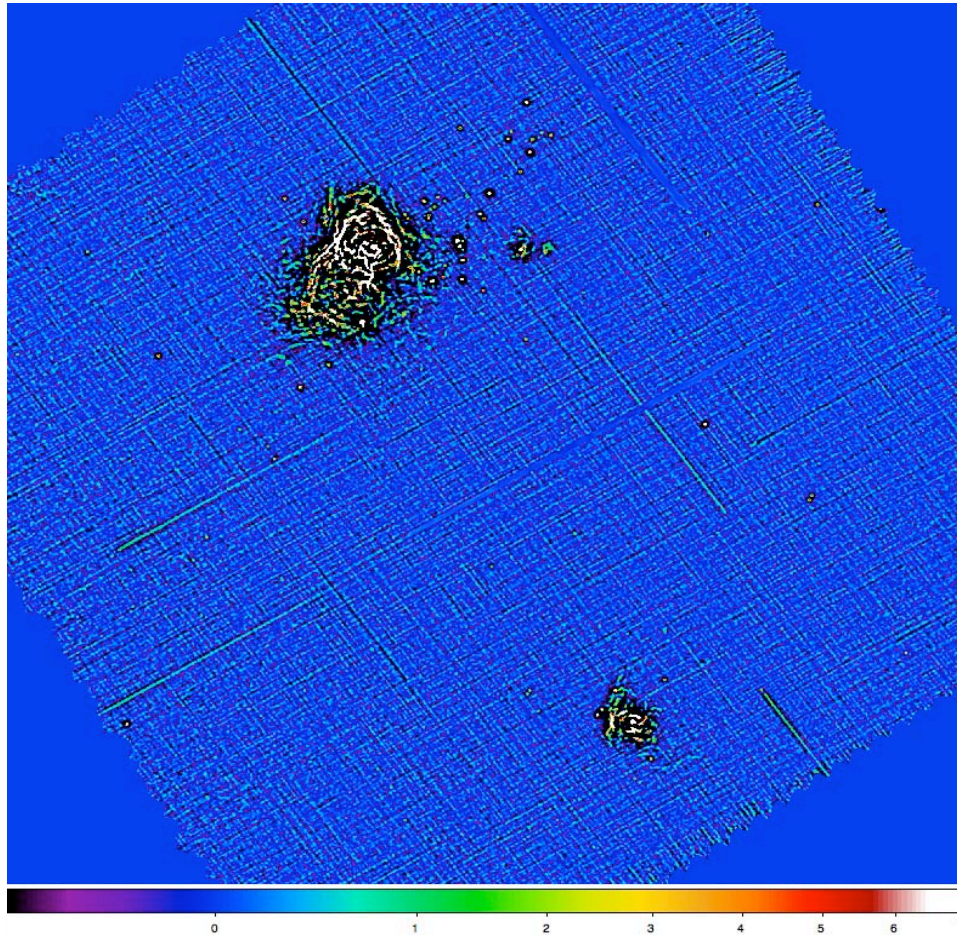
1.2°



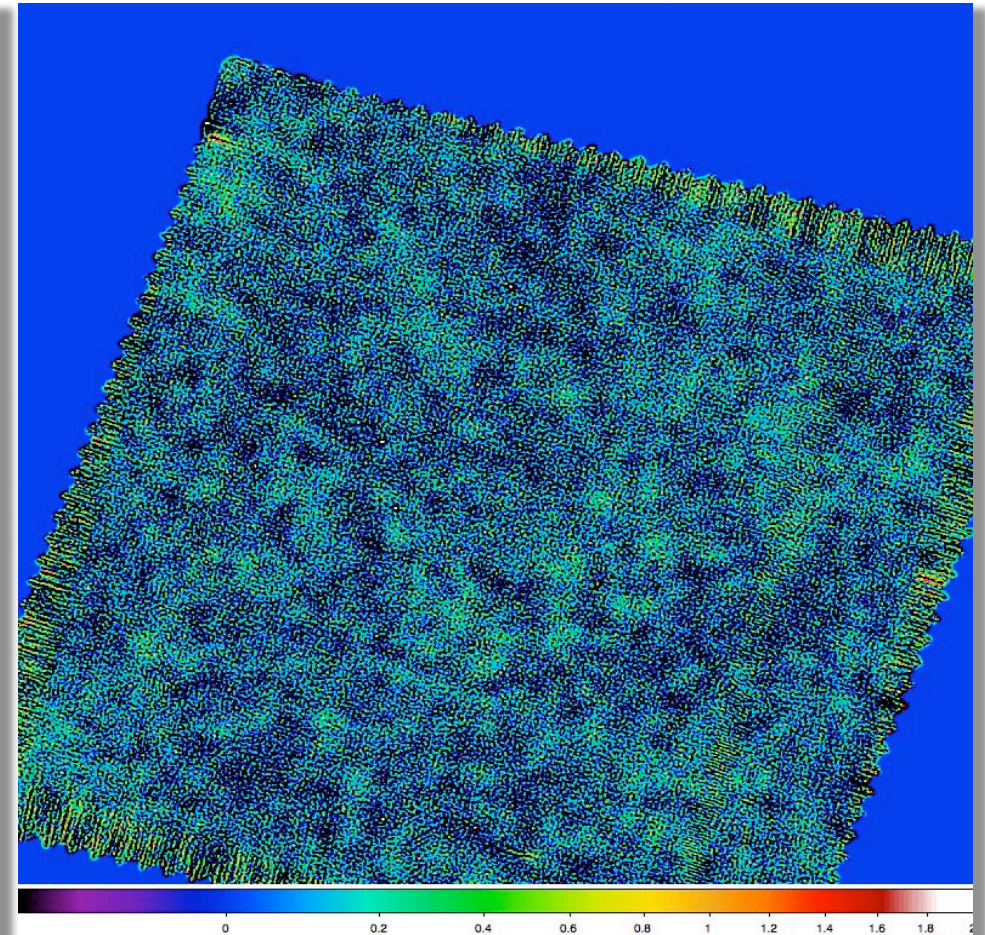
1.2°

Filamentary Structures at All *Herschel* Wavelengths

Aquila and Polaris: PACS 70 μm single scales $\sim 40''$ by *getsources*

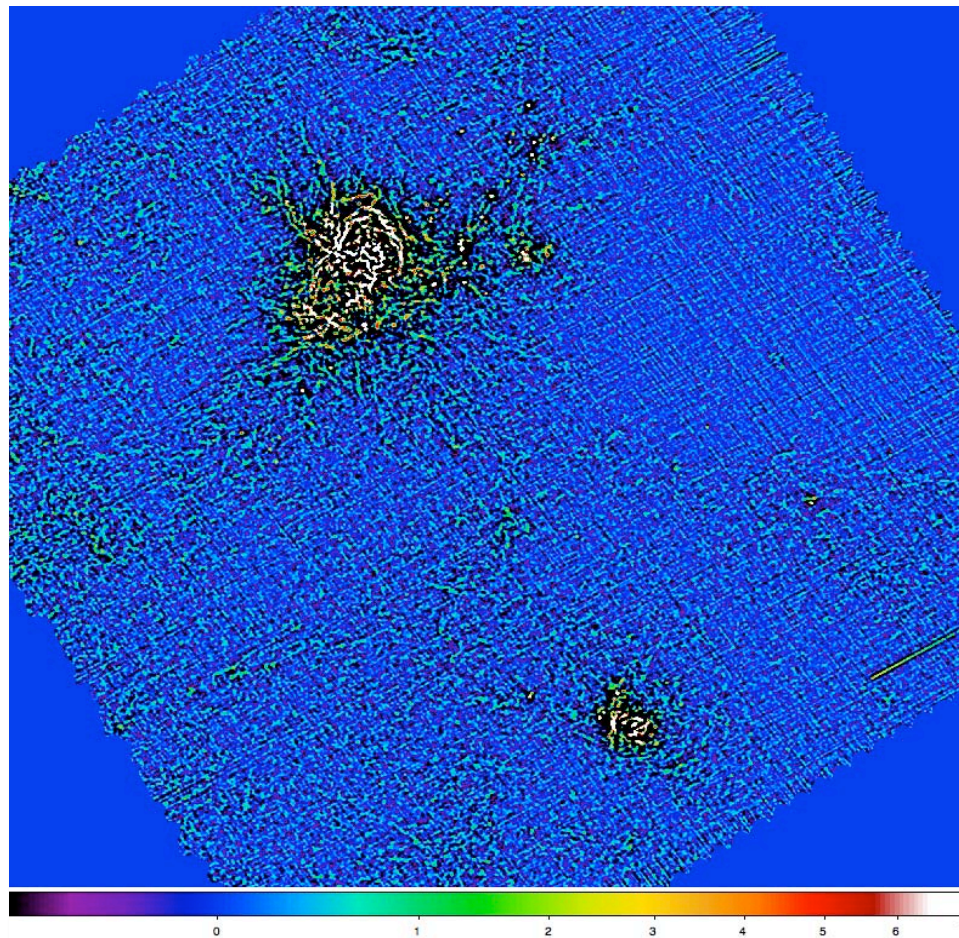


3.3°

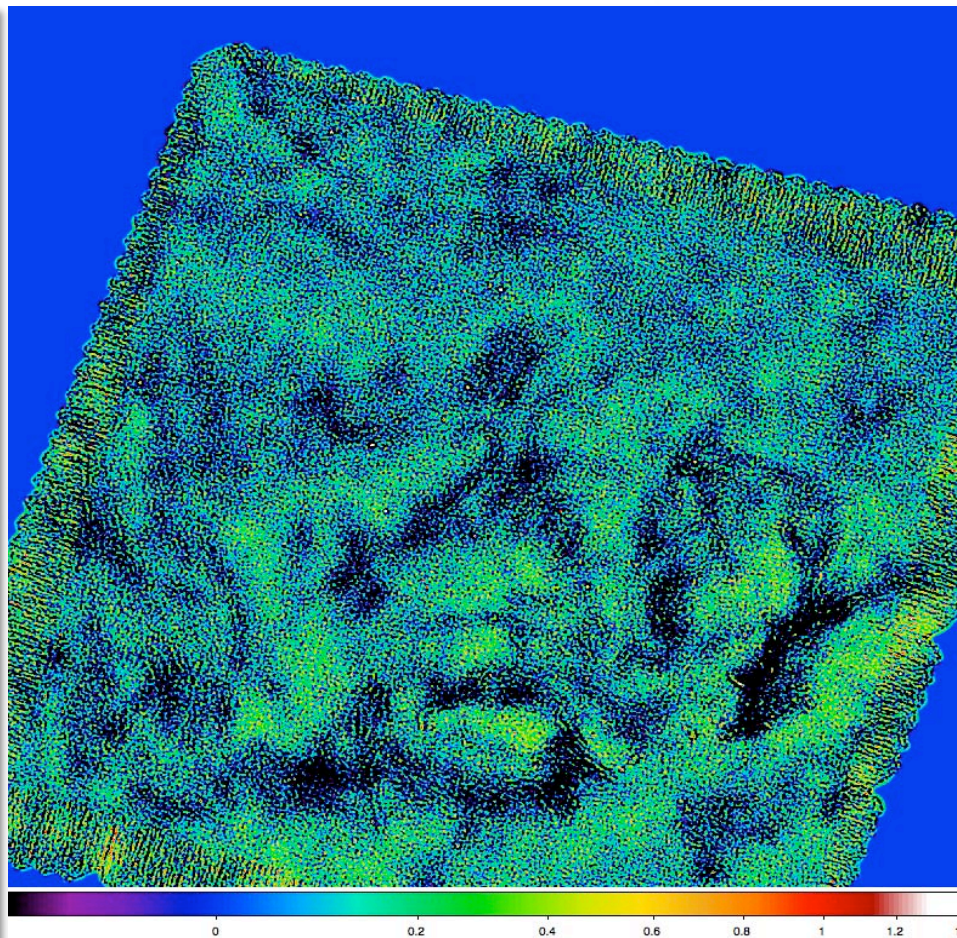


3.3°

Aquila and Polaris: PACS 160 μm single scales $\sim 40''$ by *getsources*

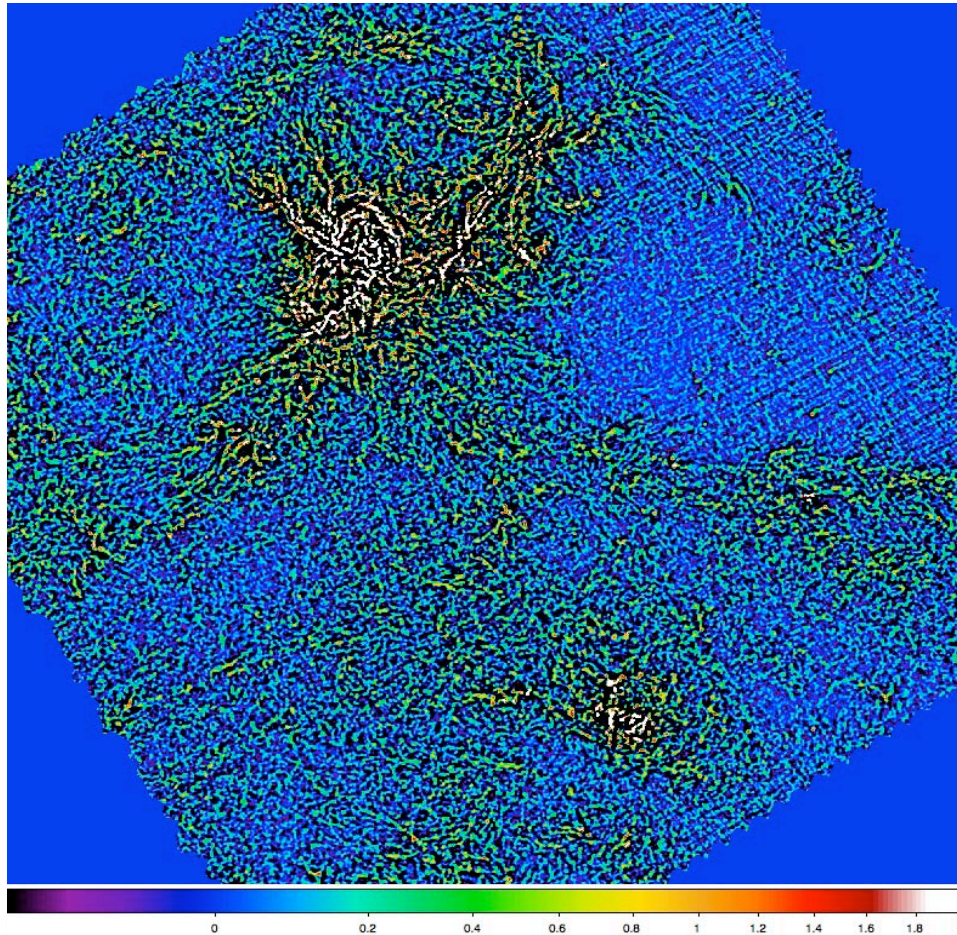


3.3°

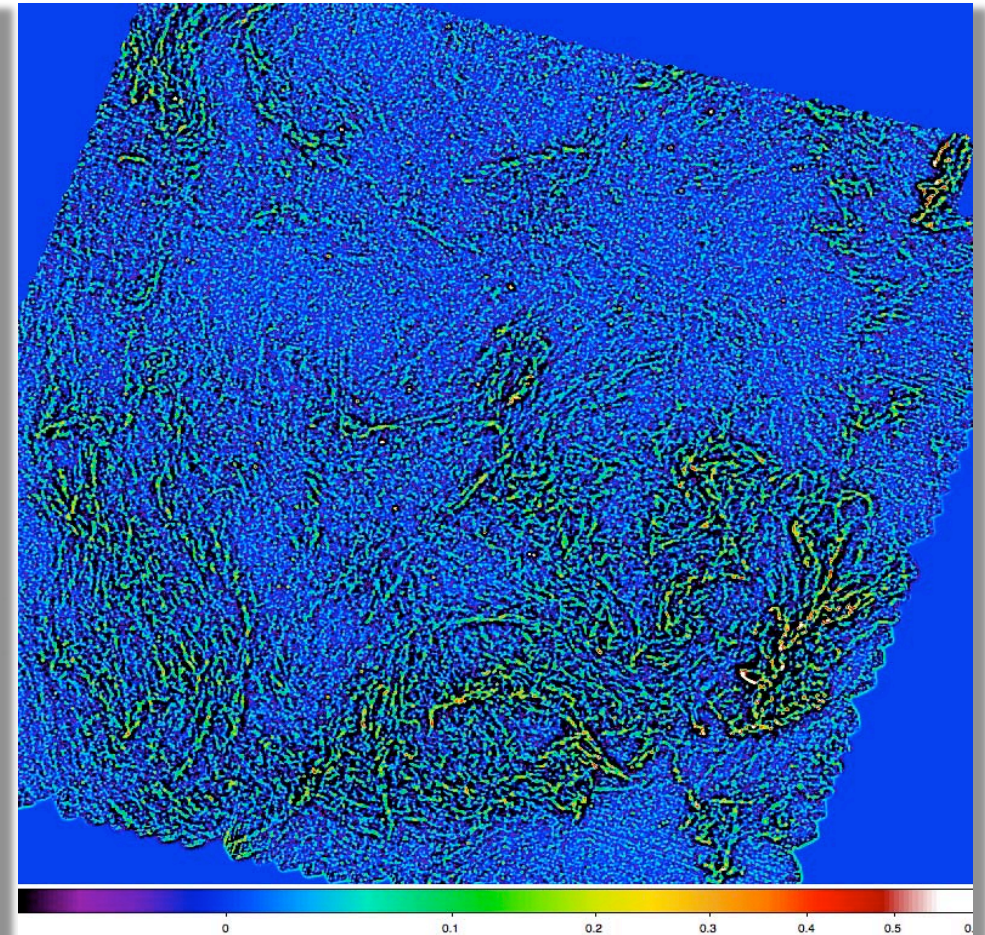


3.3°

Aquila and Polaris: SPIRE 250 μm single scales $\sim 40''$ by *getsources*

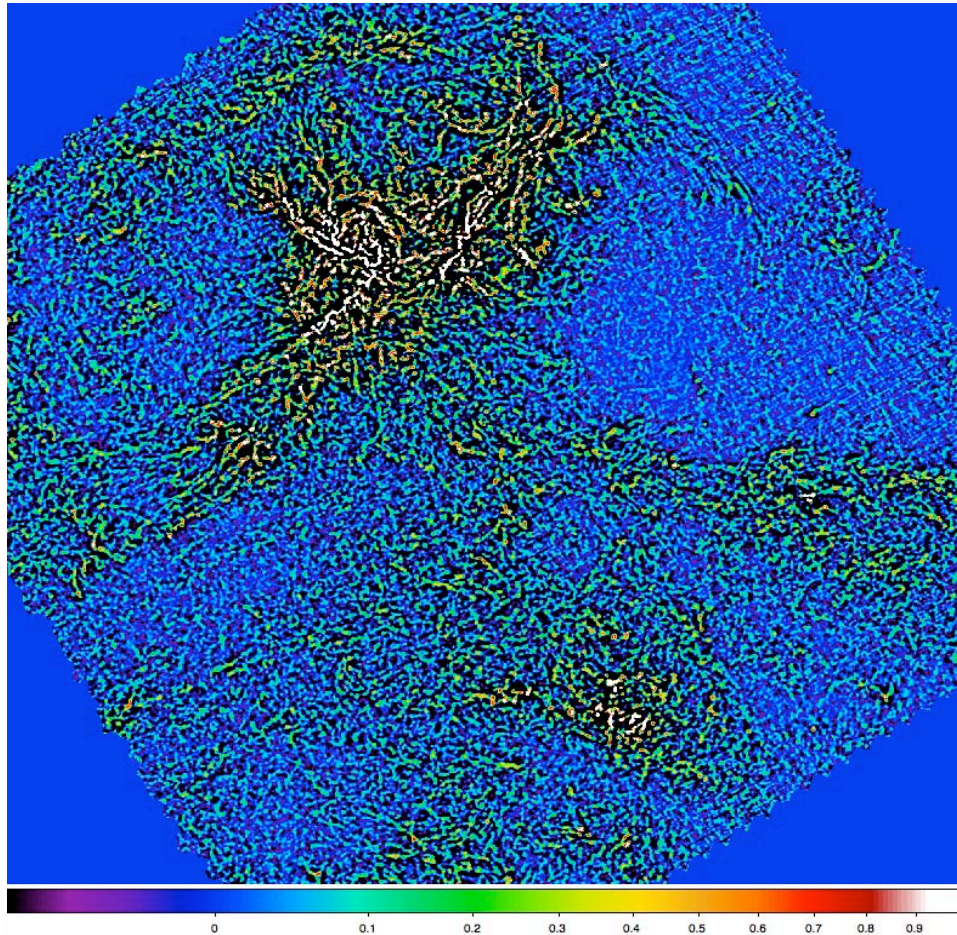


3.3°

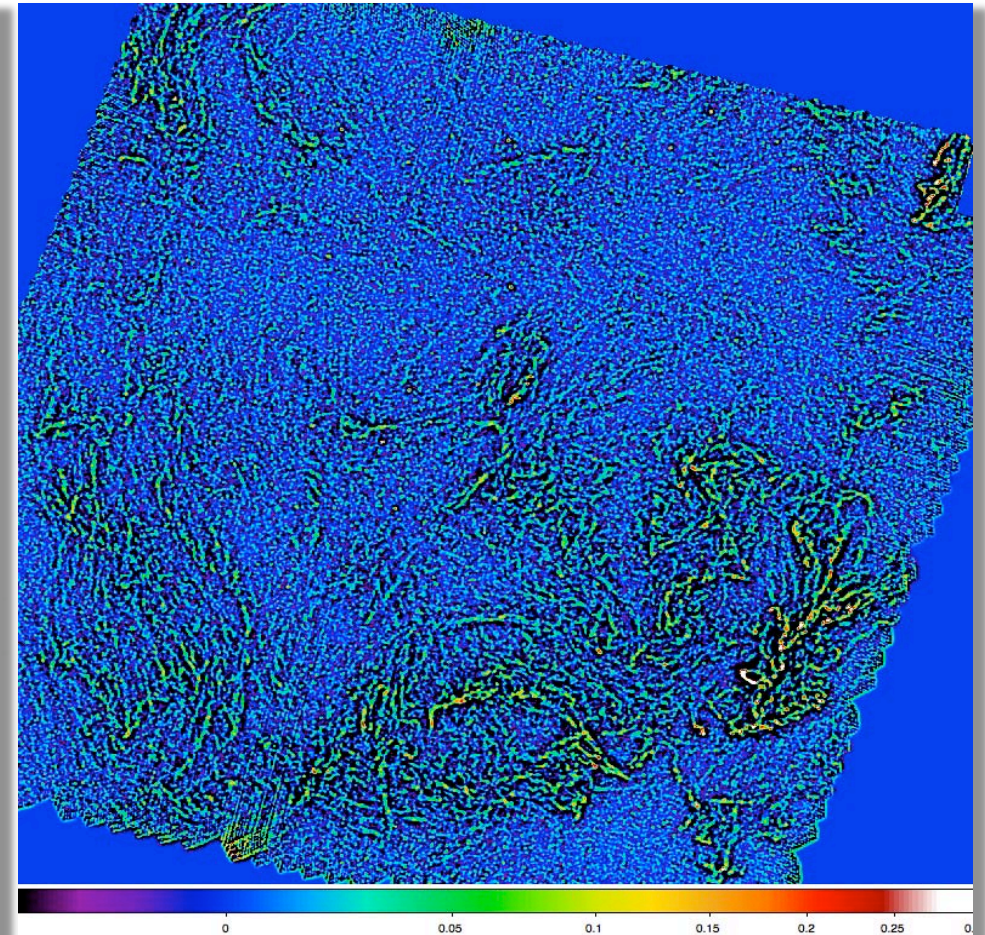


3.3°

Aquila and Polaris: SPIRE 350 μm single scales $\sim 40''$ by *getsources*

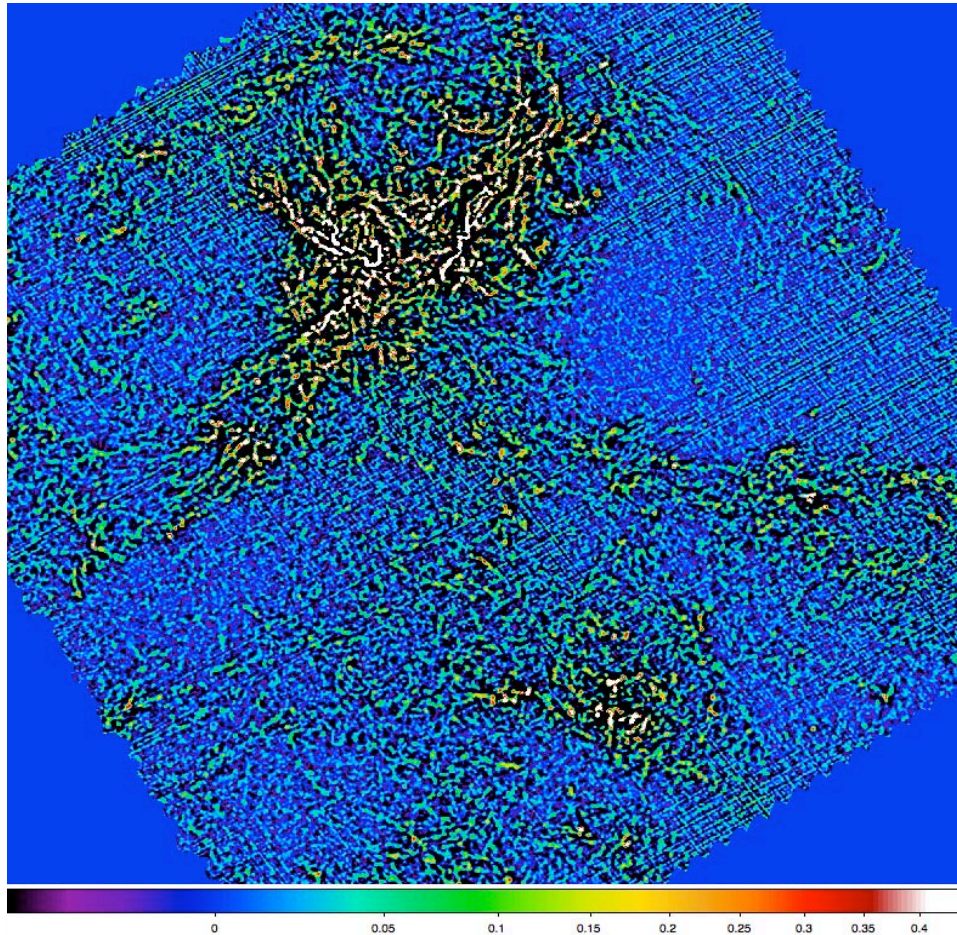


3.3°

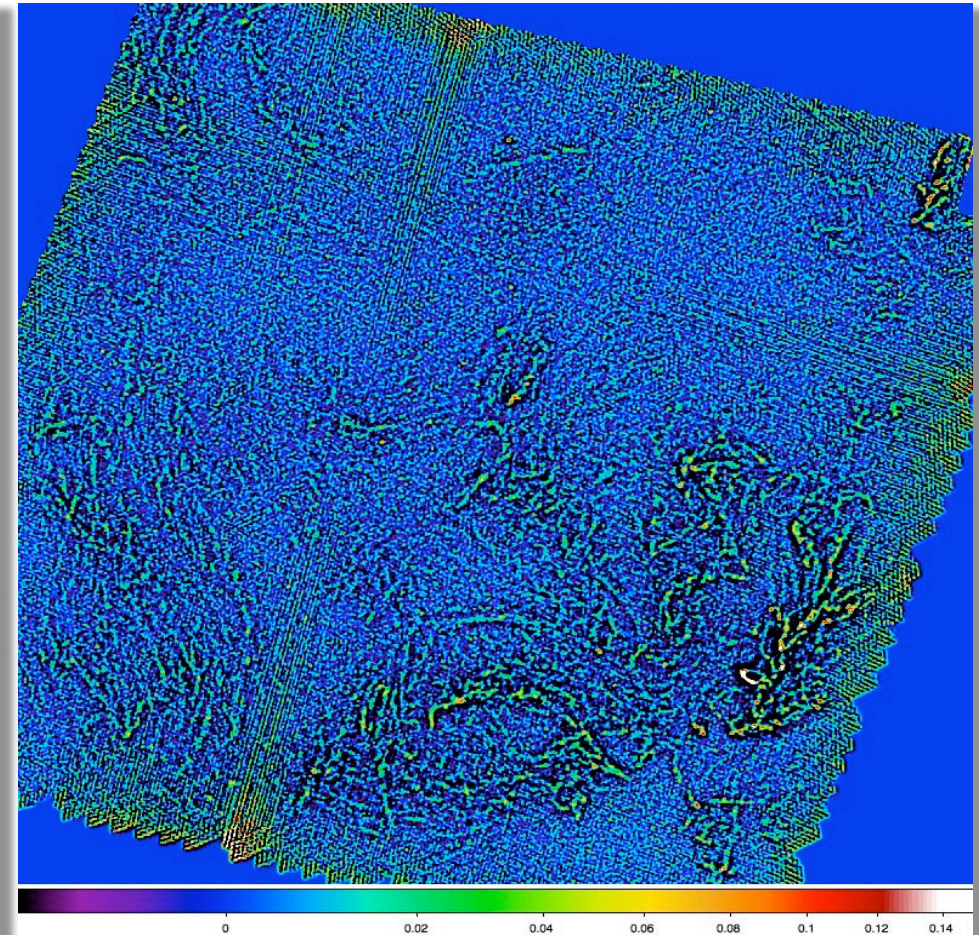


3.3°

Aquila and Polaris: SPIRE 500 μm single scales $\sim 40''$ by *getsources*

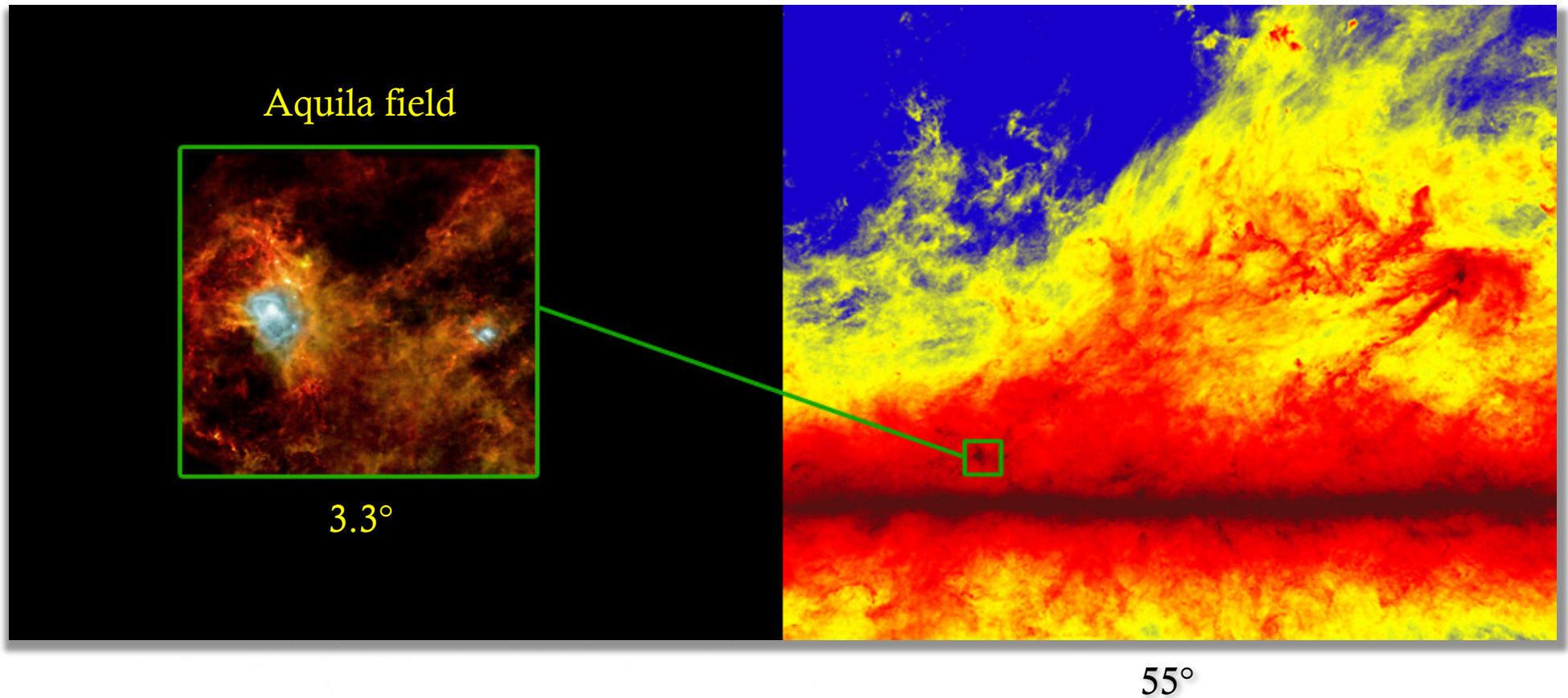


3.3°



3.3°

Herschel SPIRE/PACS and *Planck* 350 μm angular resolutions $\sim 30''$ and $300''$



Images: ESA, SPIRE, PACS, HFI Consortia, Gould Belt Key Project; <http://www.esa.int/esa-mm>

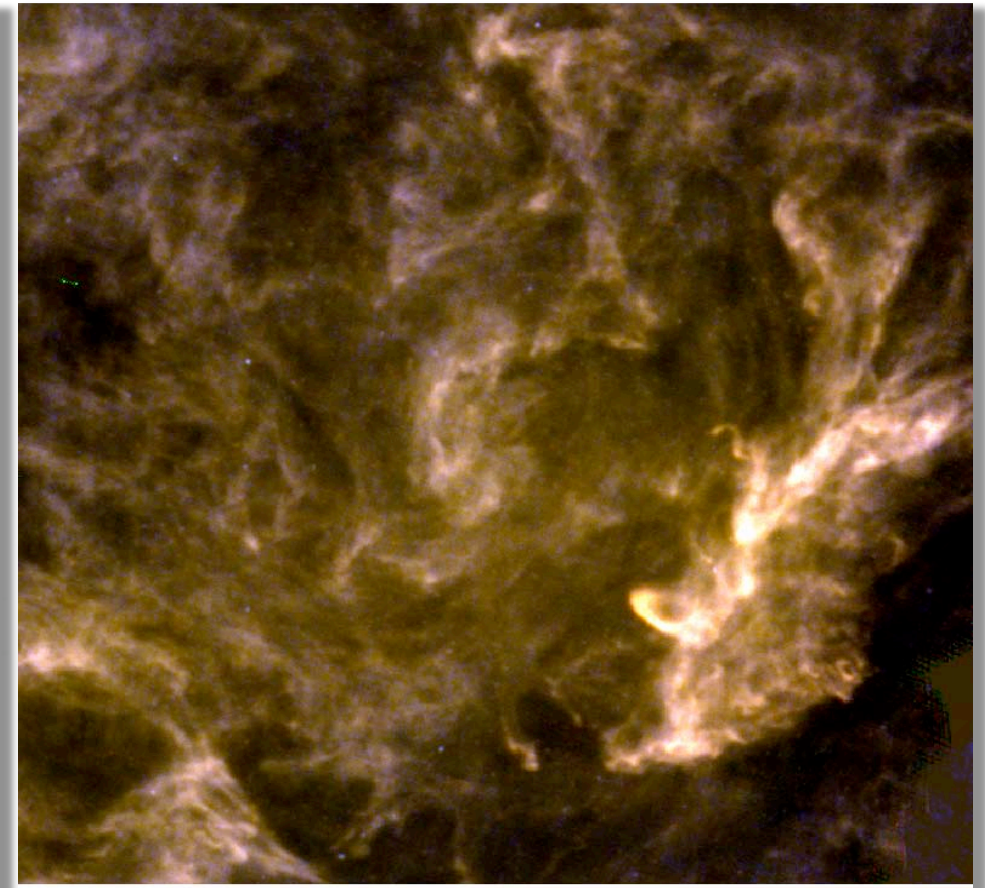
Intimate Physical Relationship of the Filaments and Cores

Aquila and Polaris Sub-Fields 1: SPIRE/PACS

RGB 350+160+70 μm and 350+250+160 μm



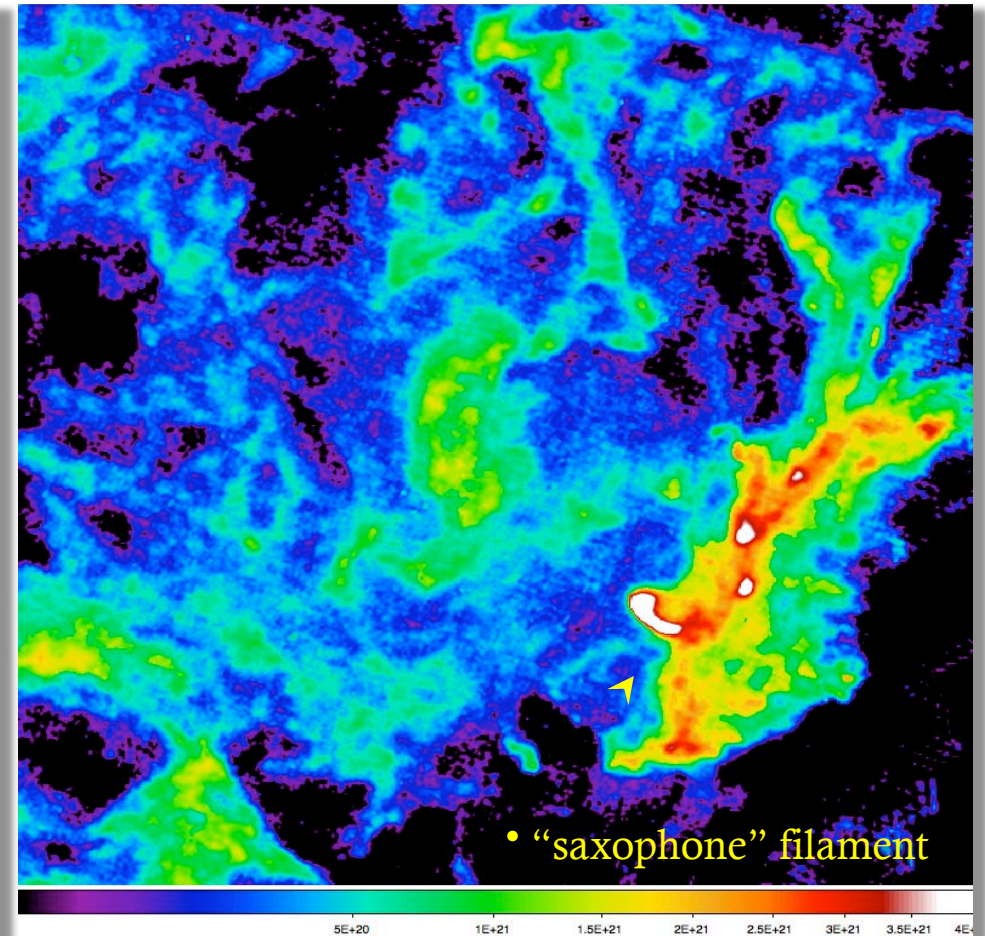
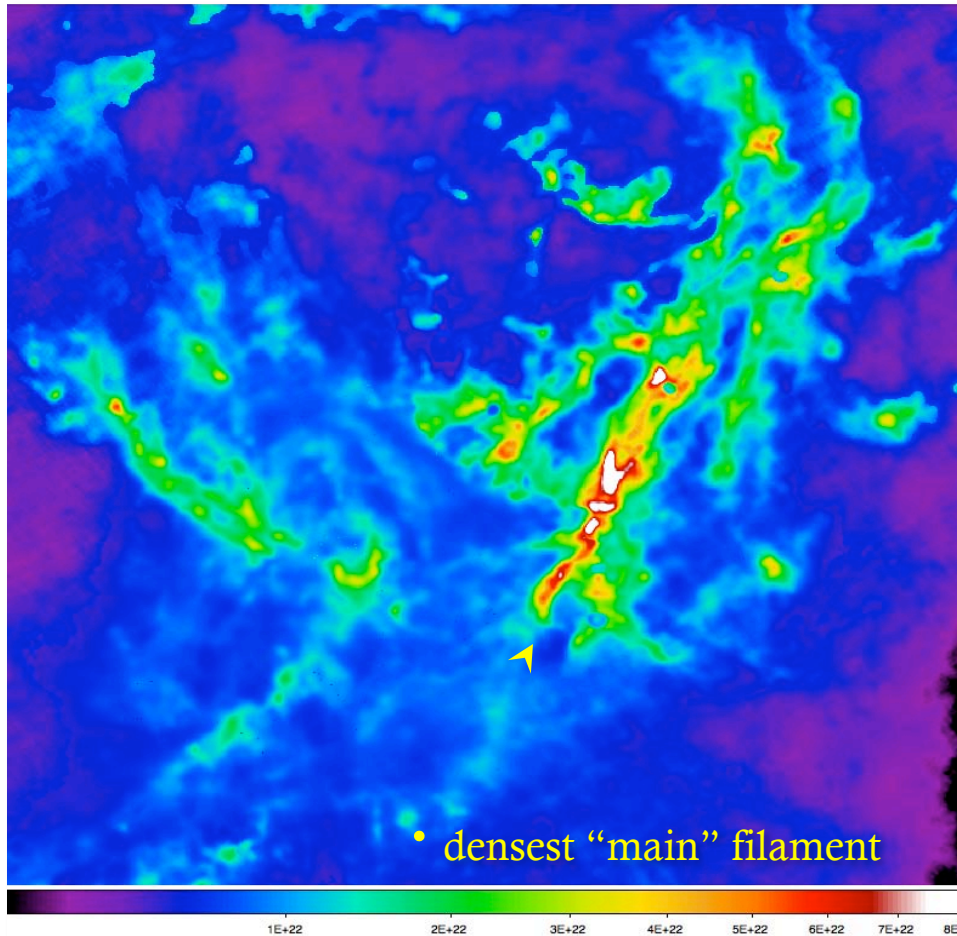
1.2°



1.2°

Aquila and Polaris Sub-Fields 1: SPIRE/PACS

column densities $N(\text{H}_2)$



$<1.4 \times 10^{23}$

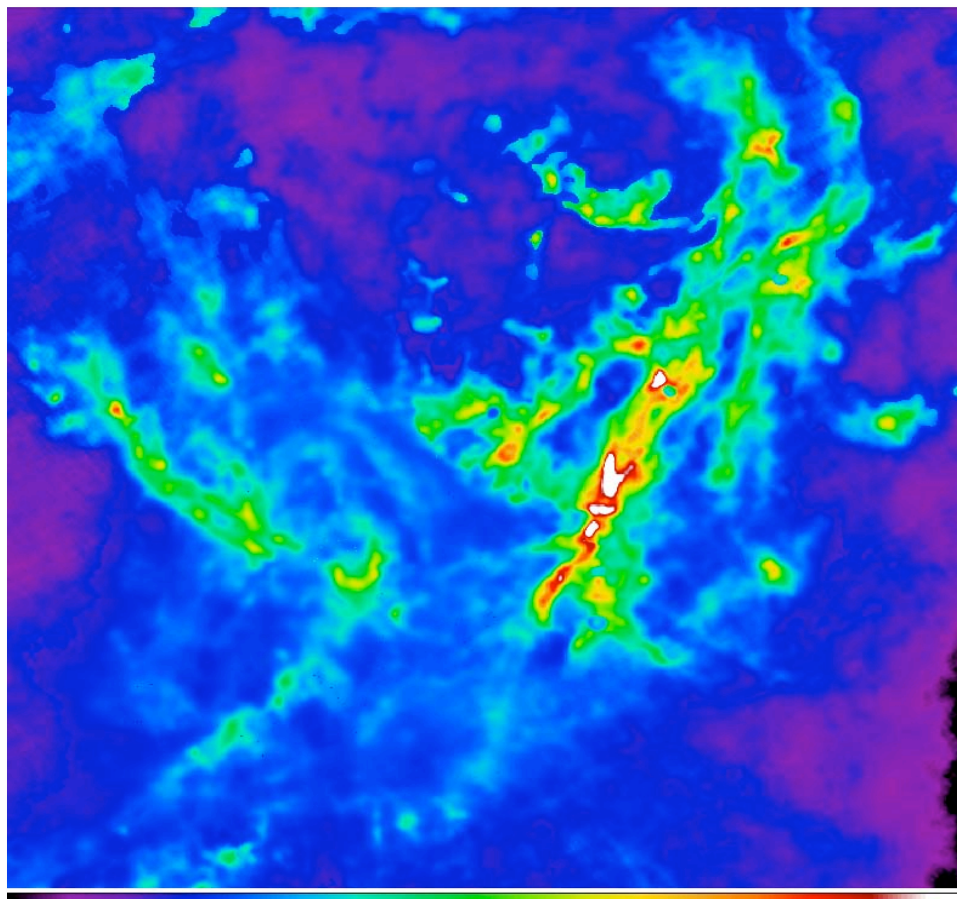
1.2°

1.2°

$<9 \times 10^{21}$

Aquila and Polaris Sub-Fields 1: SPIRE/PACS

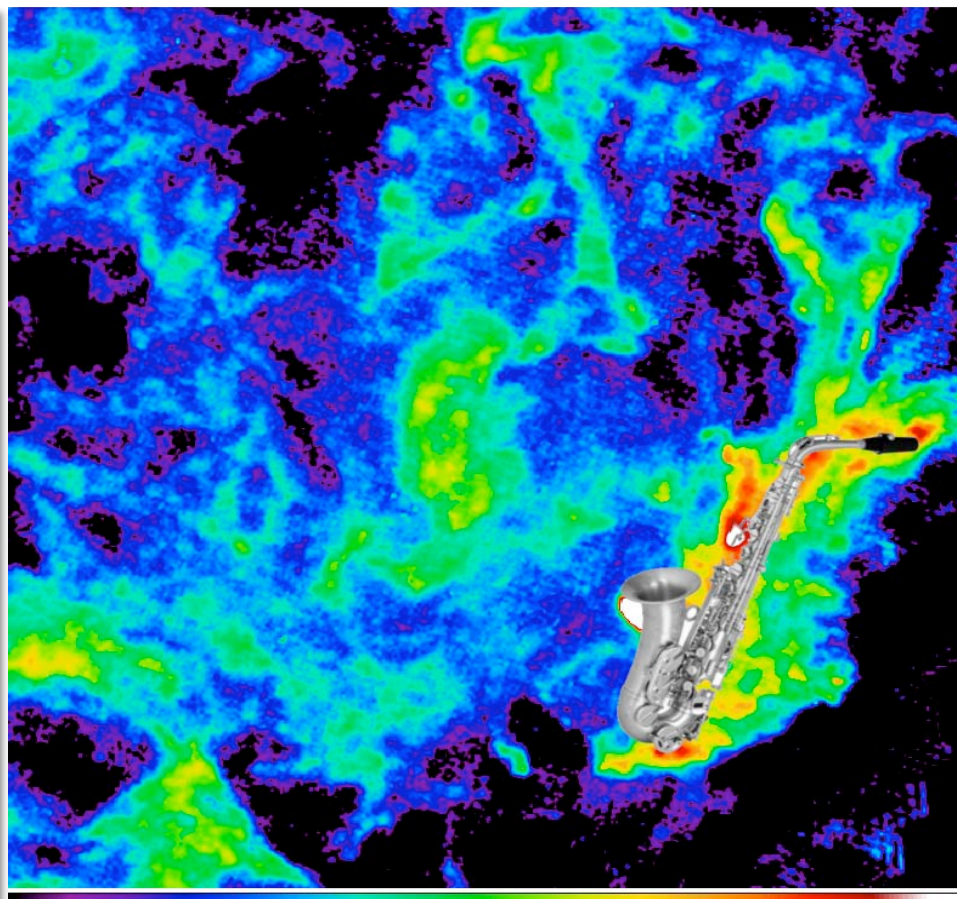
column densities $N(\text{H}_2)$



1E+22 2E+22 3E+22 4E+22 5E+22 6E+22 7E+22 8E+22

$<1.4 \times 10^{23}$

1.2°



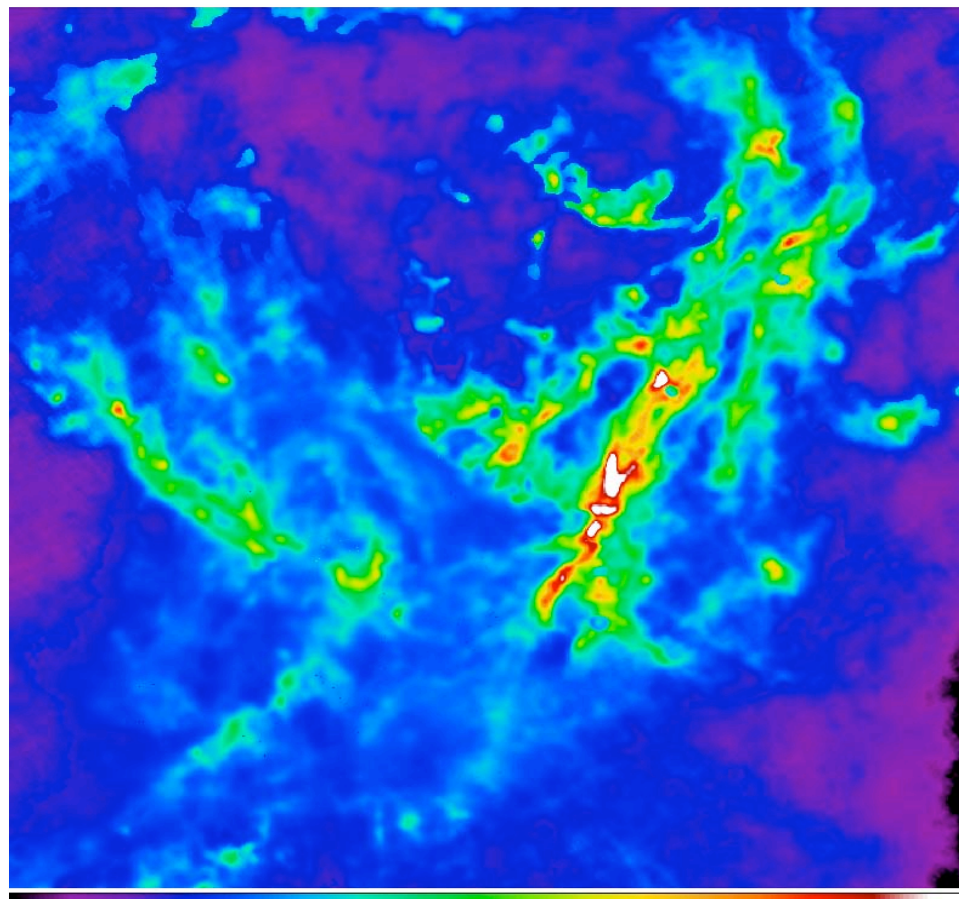
5E+20 1E+21 1.5E+21 2E+21 2.5E+21 3E+21 3.5E+21 4E+21

1.2°

$<9 \times 10^{21}$

Aquila and Polaris Sub-Fields 1: SPIRE/PACS

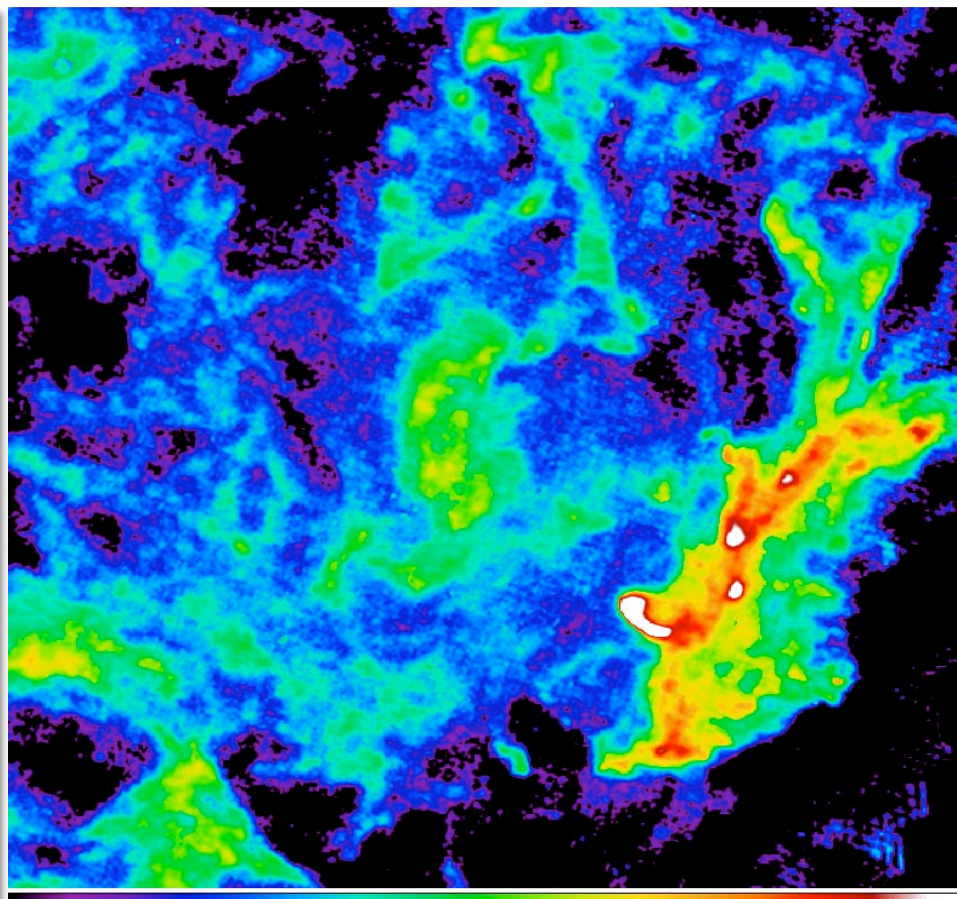
column densities $N(\text{H}_2)$



1E+22 2E+22 3E+22 4E+22 5E+22 6E+22 7E+22 8E+22

$<1.4 \times 10^{23}$

1.2°



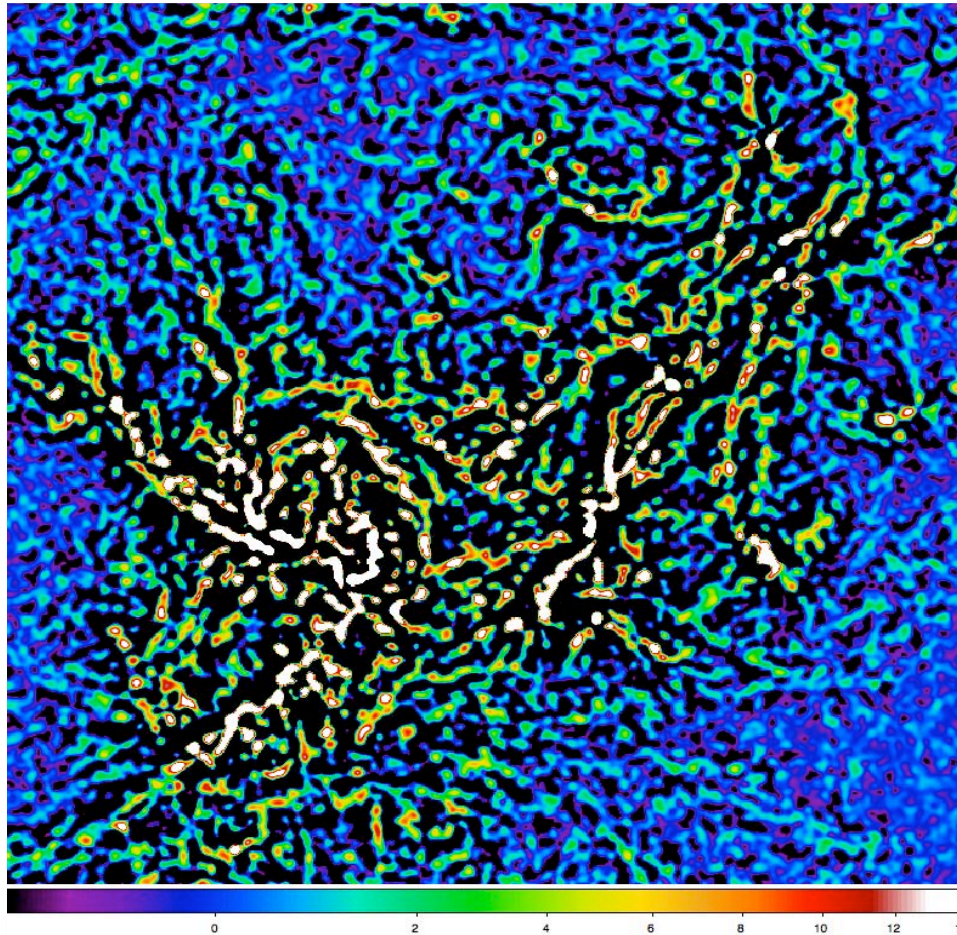
5E+20 1E+21 1.5E+21 2E+21 2.5E+21 3E+21 3.5E+21 4E+21

1.2°

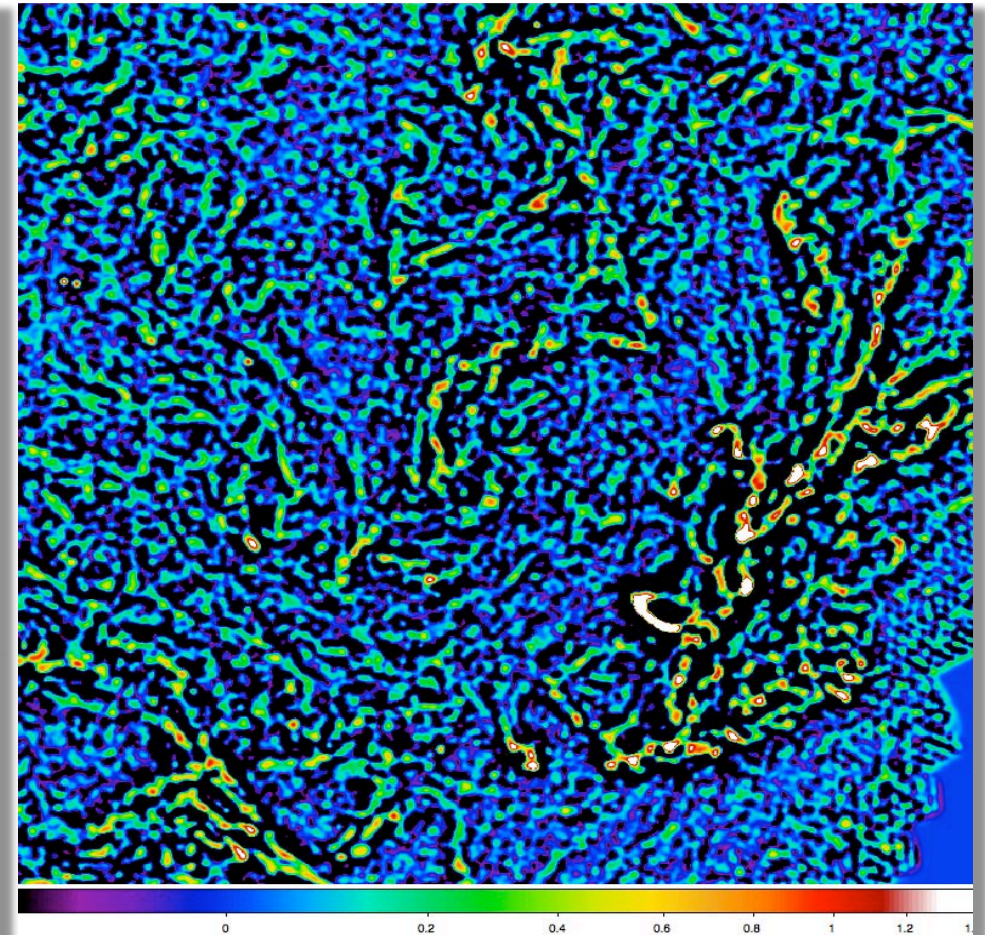
$<9 \times 10^{21}$

Aquila and Polaris Sub-Fields 1: SPIRE

single scales $\sim 40''$: high-contrast filaments and objects



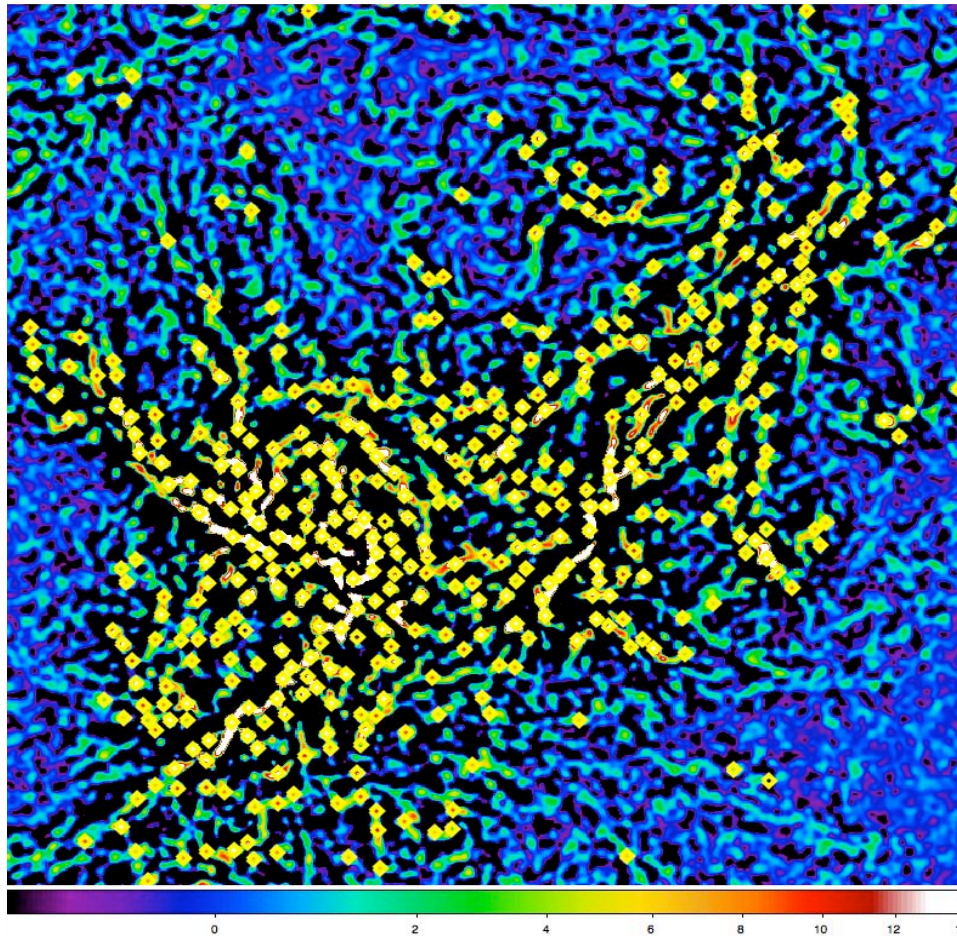
1.2°



1.2°

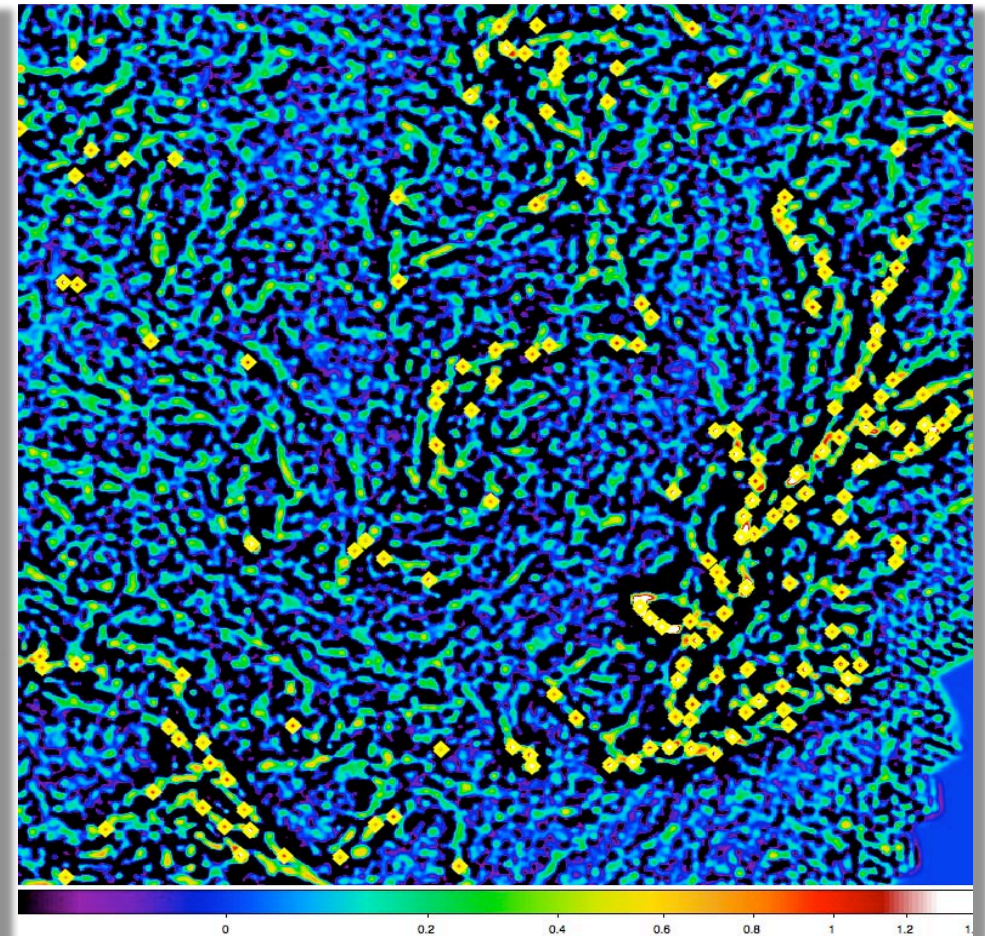
Aquila and Polaris Sub-Fields 1: SPIRE

single scales $\sim 40''$ + naive visual detection



451 objects

1.2°

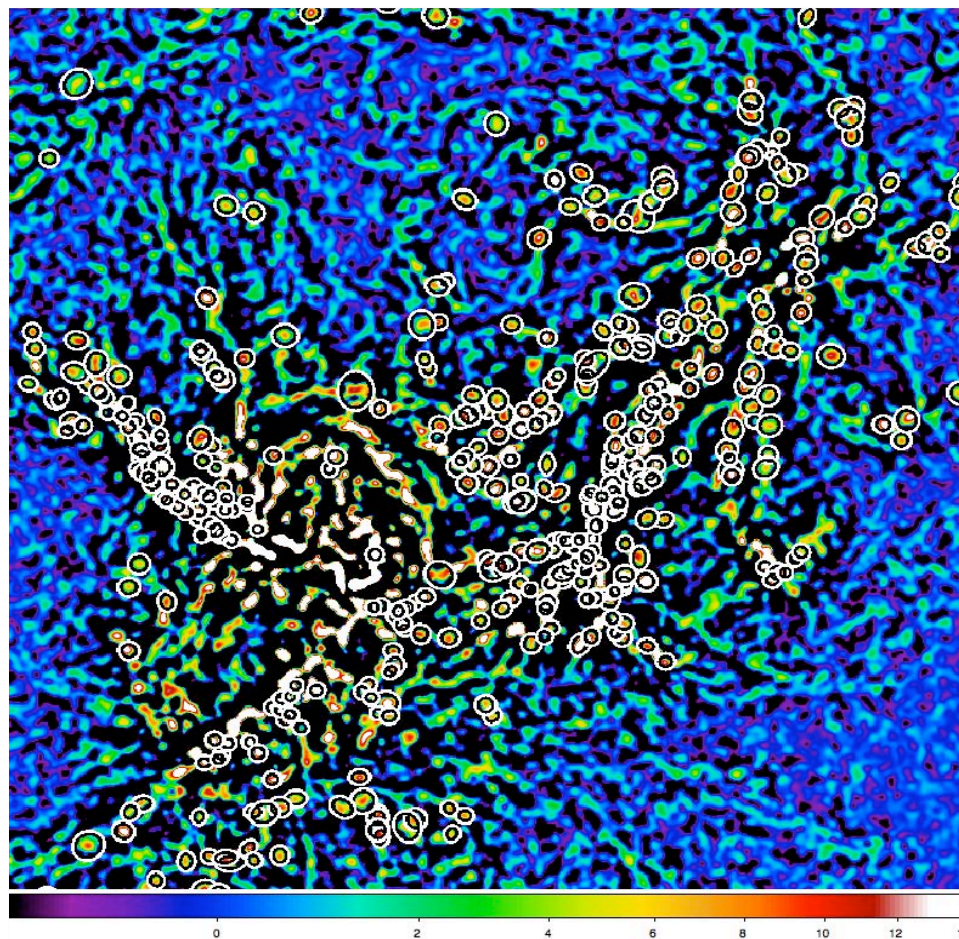


1.2°

168 objects

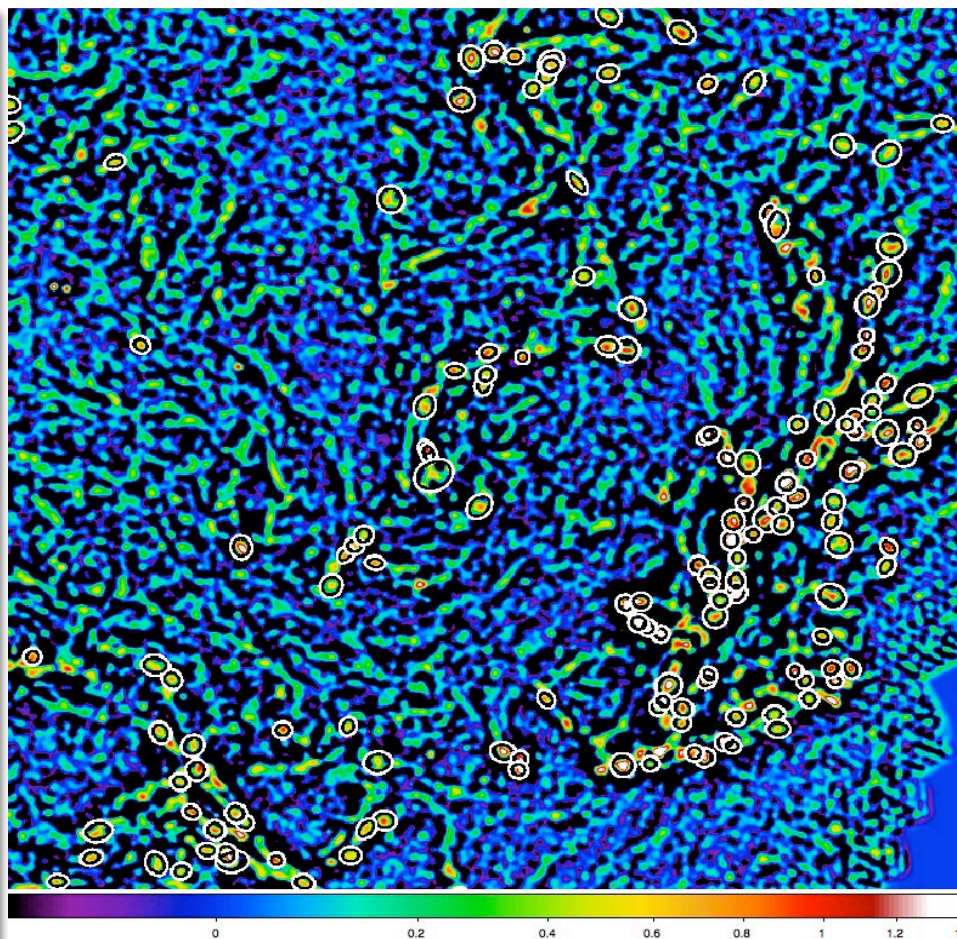
Aquila and Polaris Sub-Fields 1: SPIRE

single scales $\sim 40''$ + starless cores by *getsources*



~ 400 cores

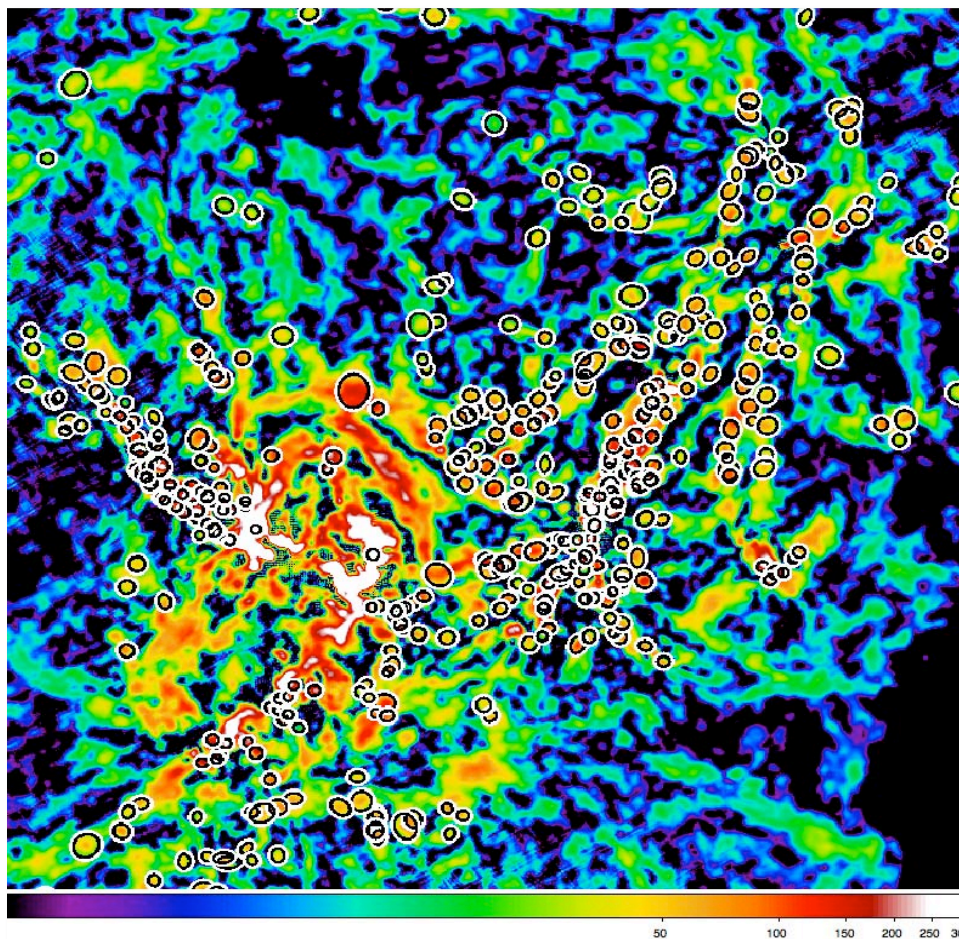
1.2°



1.2°

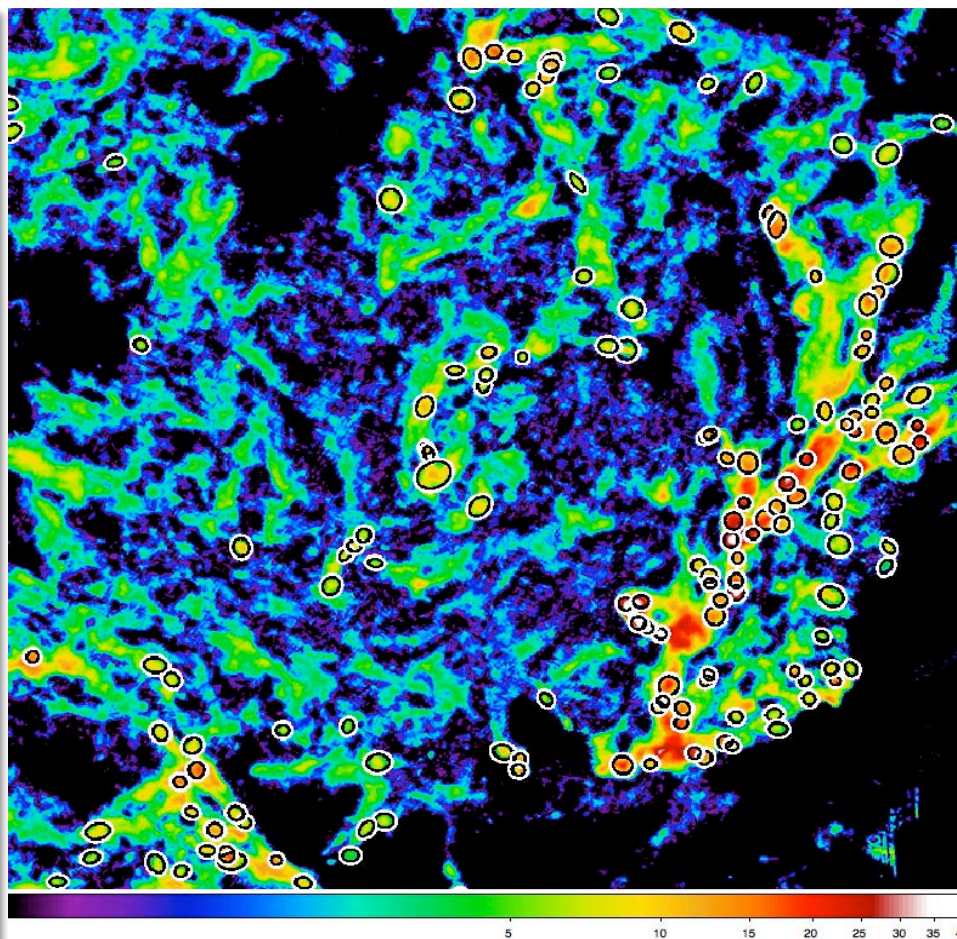
~ 160 cores

Aquila and Polaris Sub-Fields 1: SPIRE 350 μm curvelet component by *cb_mca* + starless cores by *getsources*



~400 cores

1.2°

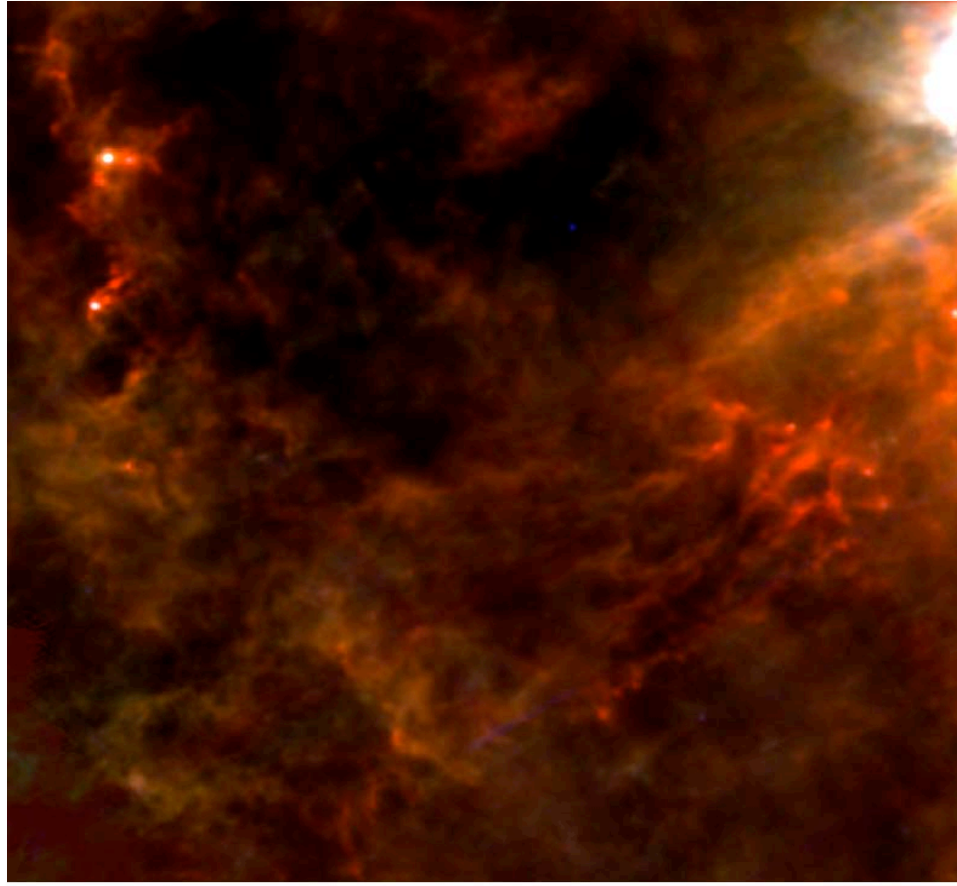


1.2°

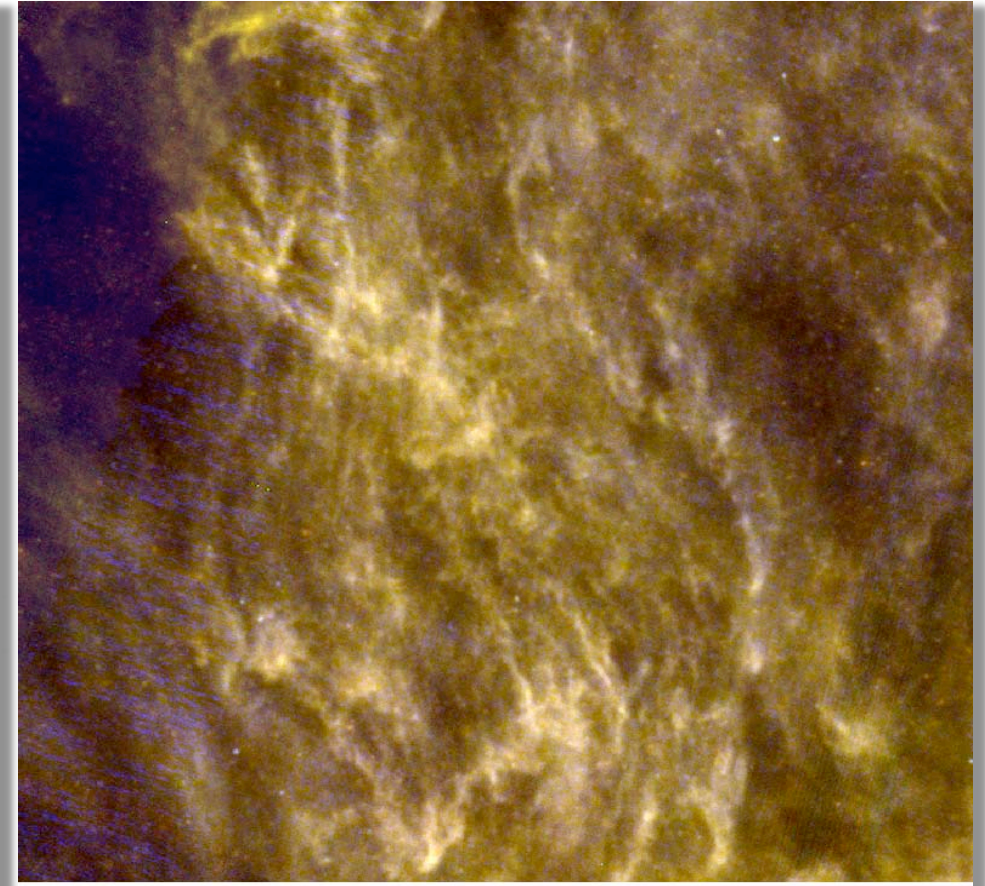
~160 cores

Aquila and Polaris Sub-Fields 2: SPIRE/PACS

RGB 350+160+70 μm and 350+250+160 μm



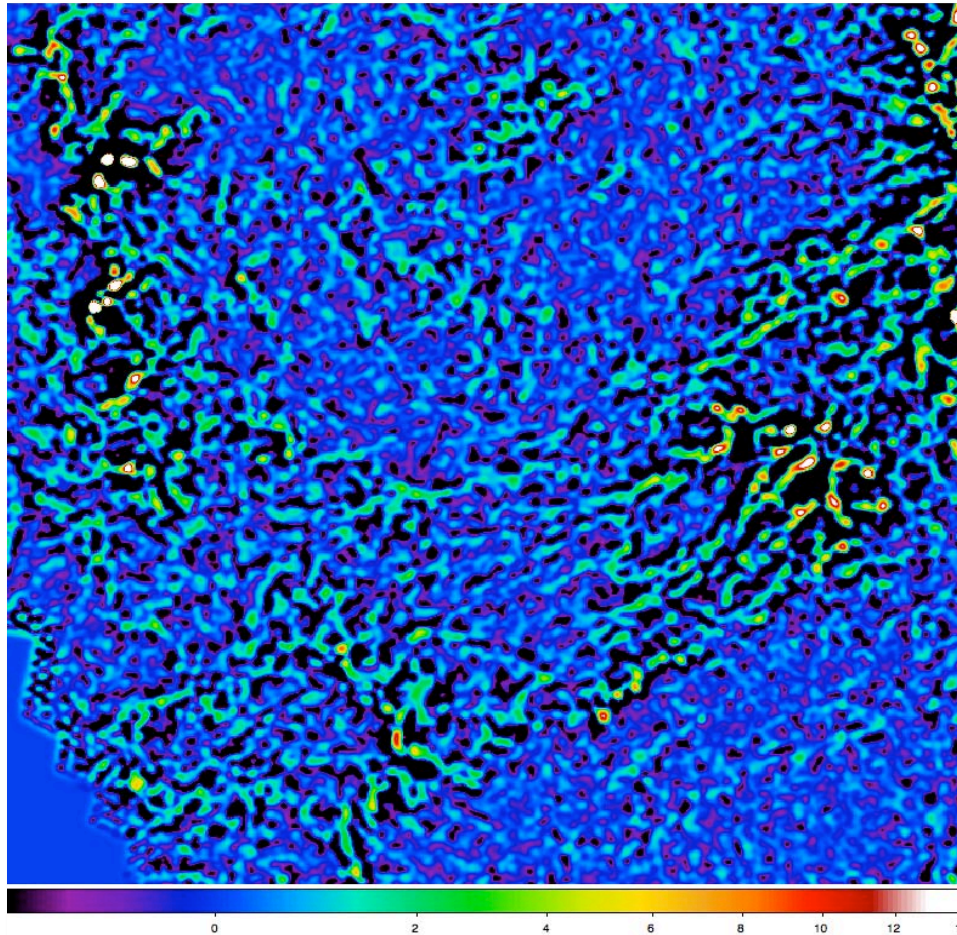
1.2°



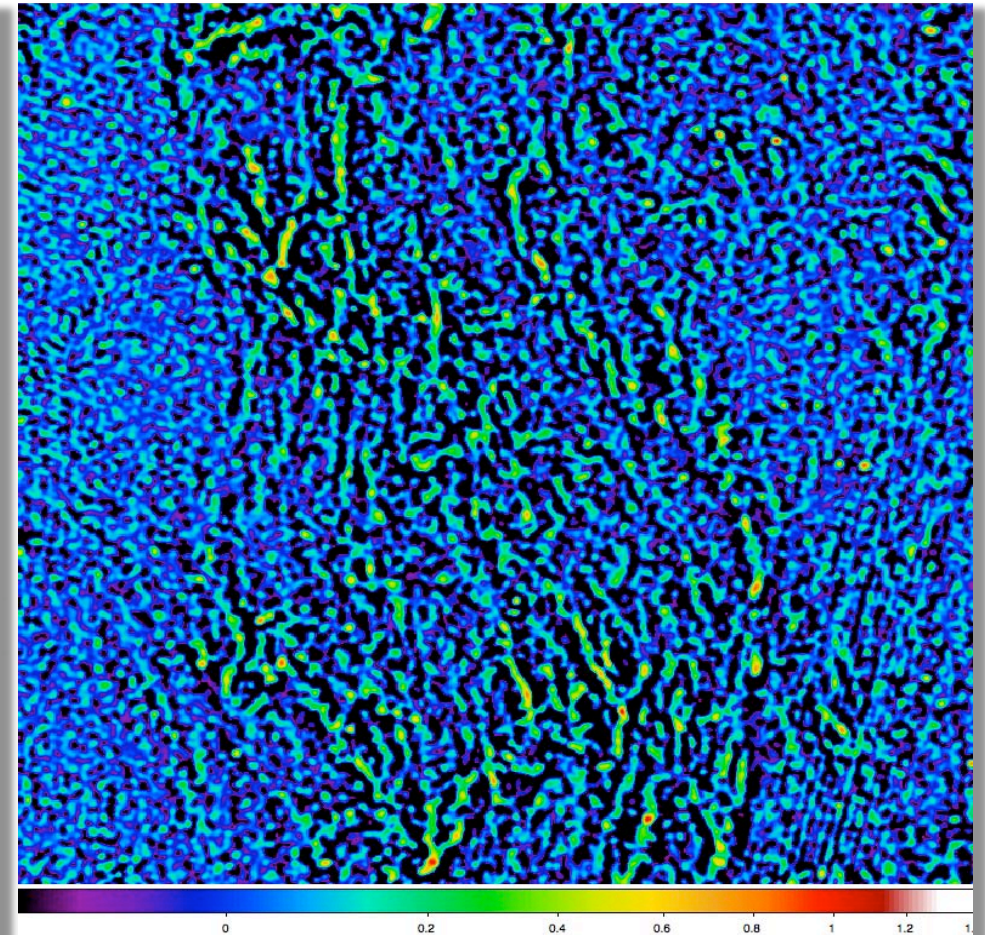
1.2°

Aquila and Polaris Sub-Fields 2: SPIRE

single scales $\sim 40''$: high-contrast filaments and objects



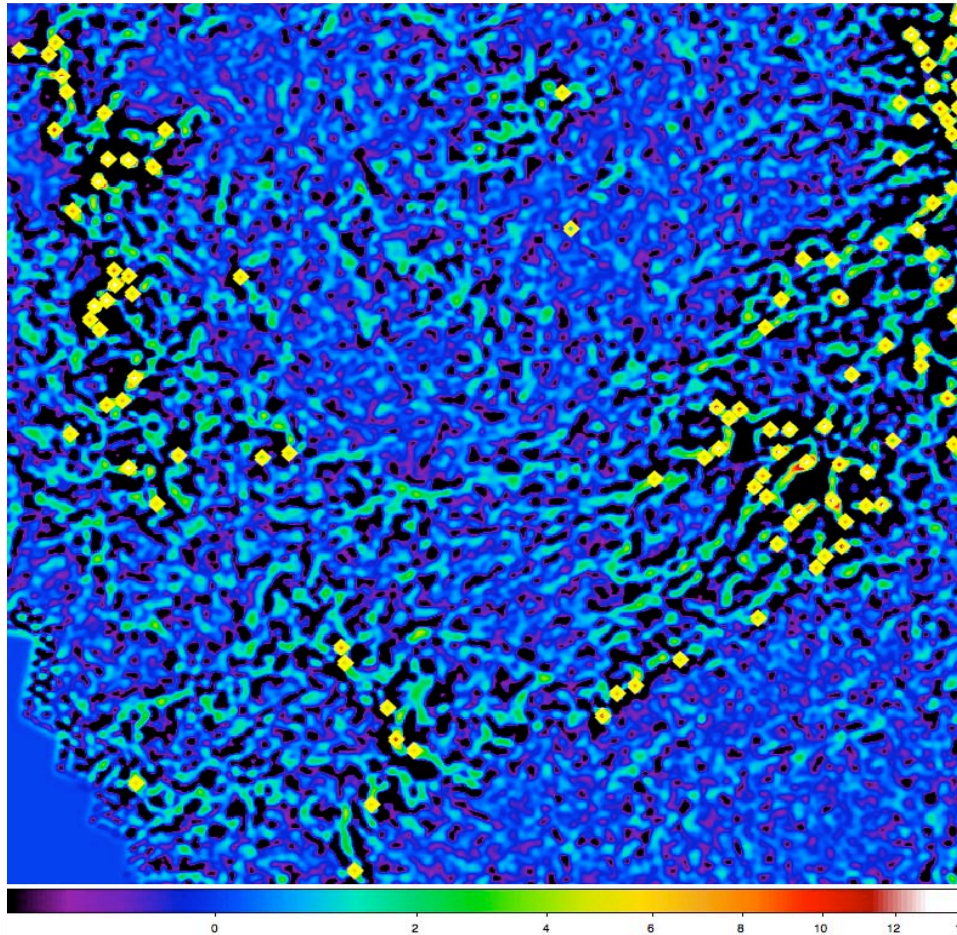
1.2°



1.2°

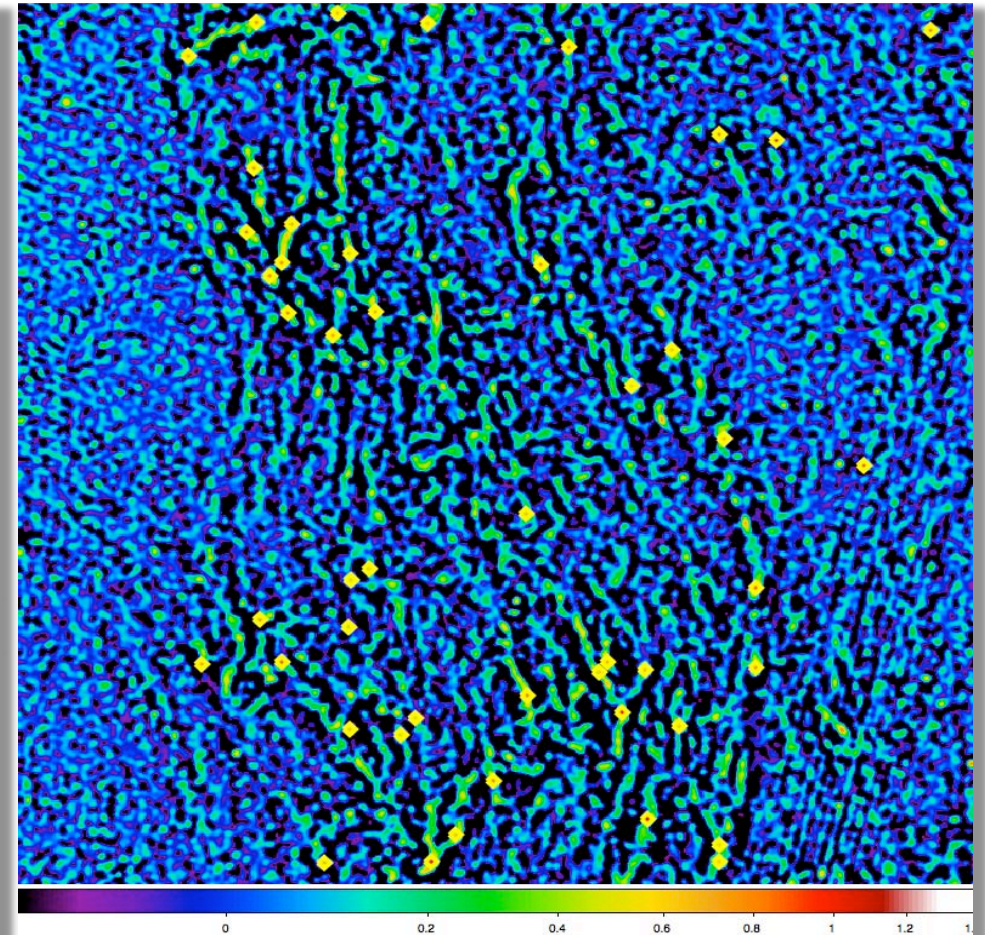
Aquila and Polaris Sub-Fields 2: SPIRE

single scales $\sim 40''$ + naive visual detection



105 objects

1.2°

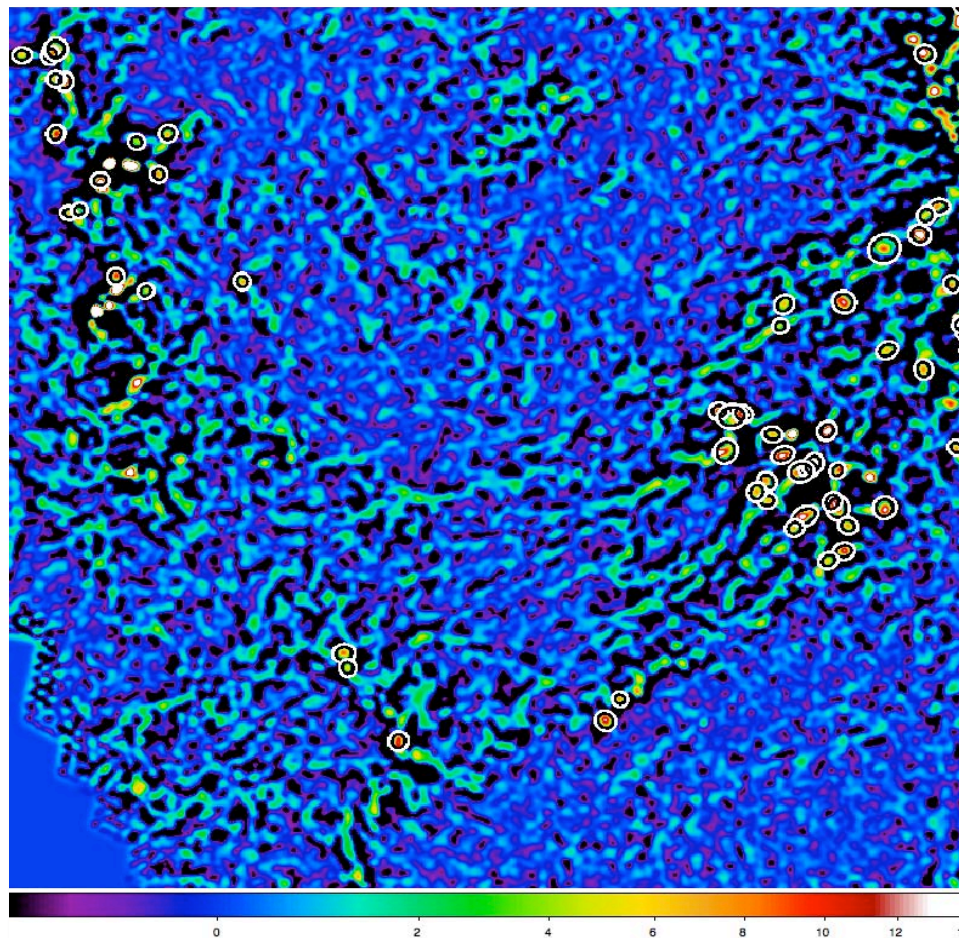


1.2°

47 objects

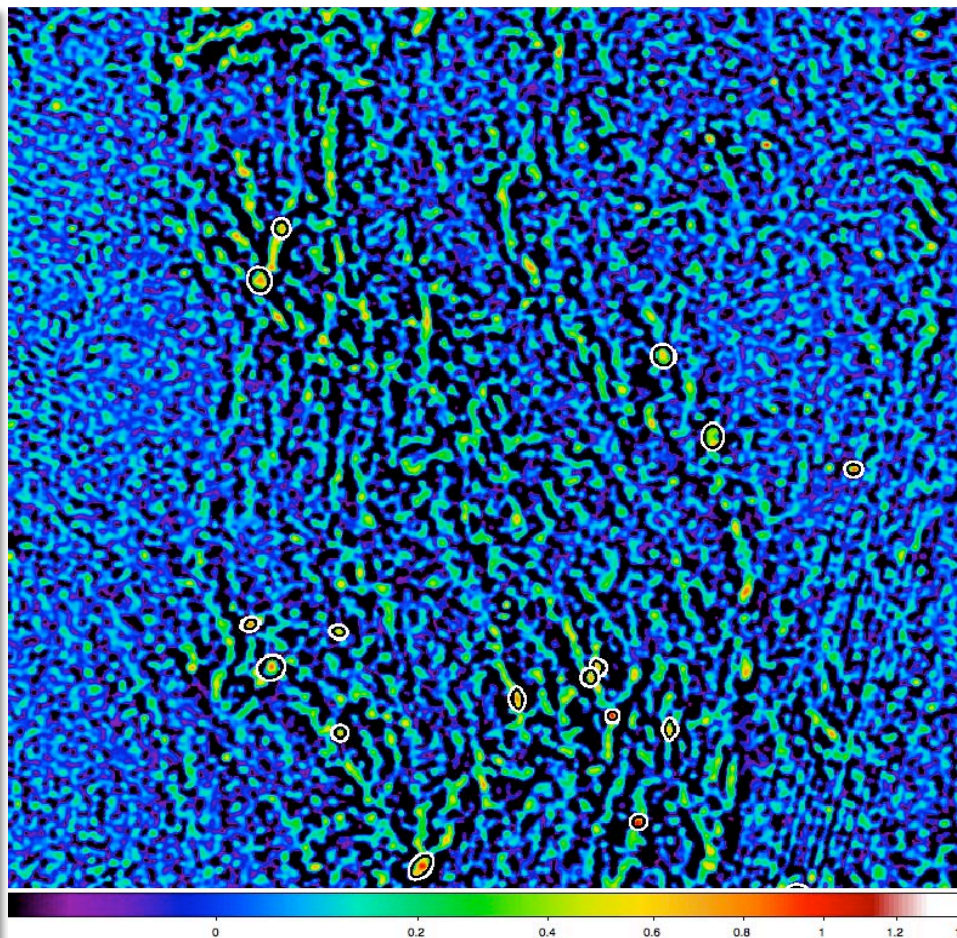
Aquila and Polaris Sub-Fields 2: SPIRE

single scales $\sim 40''$ + starless cores by *getsources*



54 cores

1.2°

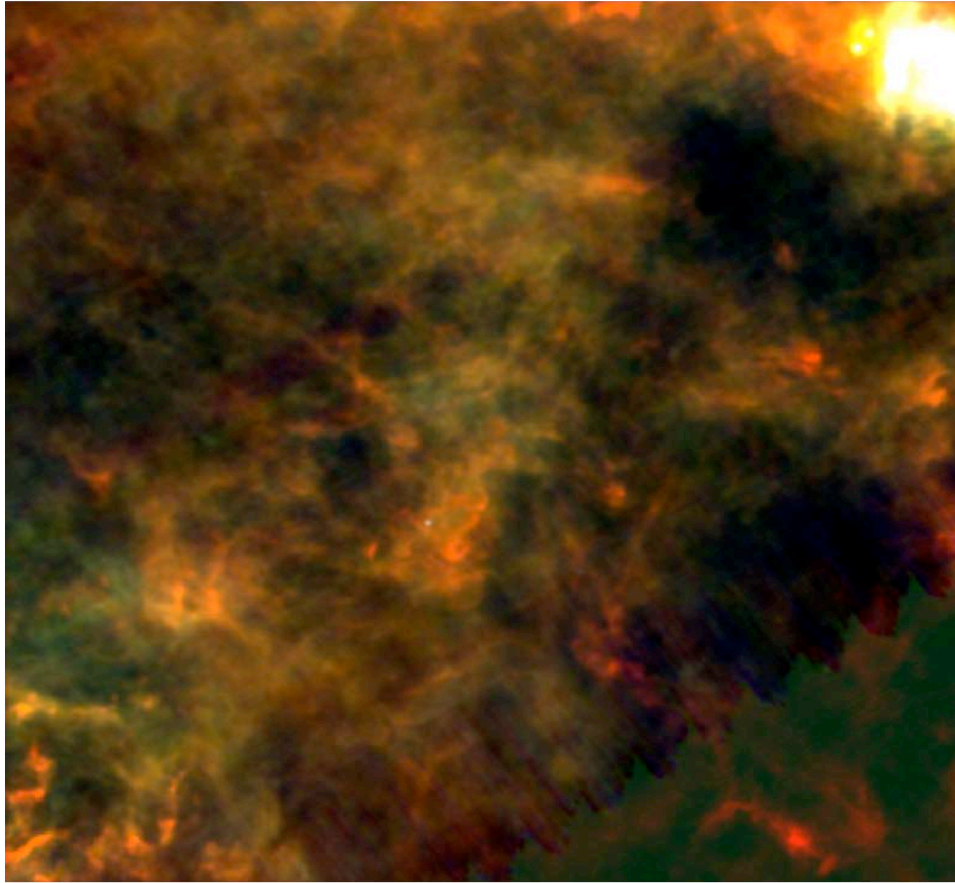


1.2°

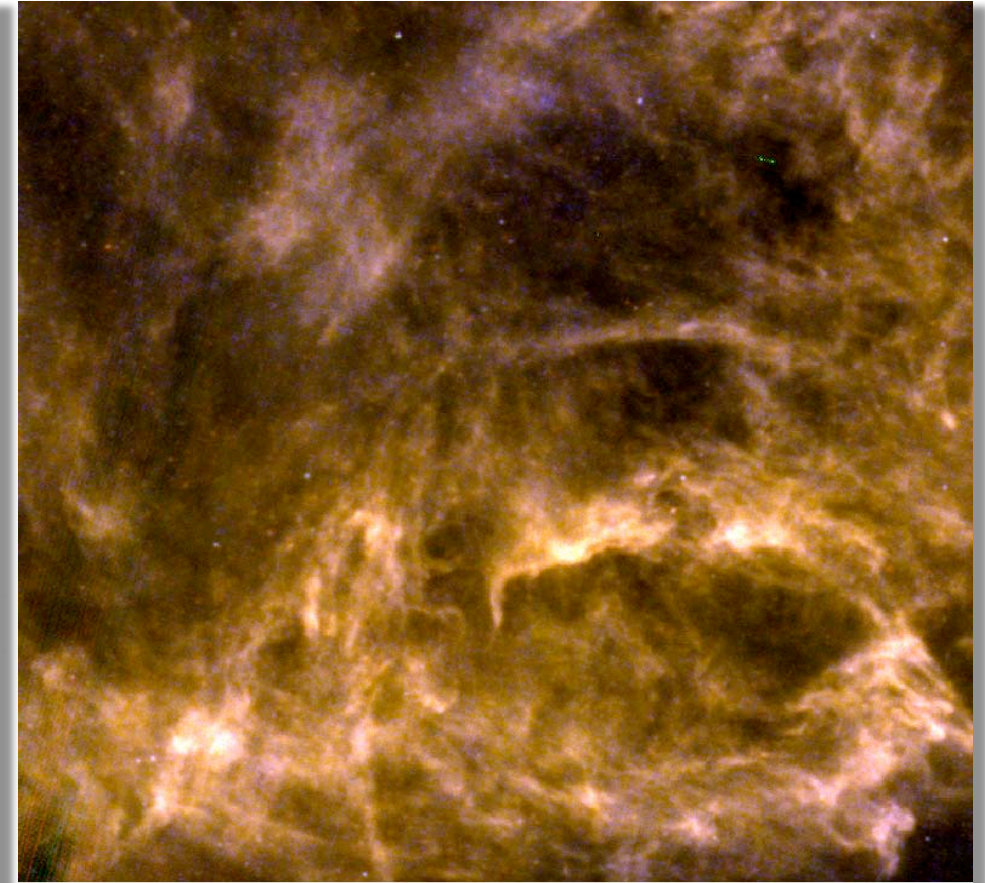
17 cores

Aquila and Polaris Sub-Fields 3: SPIRE/PACS

RGB 350+160+70 μm and 350+250+160 μm



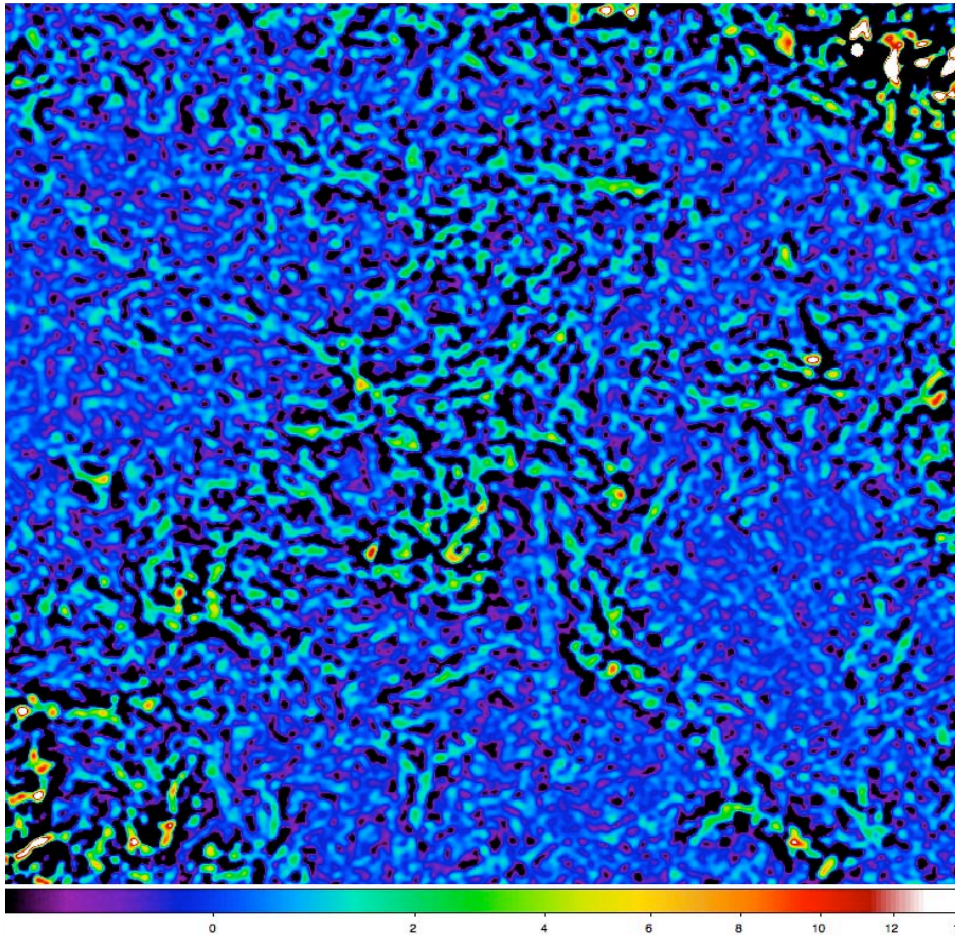
1.2°



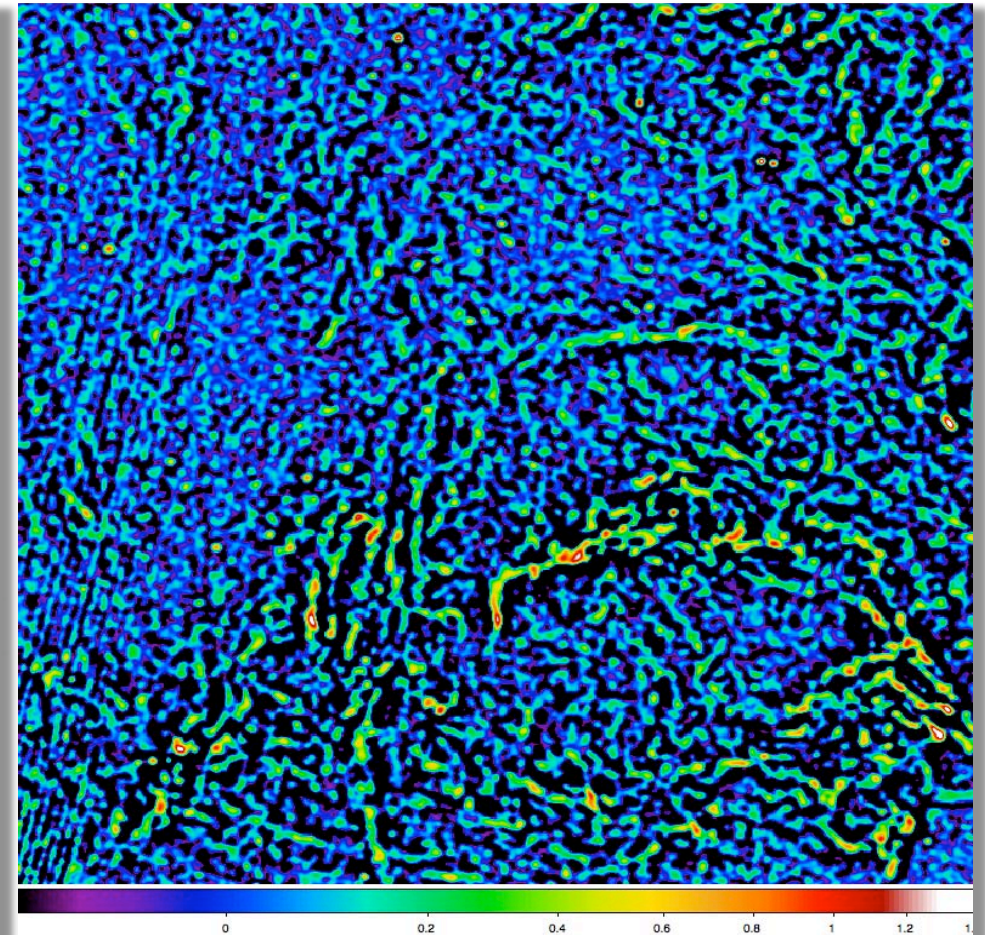
1.2°

Aquila and Polaris Sub-Fields 3: SPIRE

single scales $\sim 40''$: high-contrast filaments and objects



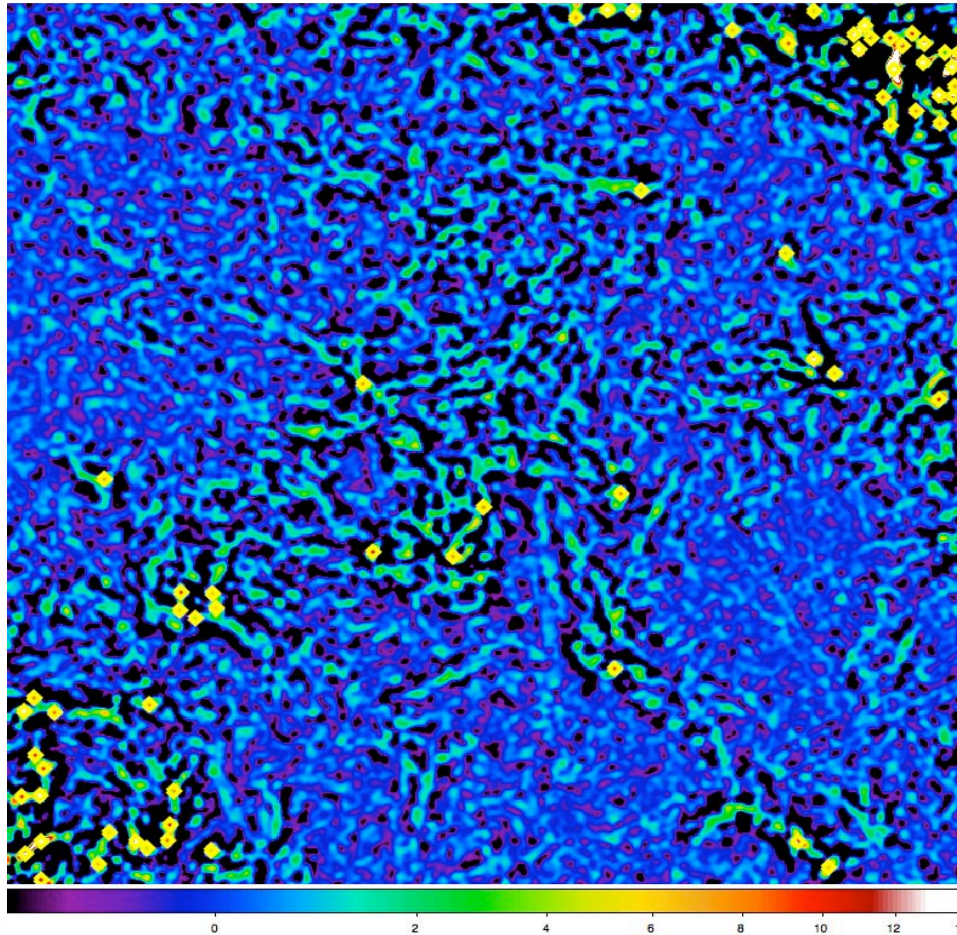
1.2°



1.2°

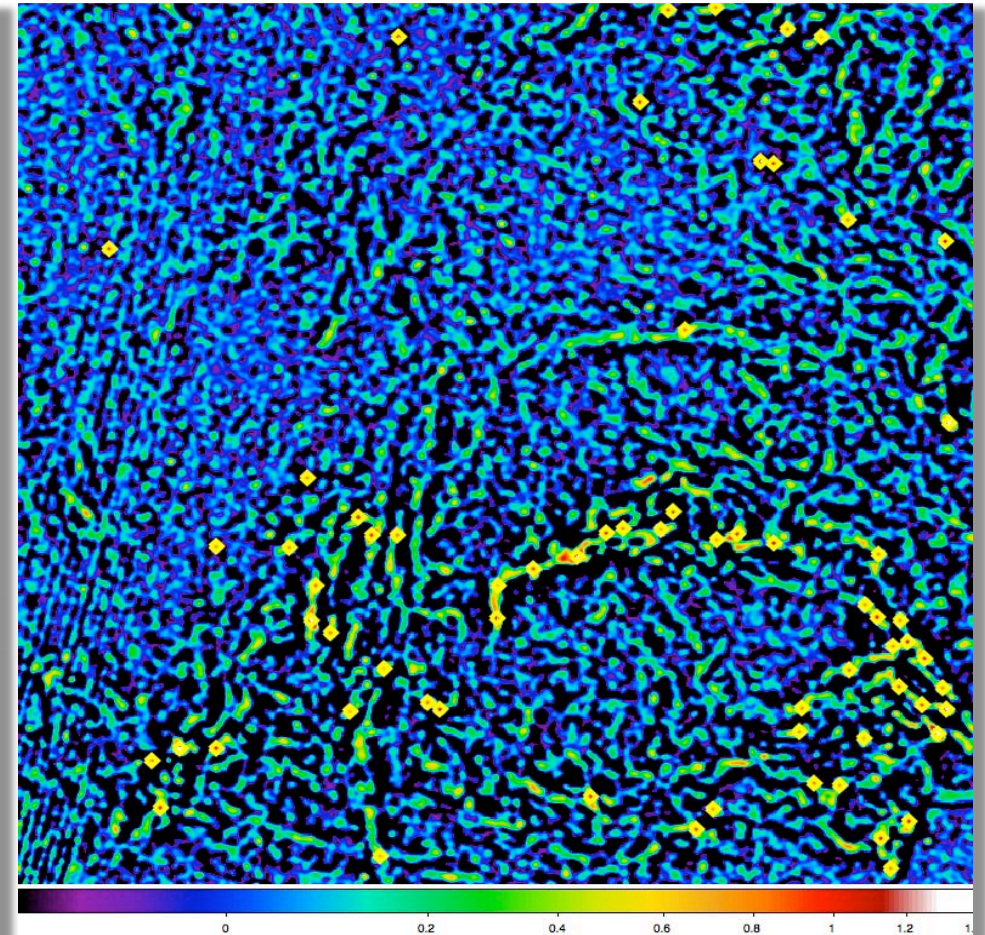
Aquila and Polaris Sub-Fields 3: SPIRE

single scales $\sim 40''$ + naive visual detection



65 objects

1.2°

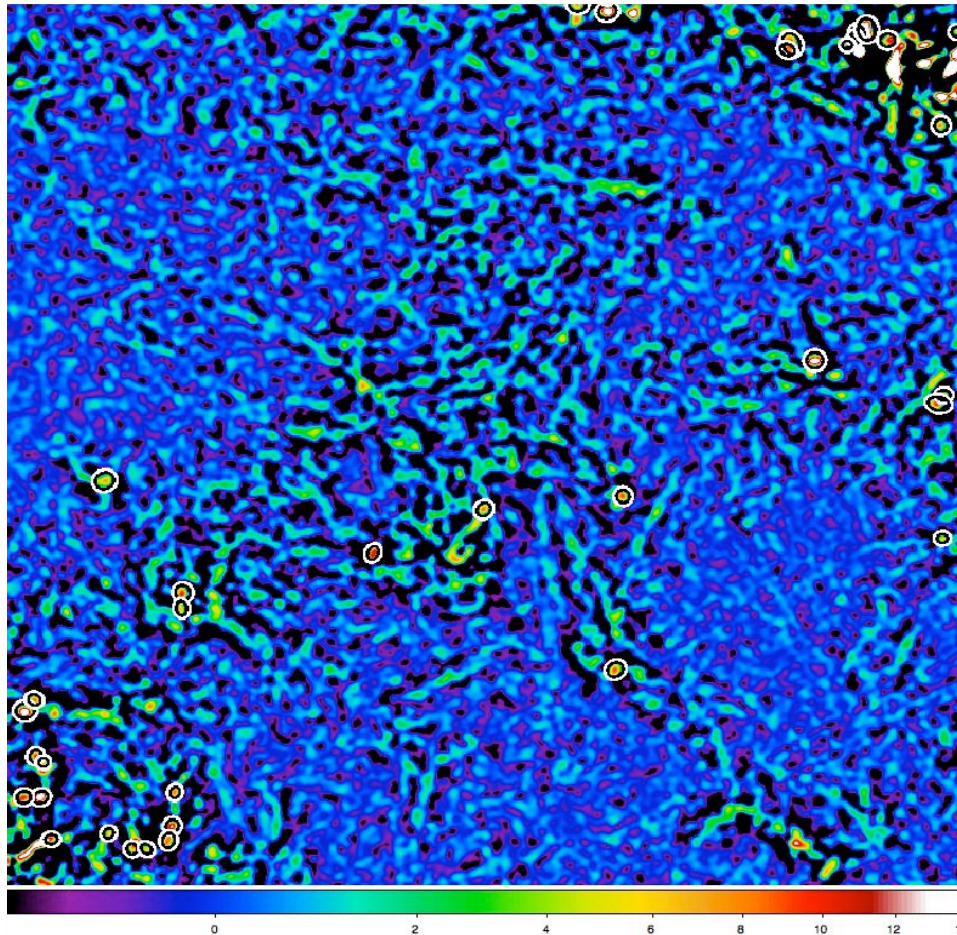


1.2°

66 objects

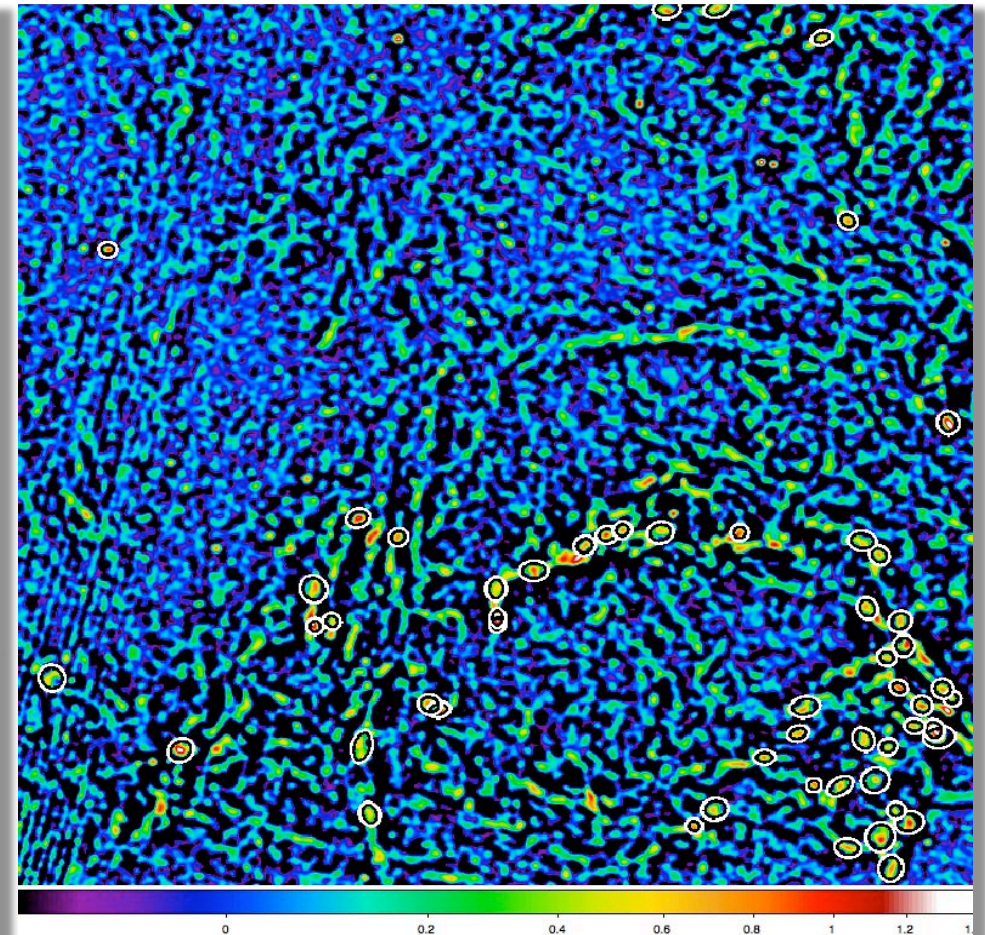
Aquila and Polaris Sub-Fields 3: SPIRE

single scales $\sim 40''$ + starless cores by *getsources*



34 cores

1.2°

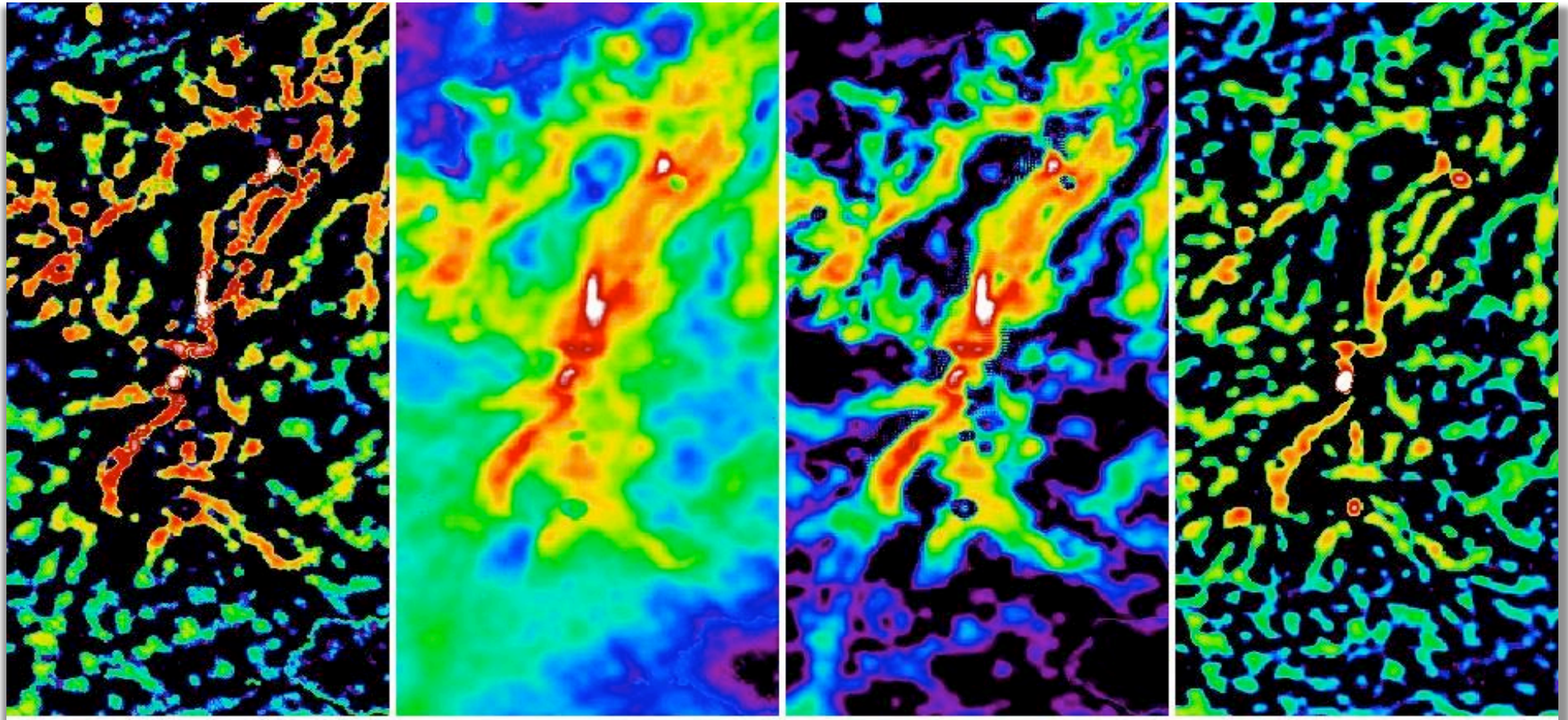


1.2°

50 cores

Two Methods, Same Structures

column density, curvelet component, and single scale



curvelet log-scaled

column density

curvelet

single scale $\sim 40''$

Filaments' Properties and Existing Models

Basic Properties of the Filaments

- Several well-behaved filaments in column density images, original images

Field	Colum H ₂	Temper	<FWHM>deconv	Maximum length	Density
Aquila	$< 1.4 \times 10^{23}$	7.5-15 K	35'' \pm 12 ~9000 AU	~0.5 deg ~few pc	$\rho \sim r^{-1.5}$
Polaris	$< 9 \times 10^{21}$	10-15 K	60'' \pm 12 ~9000 AU	~0.5 deg ~few pc	$\rho \sim r^{-2}$

- Maps of the filaments' mass per unit length (talk by Ph. André):
many Aquila filaments are gravitationally unstable, Polaris filaments are stable

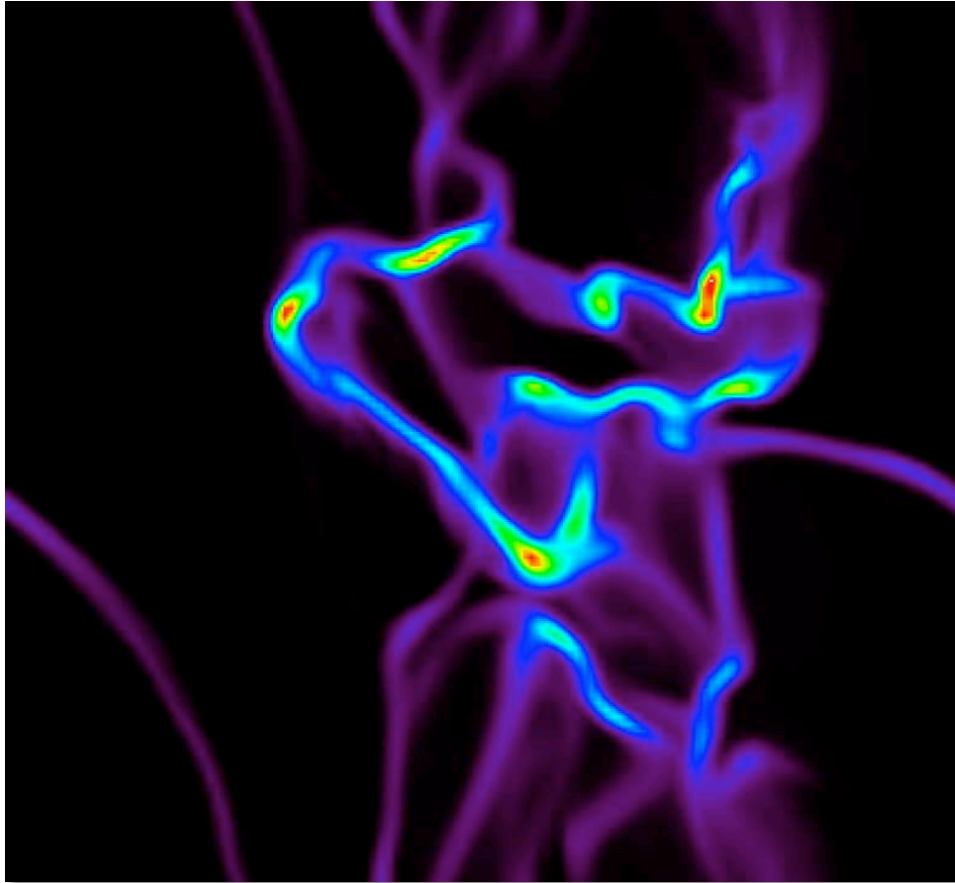
Formation of Filaments and Cores

a few selected models

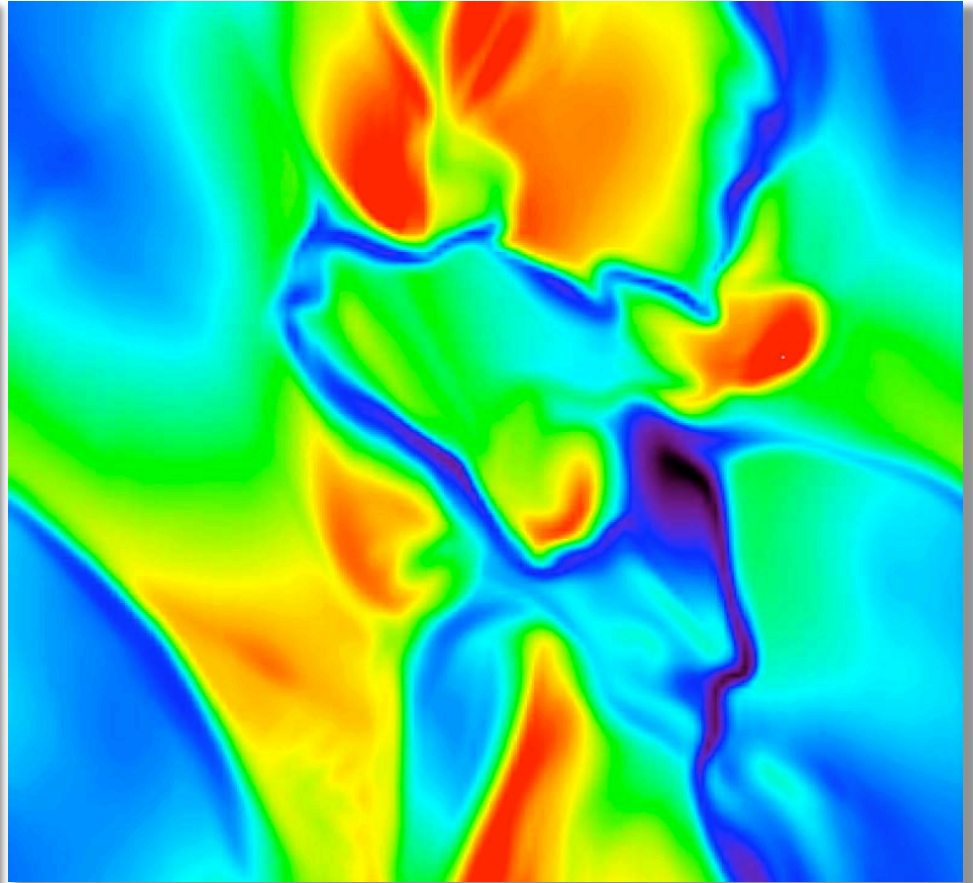
- MHD simulations of supersonic turbulent motions in weakly magnetized clouds (Padoan et al. 2001): complex system of shocks creating high-density sheets, filaments, and cores
- MHD simulations of turbulent, more strongly magnetized molecular clouds with ambipolar diffusion (Nakamura & Li 2008): sheets, filaments, and cores
- Observed profiles $\rho \sim r^{-1.5}$ and $\rho \sim r^{-2}$ are inconsistent with those of non-magnetic models of hydrostatic filaments, $\rho \sim r^{-4}$ (Ostriker 1964)
- Models of filaments with primarily toroidal or helical magnetic fields can account for profiles $\rho \sim r^{-1}$ to $\rho \sim r^{-2}$, in agreement with observations (Fiege & Pudritz 2000)

Turbulent Fragmentation, Padoan et al. (2001)

slices of the 3D density and velocity fields, Mach ~ 10



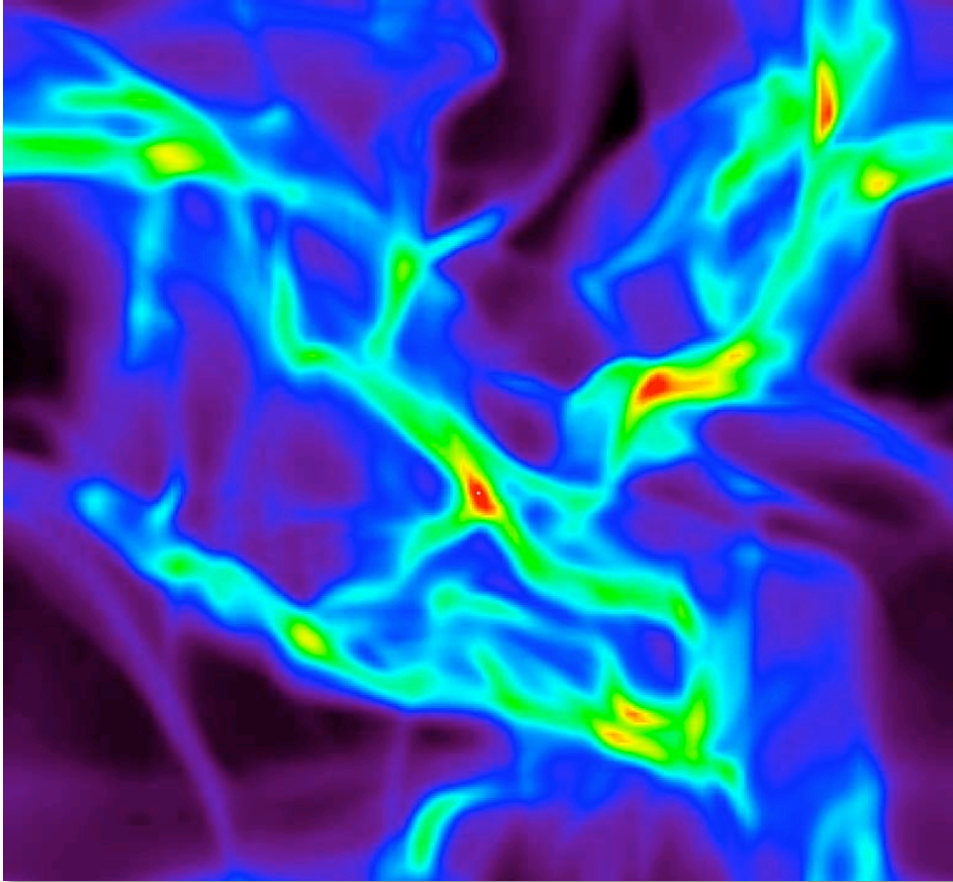
density



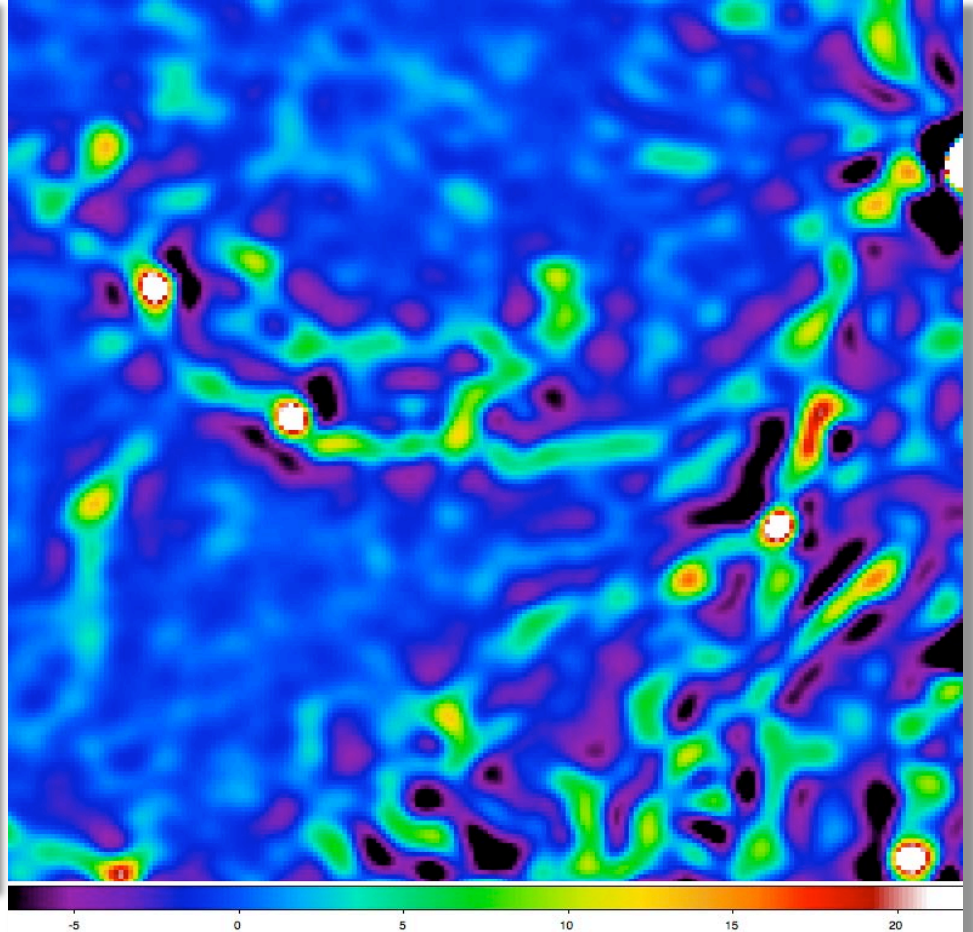
| velocity |

Turbulent Fragmentation, Padoan et al. (2001)

structural resemblance to the observed filaments



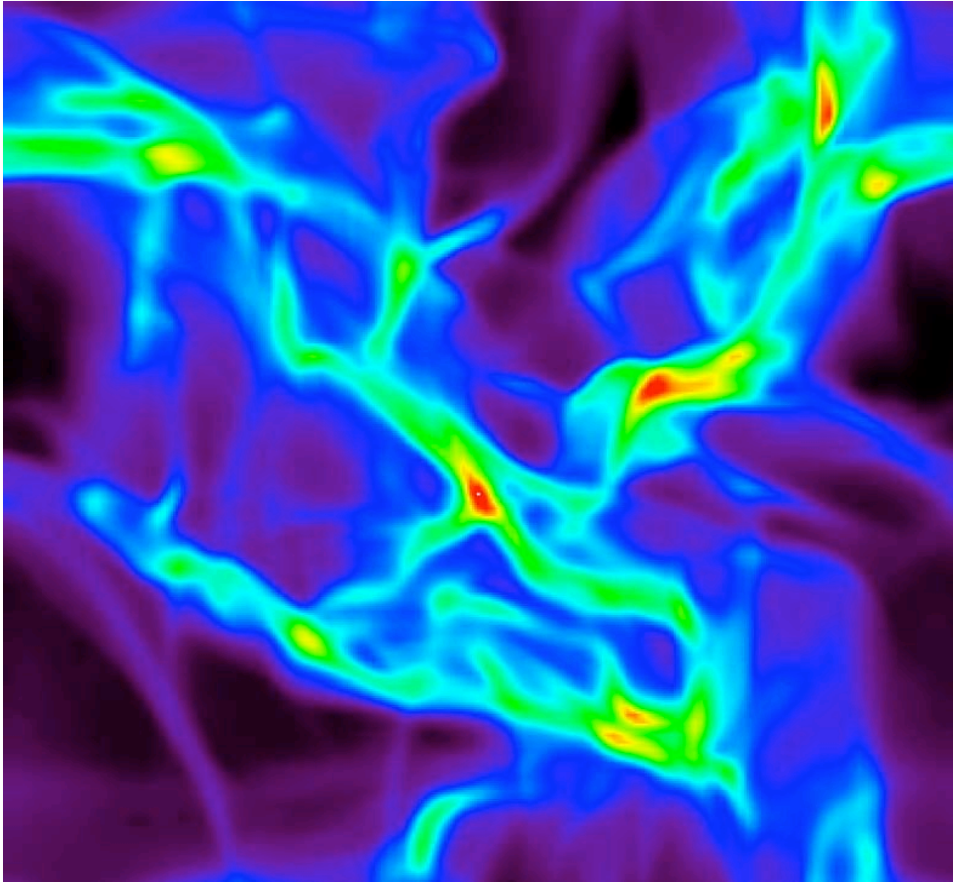
column density



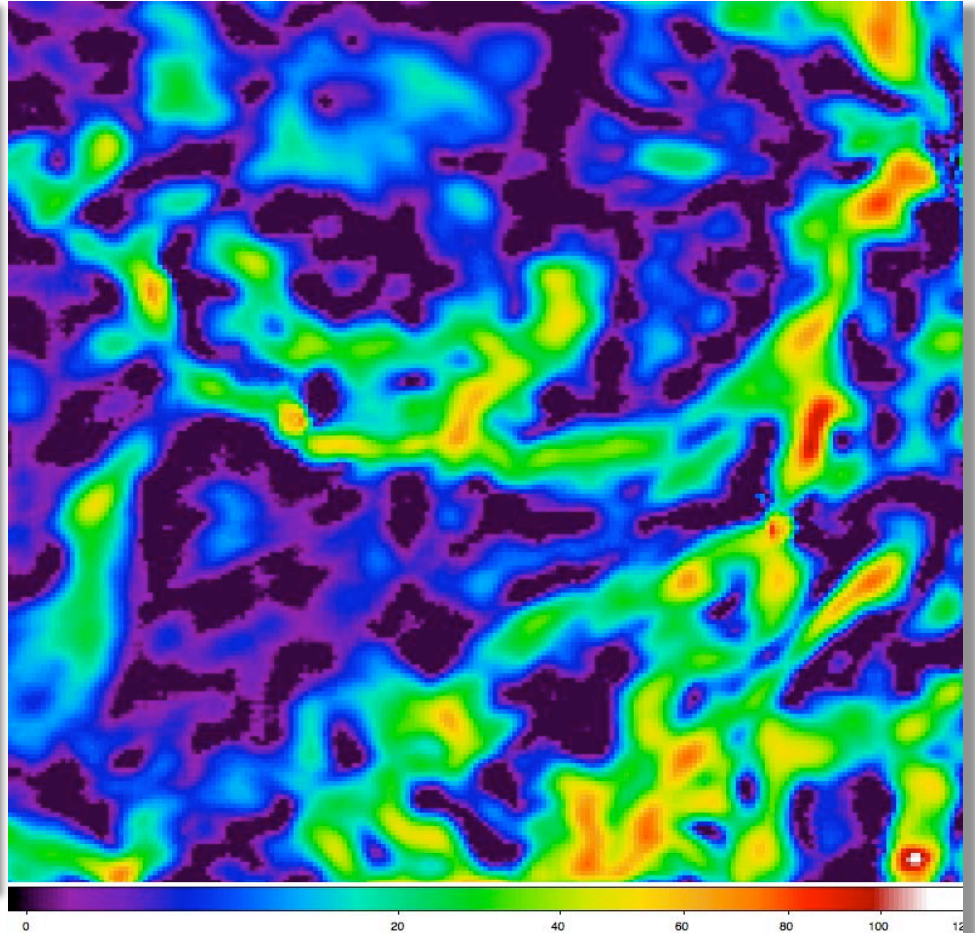
Aquila in SPIRE bands, single scale $\sim 40''$

Turbulent Fragmentation, Padoan et al. (2001)

structural resemblance to the observed filaments



column density



Aquila at 350 μm , curvelet component

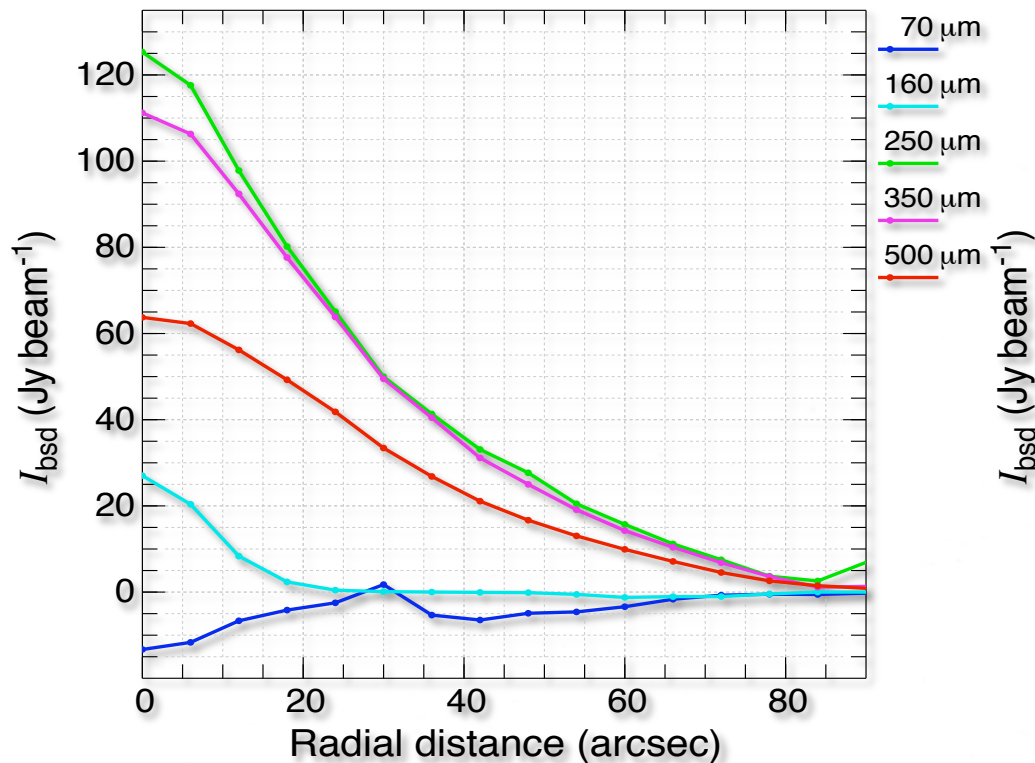
Conclusions

- Fascinating filamentary structures are *everywhere* – as deep as we can see with the sensitivity of our instruments
- All extracted objects (starless cores, prestellar cores, embedded protostars) are *physically* related to the filaments
- The observations suggest that, in general, prestellar cores *originate* in the fragmentation of complex filamentary networks
- To unravel the roles and relative importance of gravity, turbulence, and magnetic fields, we need to obtain additional *kinematic* information

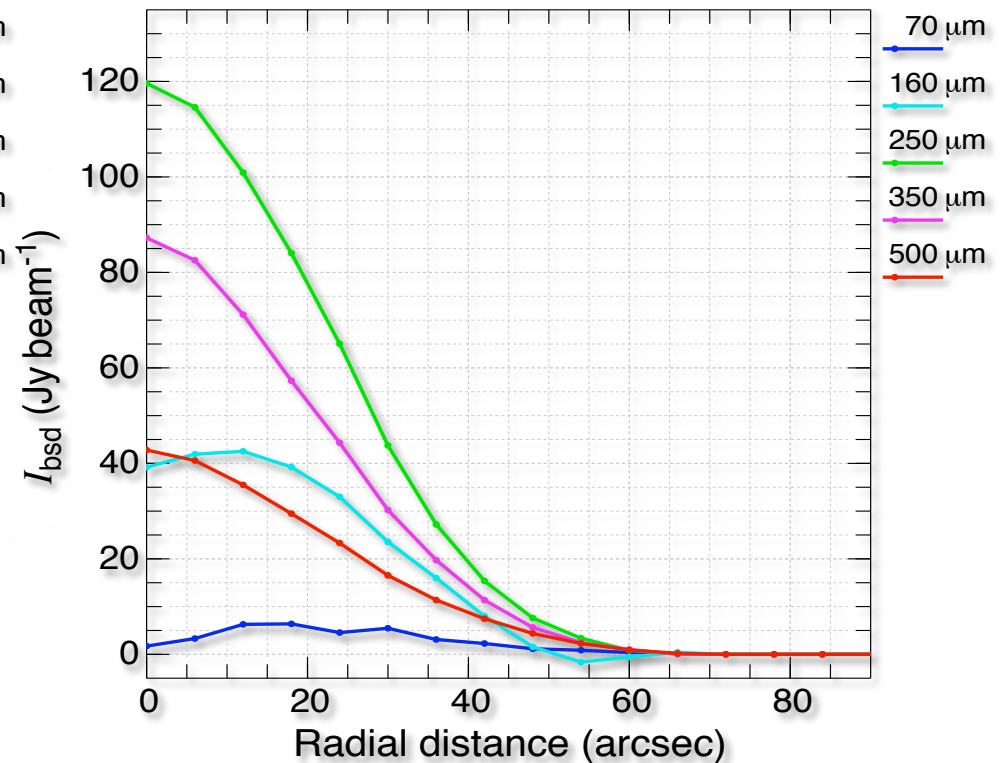
Aquila: Profiles of Selected Objects

azimuthally-averaged intensities

Intensity Profiles of Object 671



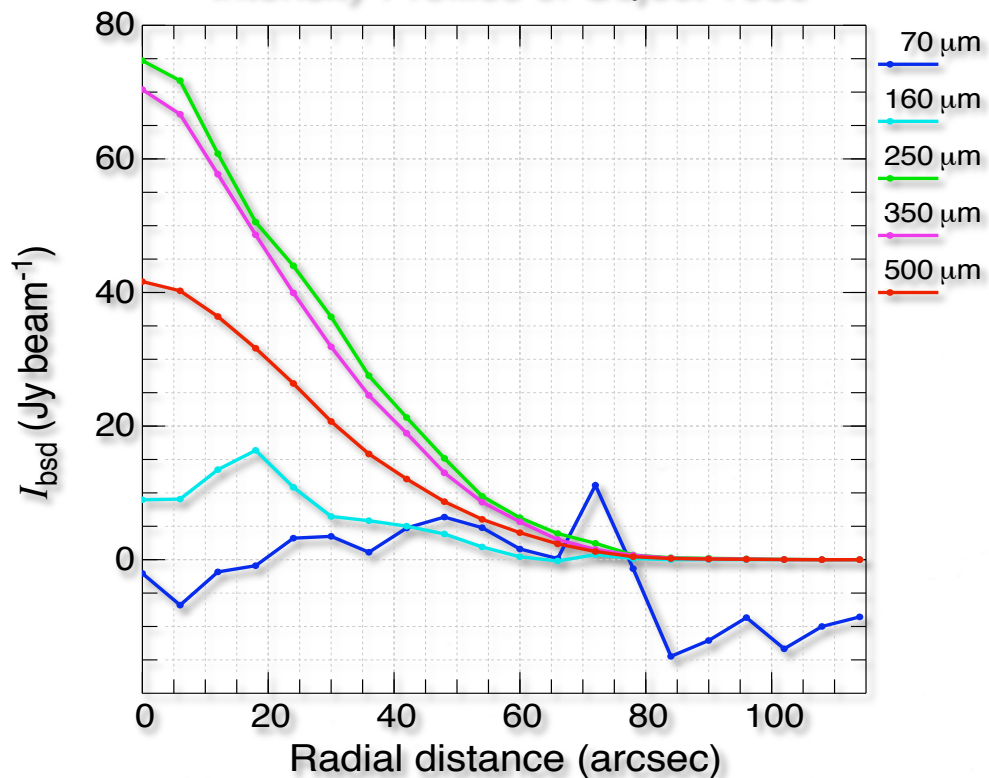
Intensity Profiles of Object 689



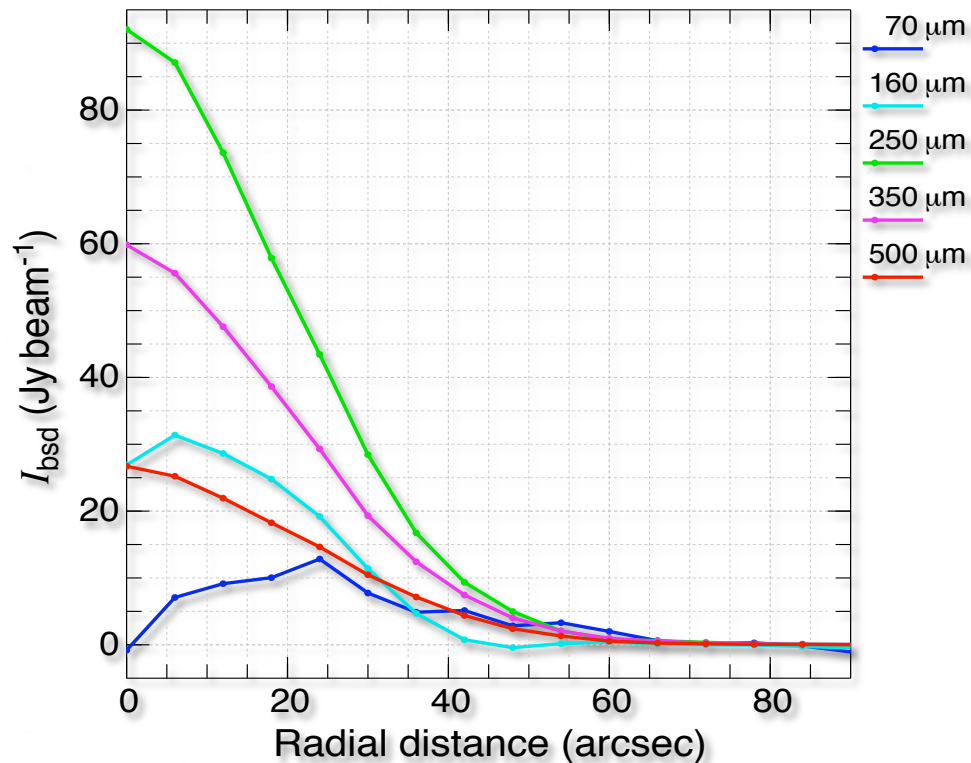
Aquila: Profiles of Selected Objects

azimuthally-averaged intensities

Intensity Profiles of Object 1050



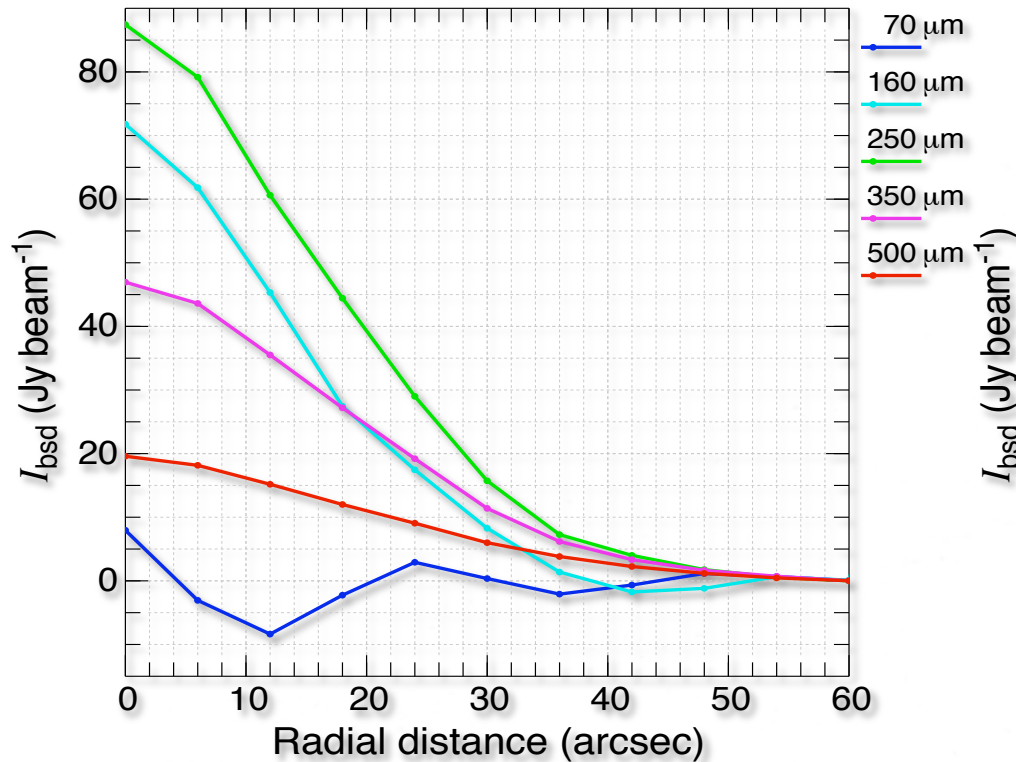
Intensity Profiles of Object 1077



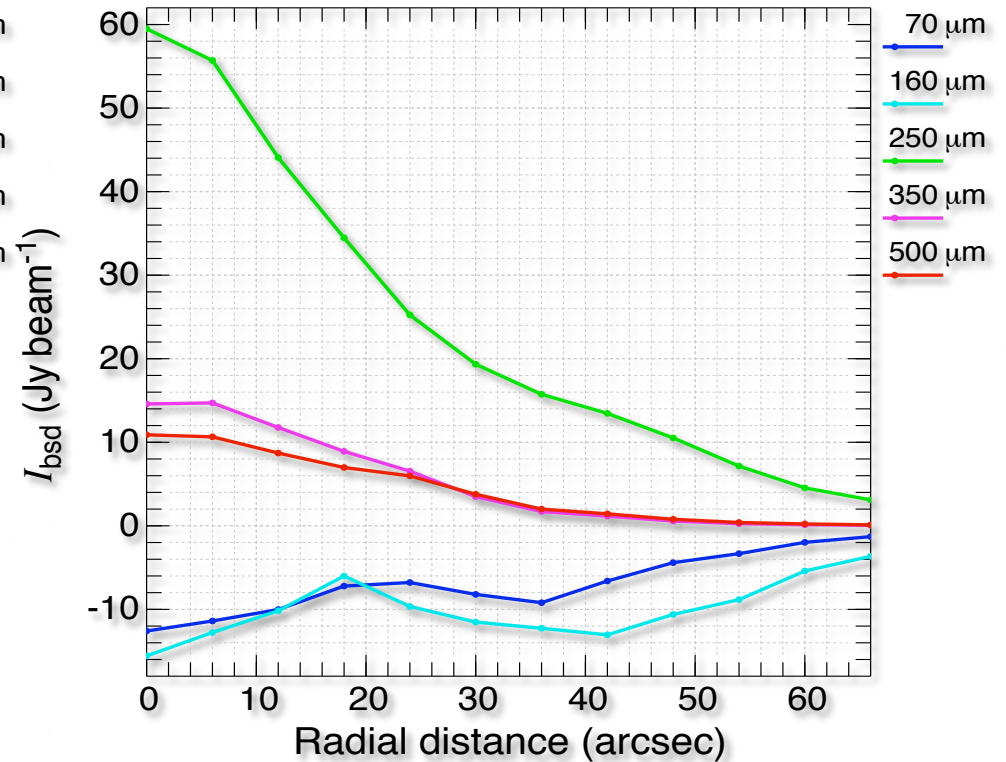
Aquila: Profiles of Selected Objects

azimuthally-averaged intensities

Intensity Profiles of Object 1213



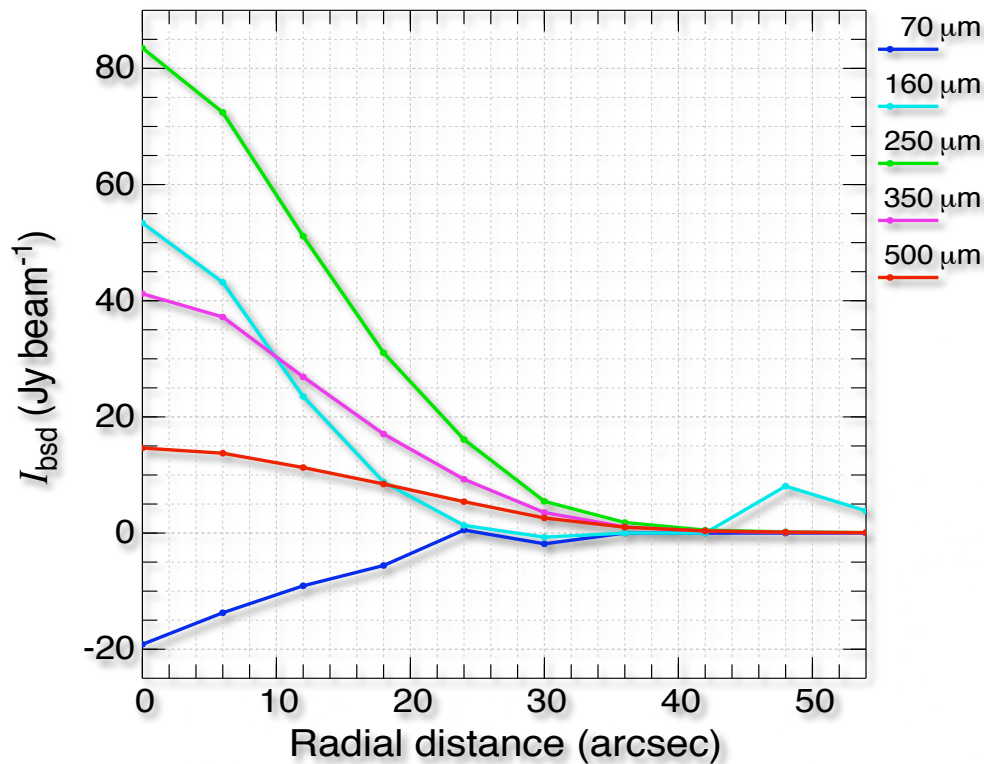
Intensity Profiles of Object 1570



Aquila: Profiles of Selected Objects

azimuthally-averaged intensities

Intensity Profiles of Object 1587



Intensity Profiles of Object 2084

